

https://dspace.org/

Turbulent hydraulic fracturing described by Prandtl's mixing length

Newman, Despina

2016-09-19
http://hdl.handle.net/10539/21080

Downloaded from a DSpace repository. https://dspace.org/

School of
Computer Science and Applied Mathematics



MSc Dissertation

Turbulent hydraulic fracturing described by Prandtl's mixing length

Student:
Despina Newman
(539077)

Supervisor:
Prof. D. P. Mason

A dissertation submitted to the Faculty of Science, University of the Witwatersrand, Johannesburg, South Africa, in fulfilment of the requirements for the degree of Master of Science.

DECLARATION

I declare that this dissertation is my own unaided work. Where other sources of information have been used, they have been acknowledged. This dissertation is being submitted for the degree of Master of Science at the University of the Witwatersrand, Johannesburg and it has not been submitted before for any degree or examination at any other university.

Johannesburg - 21/03/2016



Despina Newman,
21/03/2016

ABSTRACT

The problem of turbulent hydraulic fracturing is considered. Despite it being a known phenomenon, limited mathematical literature exists in this field. Prandtl's mixing length model is utilised to describe the eddy viscosity and a mathematical model is developed for two distinct cases: turbulence where the kinematic viscosity is sufficiently small to be neglected and the case where it is not. These models allow for the examination of the fluid's behaviour and its effect on the fracture's evolution through time. The Lie point symmetries of both cases are obtained, and a wide range of analytical and numerical solutions are explored. Solutions of physical significance are calculated and discussed, and approximate solutions are constructed for ease of fracture estimation. The non-classical symmetries of these equations are also investigated. It was found that the incorporation of the kinematic viscosity within the modelling process was important and necessary.

ACKNOWLEDGEMENTS

I am very grateful to my wonderful supervisor, Prof. Mason, for all his wisdom and support throughout the course of this dissertation. His patience, kindness and incredible insight has been invaluable. Thank you for being a wonderful example of what an academic should be - I have learned a lot from you and I strive to be more like you.

To my dear husband, Steve, thank you for always encouraging me to achieve my dreams. Without your backing, completing this dissertation would have been impossible. Thank you for always putting up with all the stress that comes along with research and for all the immeasurable love and support throughout.

Ashleigh, thank you for being such an integral part of my life, both as a mentor and a friend. Your firm commitment to quality and excellence in your research is inspiring. The friendship we have is so precious to me and has helped me through all the tough times throughout the year.

Dr. Fareo and Dr. Kgatle, thank you for sharing your time and assisting me. Your guidance through my difficulties with the numerical methods employed in this work was of critical importance and I am very grateful.

Marcio, Jarrod and Neelam, thank you for all the laughs and discussions while writing this dissertation.

Finally, a huge thank you to the National Research Foundation for the financial support during the completion of this dissertation *(Ref. SFH14070173063)*.

CONTENTS

Introduction and background 1

1 INTRODUCTION 2
- 1.1 Literature Review 2
- 1.2 Dissertation outline 4

2 THEORY AND BACKGROUND 5
- 2.1 Hydraulic fracture models 5
- 2.2 The lubrication approximation 6
- 2.3 Turbulence 7
- 2.4 Conservation laws 7
  - 2.4.1 Direct method 8
  - 2.4.2 Method of characteristics 8
  - 2.4.3 Multiplier method 9
- 2.5 Classical symmetries 9
- 2.6 Non-classical symmetries 10
- 2.7 Numerical methods for solving non-linear boundary value problems 12
  - 2.7.1 The shooting method 12
  - 2.7.2 Quasi-linearisation 13

Mathematical models and analysis 16

3 MATHEMATICAL MODEL AND GOVERNING EQUATIONS 17
- 3.1 Problem Model 17
- 3.2 Assumptions 17
- 3.3 Equation derivation 19
  - 3.3.1 The Continuity Equation 19
  - 3.3.2 The Navier-Stokes Equation 20
  - 3.3.3 Boussinesq's Closure Model 22
  - 3.3.4 Implementation of the lubrication approximation 22
  - 3.3.5 Prandtl's mixing length hypothesis 26
  - 3.3.6 Boundary and initial conditions 26
  - 3.3.7 Final equation 28
  - 3.3.8 Comparison with other models for a turbulent fracture 32

4 FULL TURBULENCE MODEL ANALYSIS 33
- 4.1 Conservation laws 33
- 4.2 Lie point symmetries and group invariant solution 38
  - 4.2.1 Constant Mixing Length 41
- 4.3 Solutions 43
  - 4.3.1 Exact analytical solutions 43
  - 4.3.2 Asymptotic solutions 46
  - 4.3.3 Numerical solution using the shooting method 47

4.3.4 Numerical solution using quasi-linearization 55
4.3.5 Graphical results 56
4.3.6 Solutions of physical importance 56
4.3.7 Comparison of average fluid velocity and fracture length propagation speed 69
4.3.8 Special symmetry solutions 78
4.4 Non-classical Symmetries 81
4.4.1 Case: $a(t) = c(t) = 0$ 81
4.4.2 Other non-classical symmetry cases 83
4.5 Analysis of results and conclusions 83
5 TRANSITIONAL TURBULENCE MODEL ANALYSIS 88
5.1 Conservation laws 88
5.2 Symmetries and group invariant solution 90
5.3 Solutions 93
5.3.1 Asymptotic solutions 93
5.3.2 Numerical solutions 94
5.4 Non-classical Symmetries 97
5.4.1 Case: $c(t) = 0$ 98
5.5 Analysis of results and conclusions 99

Conclusions 101
6 CONCLUSIONS 102

Appendix 104
A APPENDIX A 105
A.1 Lie point symmetries of the governing PDE (3.65) 105
A.2 Non-classical symmetries of the governing PDE (3.65) 111
B APPENDIX B 116
B.1 Lie point symmetries of the governing order ν equation 116
B.2 Non-classical symmetries of the governing order ν equation (3.74) 123

LIST OF FIGURES

Figure 1.1 A graph showing the simplified behaviour of the relationship between fluid pressure and fluid volume in a fracture during hydraulic fracturing, adapted from [18]. **(a)** Initially, the fracture is filled with the fluid at great pressures. **(b)** Once the fracture is filled, if the fluid pressure is great enough to overcome the rock's tensile strength and the least principal stress component, **(c)** then the fracture will extend spontaneously, making the fluid pressure approximately constant after this point, while the volume of fluid in the cavity increases. 3

Figure 2.1 A simplified diagram of the PKN fracture model, adapted from [37]. 6

Figure 3.1 A simplified diagram of the two-dimensional fracture being modelled. The fracture is within a rock mass and it is of length $L(t)$ with boundaries $z = \pm h(t, x)$. A viscous, incompressible fluid is injected at high pressures into the fracture at $x = 0$, and the flow of this fluid within the fracture is turbulent. The fracture expands due to the high pressure fluid causing the rock to fail. 18

Figure 3.2 A simple diagram of the two-dimensional fracture at $t = 0$ illustrating the characteristic lengths L and H within the hydraulic fracture problem, whereby $H << L$. 23

Figure 4.1 A graph illustrating the exact analytic solution for $\alpha = \frac{2}{7}$ (orange) and numerical solution (blue) on the same set of axes. The box within the graph is a zoomed up portion of the graph from $u = 0.9$ to $u = 0.9001$, to allow for closer inspection of the difference between the two graphs. 54

Figure 4.2 A graph illustrating the exact analytic solution for $\alpha = 1$ (orange) and numerical solution (blue) on the same set of axes. The box within the graph is a zoomed up portion of the graph from $u = 0.9$ to $u = 0.905$. 54

Figure 4.3 Graphs illustrating the effect of the parameter α on **(a)** the initial fracture profile, **(b)** the fracture length and **(c)** the fracture volume. Here, the parameters $\frac{2K}{5l_0} = 1$ and α takes on the values $\frac{2}{7}$, 0.5, 1, 1.5 and 2. 57

Figure 4.4 A graph showing the fracture half-width for $\alpha = 0.5$, at a fixed value of $p = \frac{2K}{5l_0} = 1$, where t varies, taking on the values $t = 0, 1, 5, 10$ and 100. 58

Figure 4.5 A graph showing the fracture half-width for $\alpha = 2$, at a fixed value of $p = \frac{2K}{5l_0} = 1$, where t varies, taking on the values $t = 0, 1, 5, 10$ and 50. 58

Figure 4.6 Graphs illustrating **(a)** the fracture half-width, **(b)** the fracture length and **(c)** the fracture volume, for $\alpha = 0.5$, at a fixed value of $t = 1$, where $p = \frac{2K}{5l_0}$ varies, taking on the values $p = 0, 1, 5, 10$, and 100. 59

Figure 4.7 Graphs illustrating **(a)** the fracture half-width, **(b)** the fracture length and **(c)** the fracture volume, for $\alpha = 2$, at a fixed value of $t = 1$, where $p = \frac{2K}{5l_0}$ varies, taking on the values $p = 0, 1, 5, 10$ and 100. 60

Figure 4.8 Graphs illustrating the fracture half-width varying across t and u for $\alpha = \frac{2}{7}$, at different view points. Here, the parameter $\frac{2K}{5l_0} = 1$. 61

Figure 4.9 Graphs illustrating the fracture half-width varying across t and u for $\alpha = 1$, at different view points. Here, the parameter $\frac{2K}{5l_0} = 1$. 61

Figure 4.10 Graphs illustrating the fracture half-width varying across t and u for $\alpha = 2$, at different view points. Here, the parameter $\frac{2K}{5l_0} = 1$. 62

Figure 4.11 Graphs illustrating **(a)** the fracture half-width for different t at a fixed $p = \frac{2K}{5l_0} = 1$, **(b)** the fracture half-width for varying $p = \frac{2K}{5l_0}$ at $t = 1$ and **(c)** the fracture length for different $p = \frac{2K}{5l_0}$, where $\alpha = \frac{2}{7}$, corresponding to a constant fracture volume. 64

Figure 4.12 Graphs illustrating **(a)** the fracture half-width for different t at $p = \frac{2K}{5l_0} = 1$, **(b)** the fracture half-width for different $p = \frac{2K}{5l_0}$ at $t = 1$ and **(c)** the fracture volume for varying $p = \frac{2K}{5l_0}$, where $\alpha = 0.857143$, corresponding to a constant rate of change of volume. 66

Figure 4.13 Graphs illustrating **(a)** the fracture half-width for different t for $p = \frac{2K}{5l_0} = 1$, **(b)** the fracture half-width for different values of $p = \frac{2K}{5l_0}$ at $t = 1$ and **(c)** the fracture length for varying $p = \frac{2K}{5l_0}$, where $\alpha = 1$, corresponding to a constant speed of propagation of the fracture. 68

Figure 4.14 Graphs illustrating **(a)** the fracture half-width for different t at $p = \frac{2K}{5l_0} = 1$, **(b)** the fracture length for different $p = \frac{2K}{5l_0}$ and **(c)** the fracture volume for varying $p = \frac{2K}{5l_0}$, where $\alpha = \frac{2}{3}$, corresponding to a constant pressure at the fracture entry. 70

Figure 4.15 A graph illustrating the ratios $\frac{\bar{v}_x^*}{L'(t)}$ for $\alpha = \frac{2}{7}, 0.5, 0.8, 1, 1.5, 2$ and 5. 71

Figure 4.16 A figure illustrating the ratio graph for $\frac{\bar{v}_x^*}{L'(t)} = 1$ corresponding to $\alpha = 1$, and for $\frac{\bar{v}_x^*}{L'(t)}$ for some $\frac{2}{7} < \alpha < 1$. 72

Figure 4.17 Graphs of $\frac{\bar{v}_x^*}{L'(t)}$ compared with their approximations $\alpha = 0.3$, $\alpha = 0.5$, $\alpha = 0.7$ and $\alpha = 0.9$. 73

Figure 4.18 The numerical solution of $h(t, u)$ plotted against the approximate solution obtained for $\alpha = 0.3$ and $\alpha = 0.5$ respectively. Here, $t = 1$ and $p = 2$. 74

Figure 4.19 The numerical solution of $h(t,u)$ plotted against the approximate solution obtained for $\alpha = 0.7$ and $\alpha = 0.9$ respectively. Here, $t = 1$ and $p = 2$. 75

Figure 4.20 Illustration of the graph of the ratio $\frac{\bar{v}_x^*}{L'(t)} \geqslant 1$ plotted against u corresponding to $\alpha \geqslant 1$. 76

Figure 4.21 The numerical solution of $h(t,u)$ plotted against the approximate solution obtained for $\alpha = 1.5$ and $\alpha = 2$ respectively. Here, $t = 1$ and $p = 2$. 77

Figure 4.22 Graphs illustrating the non-classical symmetry solution for **(a)** the fracture profile for $p = \frac{2K}{5l_0} = 1$, **(b)** the fracture profile for $t = 1$, **(c)** the fracture length and **(d)** the fracture volume. 84

Figure 5.1 The fracture half-width, $h(t,u)$ plotted against u at $t = 3$ for $p = 1$ and $q = 0,\ 0.01,\ 0.05,\ 0.1,\ 0.15$ and 0.2. 95

Figure 5.2 The fracture length, $L(t)$ plotted against time t for $p = 1$ and $q = 0,\ 0.05,\ 0.1,\ 0.15$ and 0.2. 95

Figure 5.3 The fracture volume, $V(t)$ plotted against time t for $p = 1$ and $q = 0,\ 0.05,\ 0.1,\ 0.15$ and 0.2. 96

Figure 5.4 The fracture half-width $h(t,u)$ plotted against u for $p = 1$, $q = 0.1$ and $t = 0,\ 1,\ 5$ and 10. 96

Figure 5.5 Comparison of the solution for the half-width (4.107) for $\nu = 0$ and $\alpha = 2$ with the solution (5.54) for $\nu \neq 0$ at $t = 3$, $p = 1$ and (a) $q = 0$ and (b) $q = 0,\ 0.05,\ 0.1$ and 0.2. 97

LIST OF TABLES

Table 3.1 The characteristic quanitites selected in this problem. 23

Table 4.1 The values of the approximate numerical solution of ODE (4.133), $G^*(u)$, the analytic solution, $G(u)$, and the error between the two, for $\alpha = \frac{2}{7}$. 52

Table 4.2 The values of the approximate numerical solution of ODE (4.133), $G^*(u)$, the analytic solution, $G(u)$, and the error between the two, for $\alpha = 1$. 53

Table 4.3 Table illustrating values of the parameter α that correspond to physically significant scenarios. 62

Table 4.4 A table showing the corresponding q value for each choice of α, where q is obtained by solving equation (4.197). 73

Table 4.5 The value of r for each choice of α. 78

INTRODUCTION AND BACKGROUND

1 INTRODUCTION

Hydraulic fracturing occurs when a viscous, incompressible fluid is injected into a small rock cavity at sufficiently high pressures that the fluid is able to overcome both the rock's tensile strength and its smallest principal stress. This causes the rock to fail and a fracture to propagate throughout it [14, 18, 21].

Hydraulic fracturing can occur by natural means [18], for example turbulent hydraulic fracturing caused by certain types of magma flows [14]. However, this process is also artificially employed in mining applications [14, 15, 18, 21]. In this context, it is used to fracture rock in order to access underground resource reserves, such as oil or natural gas [15, 18]. This is done by pumping a fluid containing a propping agent into a prepared fracture in order to extend it. The fluid used is usually water, with sand as a propping agent, with small quantities of other chemicals that aid in the fracturing process [18, 21].

This technique has become crucial in mining, as it can be utilized to increase the recovery rate of resources, for example, oil, from a reservoir [18, 21, 23, 37]. Hydraulic fracturing also has major economic benefits as it allows for additional extraction of resources from otherwise depleted reservoirs, giving access to dwindling non-renewable energy resources [21].

The aim of this research is to examine turbulent hydraulic fracturing, as justified in [14], as it has not been greatly studied in literature. This research will give insight on how a fracture will expand and propagate as a result of turbulent fluid flow. A model will be formed to represent how the fluid behaves during this process and how it affects the fracture's growth. Prandtl's mixing length model will be utilized to describe the effect of turbulent fluctuations on the mean flow, which drives fracturing.

This document will be divided into the examination of two sub-problems: turbulent flow where the turbulence is the dominant feature of the fluid flow, and flow with minor turbulence where the kinematic viscosity still plays an important role in the fluid flow.

1.1 Literature Review

The mechanism behind hydraulic fracturing is as follows: the injected fluid fills the fracture and the pressure increases. If the fluid pressure is great

enough to overcome both the material strength and stress configuration of the rock, then the fracture will propagate [14, 15, 18, 21]. At this point, the pressure will approximately stabilize and the fracture will continue to extend. A graph illustrating this principal is illustrated in Figure 1.1.

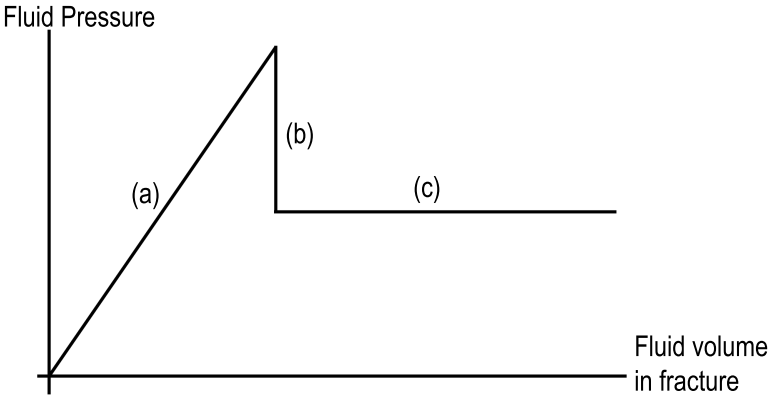


Figure 1.1: A graph showing the simplified behaviour of the relationship between fluid pressure and fluid volume in a fracture during hydraulic fracturing, adapted from [18]. **(a)** Initially, the fracture is filled with the fluid at great pressures. **(b)** Once the fracture is filled, if the fluid pressure is great enough to overcome the rock's tensile strength and the least principal stress component, **(c)** then the fracture will extend spontaneously, making the fluid pressure approximately constant after this point, while the volume of fluid in the cavity increases.

During the process of hydraulic fracturing, the fracture will propagate in the direction of least resistance [18]. This is generally, in isotropic, homogeneous rock, the direction perpendicular to the smallest principal stress in the rock [18, 21, 23].

The manner in which a fracture will expand during the hydraulic fracturing process is determined strongly by the fracture's geometry [37] as well as the fluid injection rate into the rock cavity [14]. The fluid pressure required to split the rock is dependent on the rock's material properties in conjunction with pre-existing stresses [23].

Within the field of hydraulic fracturing, there is much literature relating to laminar hydraulic fracturing. Notable works that include detailed modelling of 2-dimensional laminar hydraulic fractures are [15] and[17], which examine permeable and impermeable rock cases respectively. The PKN and lubrication approximations are implemented and justified in both of these papers and Lie group analysis is performed on the governing equation. A detailed analysis of the results are also provided.

Turbulent flow, on the other hand, is not as well-documented in existing literature, although there is evidence of this phenomena occurring. Fluids with small kinematic viscosities and 'rough' fractures greatly influence the likelihood of turbulent fracturing taking place [14].

Anthonyrajah et. al [2] have examined 2-dimensional turbulent hydraulic fracturing for a pre-existing fracture. In this paper, the mean flow components of the fluid velocity are averaged spatially across the fracture width. Once again, the PKN and lubrication approximations are utilized when deriving the governing equation. The turbulence is introduced through the Blasius wall shear stress at the fracture boundaries. The governing equation obtained contains parameters m and n that correspond to different types of laminar or turbulent flow, depending on their value. Lie group analysis is performed and solutions are obtained, both analytically for special parameter cases and numerically.

There is room for further exploration of turbulent hydraulic fractures. Turbulent fluid flow variables where the mean flow variables are averaged over time can be explored. Closure models such as those presented by Boussinesq [6] and modifications like Prandtl's mixing length [3, 12, 26] can be considered to examine this problem further.

1.2 Dissertation outline

This dissertation is structured as follows:

- Chapter 2 will detail the required mathematical background and theory relevant to the research.
- Chapter 3 will describe the model formulation and derivation of the governing equations in detail, and outline all assumptions and approximations made. A fully turbulent fracturing equation as well as a transitional turbulence fracturing equation will be obtained.
- A detailed analysis of the fully turbulent fracturing equation will be presented in Chapter 4. Conservation laws of the governing equation will be found, symmetry solutions will be obtained, and solutions (both analytical and numerical) will be presented and discussed.
- Chapter 5 will carry out a similar analysis as in Chapter 4 on the transitional turbulence fracturing equation.
- Chapter 6 will give overall conclusions drawn from the results obtained.
- Finally, an appendix will detail the calculations of the Lie point and non-classical symmetries used within this research.

2

THEORY AND BACKGROUND

In this chapter, background information and mathematical theory relevant to the problem will be outlined.

2.1 Hydraulic fracture models

There are many models used to explain the hydraulic fracturing process. A comprehensive review of existing models is given in [27, 37]. Two of the most popular and widespread of these models are the Perkins-Kern-Nordgren (PKN) and Kristianovitch-Geertsma-De Klerk (KGD) models, with most other models being modifications of these two [37]. Both of these models make the assumptions that the height and length of a fracture are independent of one another, and that the stress configuration of the rock is of plane strain form [18]. The difference between these models is defined by the length scales present and the type of plane strain considered.

In the KGD model, the length scale is comparable to the width scale. It is often used to model miniature hydraulic fracturing tests done to determine if a site is appropriate for large-scale hydraulic fracturing [18]. The plane strain is constrained to the horizontal plane in this model.

The PKN model, however, is more relevant to this work. It is used when the length scale (L) of the fracture is considerably larger than the half-width scale (H). In other words, it is applicable when $L/H >> 1$ [18, 37]. As this is usually the geometry present within most real-world applications, this model is most often used [18]. These fractures are elliptical in shape [37]. The plane strain in this case is also confined to the vertical plane. This model is illustrated in Figure 2.1.

Mathematically, the PKN model also gives a relationship between the net pressure and the half-width of the fracture,

$$p(t,x) + \sigma_{zz}^{\infty} = \Lambda h(t,x), \tag{2.1}$$

where σ_{zz}^{∞} is the normal stress at infinity, and Λ is a parameter that can be calculated from the material properties of the medium in which the fracturing is taking place [17, 32, 35].

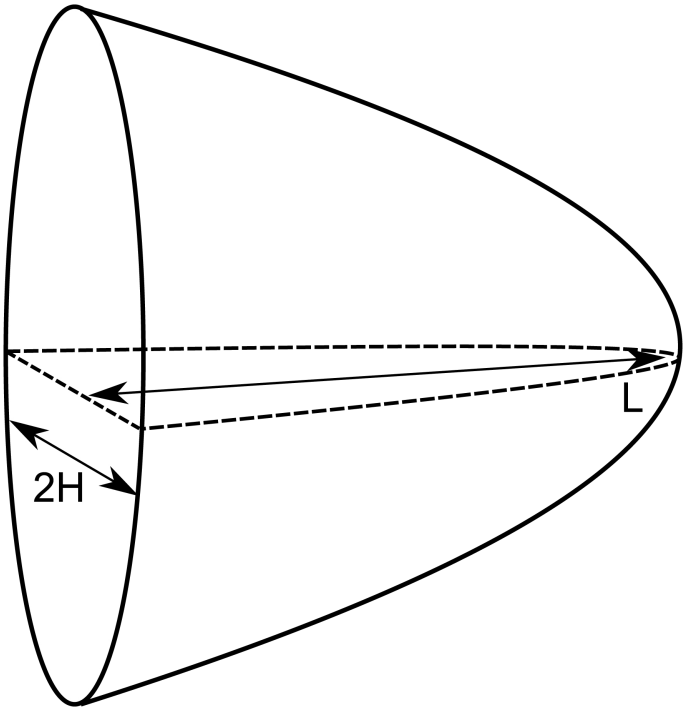


Figure 2.1: A simplified diagram of the PKN fracture model, adapted from [37].

2.2 The lubrication approximation

Occasionally, the geometry present within a problem can allow for significant simplification of equations, with minimal information loss. In problems where the length scale is substantially larger than the width scale, the lubrication approximation can be utilized [22, 34].

This approximation relies obtaining dimensionless governing equations. Upon performing the non-dimensionalization procedure, terms with the quantity

$$\frac{H}{L} << 1, \tag{2.2}$$

may be neglected as the terms are minuscule and thus do not affect the behaviour greatly [34].

Additionally, for problems related to fluid flow, the additional assumption is made that the product of the Reynolds number and the ratio of the width to length squared is small:

$$\left(\frac{H}{L}\right)^2 \mathrm{Re} << 1. \tag{2.3}$$

The left hand side of equation (2.3) is referred to as the reduced Reynolds number [22]. While the Reynolds number may potentially be large, as long as the reduced Reynolds number is significantly smaller than one, the lubrication approximation will still hold.

As a result of implementing this approximation within the Navier-Stokes equations, the inertial terms can be neglected while the viscous and pressure gradient terms dominate the behaviour [34]. The non-linearity of the equations is also removed [22].

The examination of hydraulic fracturing allows the use of this approximation, as the fracture length is indeed longer than the fracture width [18].

2.3 Turbulence

Most fluid flow that occurs in nature and in industrial applications is turbulent [34, 39, 40]. Turbulence arises when flows with high Reynolds numbers experience instabilities [26, 39, 41], and it has a random component to it. This requires the use of statistics to describe the flow behaviour, increasing the equation complexity significantly [40, 41].

Turbulent flow is often considered in terms of eddies, which are groups of fluid that retain their structure for a certain amount of time [34]. Within turbulence, there are eddies of all different length scales, the smallest of which dissipate energy [26, 34]. As a result, turbulence requires a continual supply of energy to be sustained [40].

When mathematically modelling turbulence, the Navier-Stokes equations can be used. However, unlike with laminar flow, the fluid variables are broken up into a mean flow and a random fluctuation component [34, 39, 40, 41]. The derivation of these equations is presented in detail in [40].

A feature of these equations is that they are not a closed system and thus cannot be solved without a further relationship between the variables. Closure models as presented by Boussinesq [6, 39] and further modifications such as Prandtl's mixing length [39, 34, 41] are popular relations utilized in closing these equations.

2.4 Conservation laws

Equations found in various fields of study often express the conservation of certain quantities. When such equations relate to physical problems, the conserved quantities may be of physical significance and useful for analysis [30, 31]. However, even those that are not physically understandable are of importance, as they can be indicative of an equation's integrability [28, 30].

There are many different ways of systematically obtaining the conservation laws for a differential equation. A comprehensive outline and comparison of popular methods with examples of their application is outlined in [31]. The basic theory required to understand the calculation of the conservation laws

for a single differential equation as well as an overview of selected methods will be presented here.

Consider an m^{th}-order partial differential equation given by

$$F(\underline{x}, u, u_{(1)}, \ldots, u_{(m)}) = 0, \tag{2.4}$$

where $\underline{x} = (x_1, x_2, \ldots, x_n)$ are the n independent variables and $u_{(i)}$ is the collection of i^{th}-order partial derivatives of the dependent variable u. The local conservation law for equation (2.4) is given by

$$D_i T^i|_{F=0} = (D_1 T^1 + \ldots + D_n T^n)|_{F=0} = 0, \tag{2.5}$$

where D_i denotes the total derivative with respect to the i^{th} independent variable. The vector $\underline{T} = (T^1, \ldots, T^n)$ is called the conserved vector [8, 28, 31, 38].

The direct method, method of characteristics and the multiplier method are three popular methods of obtaining the conserved vector for a differential equation. These will be discussed below.

2.4.1 *Direct method*

The direct method involves selecting a set of variables the conserved vector $\underline{T}$ depends on i.e. $\underline{T} = \underline{T}(\underline{x}, u, u_{(1)}, \ldots)$, and then substituting this into the conservation law

$$D_i T^i_{|F=0} = 0. \tag{2.6}$$

Upon doing this, we obtain an over-determined, linear system of equations. This system is obtained by separating the conservation law according to partial derivatives of the dependent variable. From this system, exact forms of $\underline{T}$ can be obtained [8, 31]. By allowing the conserved vector to depend on a greater number of variables, more general results may be obtained. Examples of this method being utilised are given in [1, 31].

2.4.2 *Method of characteristics*

The method of characteristics requires the definition of a characteristic function $\Lambda = \Lambda(\underline{x}, u, u_{(1)}, \ldots)$, and $\underline{T} = \underline{T}(\underline{x}, u, u_{(1)}, \ldots)$. This is used to solve the equation

$$D_i T^i = \Lambda F, \tag{2.7}$$

in a similar fashion to the direct method, by separating by partial derivatives of the dependent variable to obtain an over-determined linear system. This method is not only more general than the direct method, but also allows for the determination of a characteristic that makes the equation exact [31]. Fully illustrated examples of this method are presented in [1].

2.4.3 *Multiplier method*

This method is similar to the characteristic method in that a characteristic function $\Lambda = \Lambda(\underline{x}, u, u_{(1)}, \ldots)$ and conserved vector $\underline{T} = \underline{T}(\underline{x}, u, u_{(1)}, \ldots)$ is defined. However, instead of directly solving for both Λ and $\underline{T}$ together, the Euler operator

$$E_u = \frac{\partial}{\partial u} + \sum_{p \geqslant 1} (-1)^p D_{i_1} \ldots D_{i_p} \frac{\partial}{\partial u_{i_1 i_2 \ldots i_p}}, \tag{2.8}$$

is applied on ΛF,

$$E_u[\Lambda F] = 0, \tag{2.9}$$

resulting in a determining equation for Λ. Upon solving for Λ, this can then be substituted back into equation (2.7) to solve for $\underline{T}$ [28, 30, 31]. Examples are given in [28, 30, 31].

2.5 Classical symmetries

Classical or Lie point symmetries is a method to obtain exact analytic solutions to differential equations. It is often useful when an equation proves difficult to solve under other analytical techniques. It relies heavily on group theory. A comprehensive review of the background of this method is given in [7]. A summary of the results will be presented below with the example of a PDE with one dependent variable to illustrate.

Consider a partial differential equation F with n independent variables $x_1 \ldots x_n$ and one dependent variable u. Consider also a group G of invertible transformations,

$$x_i^* = f_i(\underline{x}, u, \epsilon), \quad u^* = g(\underline{x}, u, \epsilon), \quad i = 1, 2, \ldots, n. \tag{2.10}$$

This group is called a *symmetry group* of an equation F if and only if $F(\underline{x}, u) = 0$ when $F(\underline{x}^*, u^*) = 0$ [24].

Obtaining this group is equivalent to obtaining infinitesimal transformations [7, 24]

$$x_i^* = x_i + \epsilon \xi_i(\underline{x}, u), \quad u^* = u + \epsilon \eta(\underline{x}, u), \tag{2.11}$$

where

$$\xi_i(\underline{x}, u) = \frac{\partial f_i(\underline{x}, u, \epsilon)}{\partial \epsilon}|_{\epsilon=0}, \quad \eta(\underline{x}, u) = \frac{\partial g(\underline{x}, u, \epsilon)}{\partial \epsilon}|_{\epsilon=0}. \tag{2.12}$$

The method of obtaining these transformations for an equation F is done by defining a symmetry generator [7, 24],

$$X = \xi_1 \frac{\partial}{\partial x_1} + \xi_2 \frac{\partial}{\partial x_2} + \ldots + \xi_n \frac{\partial}{\partial x_n} + \eta \frac{\partial}{\partial u}. \tag{2.13}$$

We require that the equation $F = 0$ remains invariant under this symmetry generator. That is [7],

$$X(F)_{|_{F=0}} = 0. \tag{2.14}$$

Thus, infinitesimals $\xi^i(\underline{x}, u)$, $\eta(\underline{x}, u)$ that leave the function invariant are calculated.

In order to calculate the infinitesimals, the symmetry generator is prolonged to the order of the equation and then applied to the equation, as in equation (2.14). The resulting equation may then be split up into determining equations by the partial derivatives of the dependent variable.

This may be done as the infinitesimals are independent of the dependent variable's derivatives, and thus they must all separately vanish [7, 24]. These determining equations are an over-determined system which can allow the calculation of the infinitesimals.

If such a group of transformations is found that leave an equation $F = 0$ and its boundary conditions invariant, a group invariant solution may then be constructed by solving the differential equation resulting from [24]

$$X(u(\underline{\mathbf{x}}) - \psi(\underline{\mathbf{x}}))|_{u=\psi} = 0. \tag{2.15}$$

By substituting the resulting group invariant solution into the original equation, the number of variables present will be reduced by one. For example, if the original function is a partial differential equation with one dependent variable and two independent variables, substitution of the group invariant solution will result in an ordinary differential equation [9].

2.6 Non-classical symmetries

Non-classical symmetries are a generalization of classical symmetries [11]. They can be utilized to discover additional symmetries of an equation that are not obtainable through the classical approach [9, 11].

Classical symmetries can also be admitted via non-classical methods. An admitted symmetry from non-classical methods that is not a classical symmetry is called a non-trivial non-classical symmetry [11].

In the non-classical symmetry method, an infinitesimal symmetry generator is searched for that not only leaves the equation invariant, but some other sub-manifold as well [11, 33]. It is for this reason that non-classical symmetries are also termed conditional symmetries, as an additional condition is imposed that some sub-manifold is required to remain invariant under the symmetry generator too [33].

The most typical condition imposed in non-classical symmetries is that the invariant surface condition,

$$\xi^i \frac{\partial h}{\partial x_i} = \eta, \tag{2.16}$$

is invariant under the symmetry generator [9, 33], where i is a summation index over all the independent variables present in the problem and h is the dependent variable.

It can be noted that (2.16) can be divided through by one of the infinitesimals, provided that they are non-zero [9].

For example, if given a problem with n independent variables, the invariant surface condition is given by

$$\xi^1 \frac{\partial h}{\partial x_1} + \xi^2 \frac{\partial h}{\partial x_2} + \ldots + \xi^n \frac{\partial h}{\partial x_n} = \eta, \tag{2.17}$$

and assuming $\xi^1 \neq 0$, we can divide through by it resulting in

$$\frac{\partial h}{\partial x_1} + \xi^2_* \frac{\partial h}{\partial x_2} + \ldots + \xi^n_* \frac{\partial h}{\partial x_n} = \eta_*, \tag{2.18}$$

where

$$\xi^1_* = 1, \quad \xi^i_* = \frac{\xi^i}{\xi^1}, \quad \eta_* = \frac{\eta}{\xi^1},$$

for $i = 2, 3, \ldots n$.

This simplifies the calculation required in calculating non-classical symmetries without loss of generality.

From this point, one searches for a symmetry generator

$$X = \frac{\partial}{\partial x_1} + \xi^2 \frac{\partial}{\partial x_2} + \ldots + \xi^n \frac{\partial}{\partial x_n} + \eta \frac{\partial}{\partial h}, \tag{2.19}$$

where

$$X(F)_{|(F=0,\ (2.18))} = 0, \tag{2.20}$$

holds [9].

Practically, this entails solving the equation and invariant surface condition for different derivatives of the dependent variable. The obvious variable to solve for in the invariant surface condition (2.18) is $\frac{\partial h}{\partial x_1}$. Taking the total derivatives of this term is then done to obtain expressions that can be substituted into the determining equations. For example,

$$D_{x_i}\left(\frac{\partial h}{\partial x_1}\right) = \frac{\partial^2 h}{\partial x_1 x_i}, \qquad i = 1, 2, \ldots n. \tag{2.21}$$

The term solved for within the equation is often chosen to be the highest order derivative present in the equation.

By calculating symmetries in this manner, a non-linear system of equations is obtained, in contrast to the linear set of equations obtained in classical symmetry methods [9, 11]. These equations are often very difficult to solve exactly. Thus, special cases are taken and solved. Each special solution to the non-linear system of equations obtained is a symmetry of the equation and the invariant surface condition [9].

2.7 Numerical methods for solving non-linear boundary value problems

Consider a highly non-linear, second-order two-point boundary value problem of the form

$$y'' = f(t, y, y'), \quad t \in [a, b], \tag{2.22}$$

where

$$y(a) = \alpha, \quad y(b) = \beta. \tag{2.23}$$

Often, equations of this form arising from real-world problems cannot be solved analytically and numerical methods need to be considered [20].

2.7.1 *The shooting method*

The shooting method is a common way of solving such problems, as it is applicable to a wide range of equations [10, 20]. It is based on replacing the boundary value problem with two initial value problems [10, 16].

This replacement can be done in a variety of ways. The method that will be considered in this work will take a Lie point symmetry approach. This approach may only be taken for equations that admit scaling symmetries.

Assume equation (2.22) has a Lie point symmetry generator of the form

$$X = c_1 t \frac{\partial}{\partial t} + c_2 y \frac{\partial}{\partial y}. \tag{2.24}$$

These are scaling symmetries, which upon solution of Lie's equations yields the following invariant transformation,

$$\bar{t} = e^{c_1 p} t, \qquad \bar{y} = e^{c_2 p} y, \tag{2.25}$$

where p is the group parameter.

By letting $\lambda = e^{c_1 p}$, this transformation can be rewritten as

$$\bar{t} = \lambda t, \qquad \bar{y} = \lambda^{\frac{c_2}{c_1}} y. \tag{2.26}$$

Using this transformation on (2.22), we thus obtain the first initial value problem.

Initial Value Problem 1:

$$\bar{y}'' = f(\bar{t}, \bar{y}, \bar{y}'), \quad \bar{t} \in [\lambda a, \lambda b], \tag{2.27}$$

where

$$\bar{y}(\lambda a) = \lambda^{\frac{c_2}{c_1}} \alpha, \quad \bar{y}'(\lambda a) = k_1, \tag{2.28}$$

where k_1 is a constant to be determined, and $\bar{y}(\lambda b) = \lambda^{\frac{c_2}{c_1}} \beta$. A value for k_1 can be approximated by obtaining an asymptotic solution as $\bar{t} \to \lambda a$.

Starting with an initial guess for λ, this problem is then solved with normal IVP numerical methods. This will 'shoot' a solution. By examining the size of the error between the obtained numerical value, $\bar{y}^*(\lambda b)$, and the actual value, $\bar{y}(\lambda b)$, i.e.

$$\text{error} = \bar{y}(\lambda b) - \bar{y}^*(\lambda b) \tag{2.29}$$

we then iteratively adjust the value of λ until the solution 'shoots' to the correct point and the error between these terms is sufficiently small [16, 20]. Common methods of iterating are through binary searches or by employing the secant method [16].

From this point, the value of λ resulting in a small error can be stored and used in the solution of the second initial value problem.

Initial Value Problem 2:

$$y'' = f(t, y, y'), \quad t \in [a, b], \tag{2.30}$$

where

$$y(a) = \alpha, \quad y'(a) = \lambda^{1-\frac{c_2}{c_1}} k_1, \tag{2.31}$$

where the derivative boundary condition is derived via the transformation (2.26).

When solving this problem, the numerical estimate should satisfy $y^*(b) \approx \beta$, provided the value of λ is reasonably accurate.

2.7.2 *Quasi-linearisation*

The technique of quasi-linearisation is often utilised to solve non-linear two-point boundary value problems [4, 5, 29]. It is a generalisation of the Newton-Raphson method, making use of a Taylor series approximation in order to obtain a linearised version of the original equation [25].

This linearised equation requires some initial guess of the original function in order to be constructed [29], and it is updated at each iteration of the algorithm [5, 25]. Due to the linear nature of the equation to be solved, the numerical solving required is thus much easier than what would have been required to solve the original problem directly [25, 29].

The solutions obtained from iterating the algorithm result in a set of approximations that quadratically and uniformly converge to the original BVP [4, 25]. Proofs relating to the convergence of this method can be found in [5, 29].

An outline of the method, as presented in [29], will be presented below:

Consider a second-order problem as given by (2.22). We may define a function

$$\phi(t, y, y', y'') = y'' - f(t, y, y') = 0, \tag{2.32}$$

and enforce that the n^{th} and $(n+1)^{th}$ iteration approximations of this function vanish,

$$\phi_n = y_n'' - f_n = 0, \tag{2.33}$$

$$\phi_{n+1} = y_{n+1}'' - f_{n+1} = 0. \tag{2.34}$$

However, we can obtain a second-order Taylor series approximation of ϕ_{n+1},

$$\phi_{n+1} = \phi_n + \left(\frac{\partial \phi}{\partial y}\right)_n (y_{n+1} - y_n) + \left(\frac{\partial \phi}{\partial y'}\right)_n (y'_{n+1} - y'_n) + \left(\frac{\partial \phi}{\partial y''}\right)_n (y''_{n+1} - y''_n) = 0. \tag{2.35}$$

Implementing (2.33) and (2.34) and substituting in y''_n, this reduces to

$$y''_{n+1} - \left(\frac{\partial f}{\partial y'}\right)_n y'_{n+1} - \left(\frac{\partial f}{\partial y}\right)_n y_{n+1} = f_n - \left(\frac{\partial f}{\partial y}\right)_n y_n - \left(\frac{\partial f}{\partial y'}\right)_n y'_n, \tag{2.36}$$

where

$$y_{n+1}(a) = \alpha, \qquad y_{n+1}(b) = \beta. \tag{2.37}$$

Equation (2.36) is the linearised approximation to the original problem. By supplying an initial guess of the solution, say $y^{(0)} = f^{(0)}$, this can easily be solved using a number of simple numerical methods to obtain the next approximation of the solution, $y^{(1)}$. Equation (2.36) can then be re-updated with this approximation, and this process can be iterated until convergence.

This technique offers very good accuracy, however it must be noted that for large problems, it can be computationally demanding [4]. It works for most equations; however, some equations or initial guesses to the equations can present convergence issues [29].

MATHEMATICAL MODELS AND ANALYSIS

3

MATHEMATICAL MODEL AND GOVERNING EQUATIONS

In this chapter, a model will be formulated to examine the hydraulic fracturing process when flow inside a fracture is turbulent.

3.1 Problem Model

In this model, we consider a 2-dimensional fracture in a rock mass which has a viscous, incompressible fluid injected into it at sufficiently high pressures such that fracturing of the rock occurs, thus extending the fracture.

The x-axis is positioned along the length of the fracture, half-way along the fracture width. The distance from the x-axis to the fracture boundary is important in this work and will be termed the *half-width*. The z-axis is parallel to the fracture opening and is positioned to coincide with this opening. All quantities in this problem are independent of y. As a result of this, the fluid variables in the problem considered are given by:

$$\begin{aligned} v_x &= v_x(t,x,z), & v_y &= 0, \\ v_z &= v_z(t,x,z), & p &= p(t,x,z). \end{aligned} \tag{3.1}$$

The fracture is defined by the boundaries $z = \pm h(t,x)$, where $x \in [0,\ L(t)]$ and $t \geqslant 0$. The length of the fracture changes with the time elapsed during the hydraulic fracturing procedure and is described by $L(t)$. The fracture boundaries are given by $z = \pm h(t,x)$ and are symmetric about the x-axis. They change according to the position along the crack and over time.

Due to fluid being injected at high pressures into the crack, the rock's material strength and stresses will be overcome and the fracture will extend in both the z-plane and in the positive x-plane. A simplified diagram of the situation being examined is given in Figure 3.1.

3.2 Assumptions

The following assumptions are made within this model:

- *The fluid is viscous and incompressible:*
  Fluids used to hydraulically fracture rock are viscous liquids of some

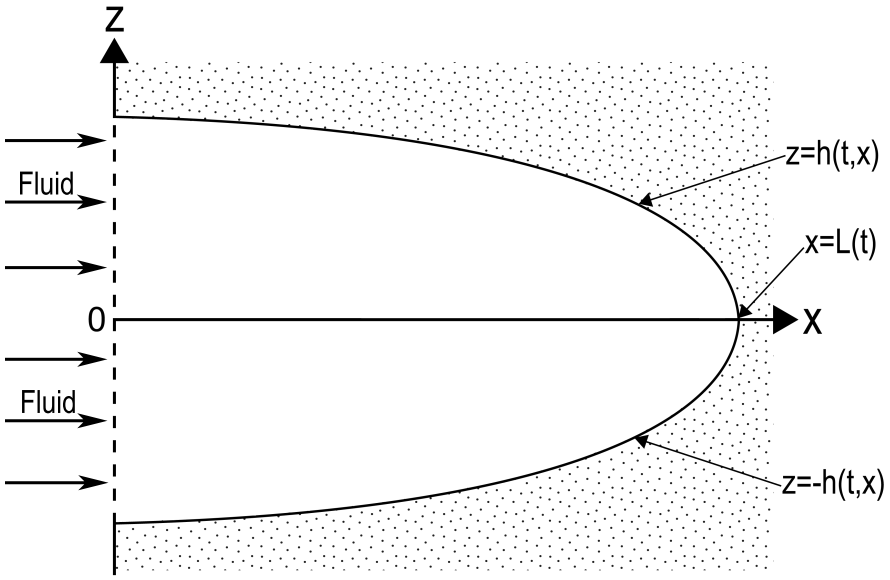


Figure 3.1: A simplified diagram of the two-dimensional fracture being modelled. The fracture is within a rock mass and it is of length $L(t)$ with boundaries $z = \pm h(t,x)$. A viscous, incompressible fluid is injected at high pressures into the fracture at $x = 0$, and the flow of this fluid within the fracture is turbulent. The fracture expands due to the high pressure fluid causing the rock to fail.

kind. The fluid most commonly used in hydraulic fracturing applications is water, mixed with trace amounts of other chemicals that aid the fracturing process [18, 21].

- *The fluid flow is turbulent:*
  Emerman et. al [14] suggest that turbulent fracturing by magma can occur for specific types of magma with relatively small kinematic viscosities. They also suggest that the degree to which the fracture has rough edges can decrease the magnitude of the Reynolds number required for turbulent flow to occur.

  Similarly, in industrial applications, the fluid used is generally water which has a small kinematic viscosity. The fractures also extend far in length during the process [18, 37]. This can create large Reynolds numbers ($Re=\frac{UL}{\nu}$), and due to the high pressures and potential roughness of the fracture, instabilities can arise creating turbulent flow.

- *The body force can be neglected:*
  As a result of the high pressures that the injected fluids are under [18, 21, 23], the effect of the body force on the behaviour of the fluid is minimal.

- *The fracture length is much greater than the width of the fracture opening:*
  With the exception of small scale hydraulic fracturing projects that are

used to test whether an area will be suitable for application of this technique, most hydraulic fracturing creates fractures where the length scale is significantly greater than the width [18, 37].

- *The fracture is symmetric about the x-axis.*
- *The rock is an impermeable medium*

3.3 Equation derivation

Turbulent fluid flow can be considered as a mean flow with random fluctuations imposed on it [12, 26]. As a result, the fluid variables (3.1) can be expressed as:

$$v_i(t,x,z) = \overline{v_i}(x,z) + v_i'(t,x,z), \qquad i = x,\ z, \tag{3.2}$$

$$p(t,x,z) = \overline{p}(x,z) + p'(t,x,z), \tag{3.3}$$

where $\overline{v_i}$ and $\overline{p}$ are the mean flow components of the turbulent flow, and v_i' and p' are the random Gaussian fluctuations, with a mean of zero [26].

The mean flow components are defined by

$$\overline{v_i}(x,z) = \frac{1}{t_f}\int_{t_0}^{t_0+t_f} v_i(t,x,z)\,dt, \qquad i = x,\ z, \tag{3.4}$$

$$\overline{p}(x,z) = \frac{1}{t_f}\int_{t_0}^{t_0+t_f} p(t,x,z)\,dt, \tag{3.5}$$

where the time interval $[t_0, t_f]$ is sufficiently large that these variables are statistically time-independent [12, 26].

As outlined in Section 3.2, the assumption that the fluid is incompressible is made. For an incompressible fluid, the Navier-Stokes equation is

$$\rho\left(\frac{\partial \underline{v}}{\partial t} + (\underline{v}\cdot\underline{\nabla})\underline{v}\right) = -\underline{\nabla}p + \mu\nabla^2\underline{v}, \tag{3.6}$$

and the continuity equation reduces to

$$\underline{\nabla}\cdot\underline{v} = 0. \tag{3.7}$$

3.3.1 *The Continuity Equation*

Consider the continuity equation (3.7). Using the fluid variables (3.2, 3.3), we obtain

$$\frac{\partial \overline{v_x}}{\partial x} + \frac{\partial v_x'}{\partial x} + \frac{\partial \overline{v_z}}{\partial z} + \frac{\partial v_z'}{\partial z} = 0. \tag{3.8}$$

Taking a time average of (3.8) while implementing that the random fluctuations are Gaussian and thus have a zero mean results in

$$\frac{\partial \overline{v_x}}{\partial x} + \frac{\partial \overline{v_z}}{\partial z} = 0. \tag{3.9}$$

Upon substituting (3.9) into (3.7),

$$\frac{\partial v_x'}{\partial x} + \frac{\partial v_z'}{\partial z} = 0. \tag{3.10}$$

Thus, the result is obtained that both the mean flow and the random fluctuation components of the turbulent flow satisfy the continuity equation separately.

3.3.2 *The Navier-Stokes Equation*

We can consider the x- and z-components of the Navier-Stokes equation (3.6) and substitute the turbulent fluid variables (3.2, 3.3) to obtain an equations governing the turbulent fluid flow in this model.

If we consider the x-component of equation (3.6) in conjunction with the fluid variables (3.1), it reduces to

$$\rho\left(\frac{\partial v_x}{\partial t} + v_x\frac{\partial v_x}{\partial x} + v_z\frac{\partial v_x}{\partial z}\right) = -\frac{\partial p}{\partial x} + \mu\left(\frac{\partial^2 v_x}{\partial x^2} + \frac{\partial^2 v_x}{\partial z^2}\right). \tag{3.11}$$

Substituting the expanded components of the turbulent variables (3.2, 3.3) results in

$$\begin{aligned}&\rho\left(\frac{\partial v_x'}{\partial t} + (\overline{v_x} + v_x')\frac{\partial \overline{v_x}}{\partial x} + (\overline{v_x} + v_x')\frac{\partial v_x'}{\partial x} + (\overline{v_z} + v_z')\frac{\partial \overline{v_x}}{\partial z} + (\overline{v_z} + v_z')\frac{\partial v_x'}{\partial z}\right)\\ &= -\frac{\partial \overline{p}}{\partial x} - \frac{\partial p'}{\partial x} + \mu\left(\frac{\partial^2 \overline{v_x}}{\partial x^2} + \frac{\partial^2 v_x'}{\partial x^2} + \frac{\partial^2 \overline{v_x}}{\partial z^2} + \frac{\partial^2 v_x'}{\partial z^2}\right).\end{aligned} \tag{3.12}$$

Taking a time average of this equation yields

$$\rho\left(\overline{v_x}\frac{\partial \overline{v_x}}{\partial x} + \overline{v_x'\frac{\partial v_x'}{\partial x}} + \overline{v_z}\frac{\partial \overline{v_x}}{\partial z} + \overline{v_z'\frac{\partial v_x'}{\partial z}}\right) = -\frac{\partial \overline{p}}{\partial x} + \mu\left(\frac{\partial^2 \overline{v_x}}{\partial x^2} + \frac{\partial^2 \overline{v_x}}{\partial z^2}\right). \tag{3.13}$$

We can re-write the fluctuation product terms as follows:

$$\overline{v_i'\frac{\partial v_x'}{\partial x_i}} = \frac{\partial}{\partial x_i}\overline{(v_i'v_x')} - \overline{v_x'\frac{\partial v_i'}{\partial x_i}}, \qquad i = x,\ z. \tag{3.14}$$

Using this result and the fact that the continuity equation is satisfied by the fluid fluctuations, equation (3.13) becomes

$$\rho\left(\overline{v_x}\frac{\partial \overline{v_x}}{\partial x} + \overline{v_z}\frac{\partial \overline{v_x}}{\partial z} + \frac{\partial}{\partial x}\overline{(v_x'v_x')} + \frac{\partial}{\partial z}\overline{(v_z'v_x')}\right) = -\frac{\partial \overline{p}}{\partial x} + \mu\left(\frac{\partial^2 \overline{v_x}}{\partial x^2} + \frac{\partial^2 \overline{v_x}}{\partial z^2}\right). \tag{3.15}$$

We can also re-write the viscous terms as follows:

$$\frac{\partial^2 \overline{v_x}}{\partial x^2} + \frac{\partial^2 \overline{v_x}}{\partial z^2} = \frac{\partial}{\partial x}\left(\frac{\partial \overline{v_x}}{\partial x} + \frac{\partial \overline{v_x}}{\partial x}\right) + \frac{\partial}{\partial z}\left(\frac{\partial \overline{v_x}}{\partial z} + \frac{\partial \overline{v_z}}{\partial x}\right), \tag{3.16}$$

also as a result of the continuity equation being satisfied by the mean flow.

Thus, equation (3.15) is reduced to

$$\begin{aligned} &\rho\left(\overline{v_x}\frac{\partial \overline{v_x}}{\partial x} + \overline{v_z}\frac{\partial \overline{v_x}}{\partial z} + \frac{\partial}{\partial x}\overline{(v_x' v_x')} + \frac{\partial}{\partial z}\overline{(v_z' v_x')}\right) \\ &= -\frac{\partial \overline{p}}{\partial x} + \mu\left(\frac{\partial}{\partial x}\left(\frac{\partial \overline{v_x}}{\partial x} + \frac{\partial \overline{v_x}}{\partial x}\right) + \frac{\partial}{\partial z}\left(\frac{\partial \overline{v_x}}{\partial z} + \frac{\partial \overline{v_z}}{\partial x}\right)\right). \end{aligned} \tag{3.17}$$

This can be re-written as follows:

$$\begin{aligned} &\rho\left(\overline{v_x}\frac{\partial \overline{v_x}}{\partial x} + \overline{v_z}\frac{\partial \overline{v_x}}{\partial z}\right) \\ &= \frac{\partial}{\partial x}\left(-\overline{p} + \mu\left(\frac{\partial \overline{v_x}}{\partial x} + \frac{\partial \overline{v_x}}{\partial x}\right) - \rho\overline{(v_x' v_x')}\right) \\ &+ \frac{\partial}{\partial z}\left(\mu\left(\frac{\partial \overline{v_z}}{\partial x} + \frac{\partial \overline{v_x}}{\partial z}\right) - \rho\overline{(v_z' v_x')}\right). \end{aligned} \tag{3.18}$$

Similarly, the z-component of (3.6) can be expressed as follows:

$$\begin{aligned} &\rho\left(\overline{v_x}\frac{\partial \overline{v_z}}{\partial x} + \overline{v_z}\frac{\partial \overline{v_z}}{\partial z}\right) \\ &= \frac{\partial}{\partial x}\left(\mu\left(\frac{\partial \overline{v_x}}{\partial z} + \frac{\partial \overline{v_z}}{\partial x}\right) - \rho\overline{(v_x' v_z')}\right) \\ &+ \frac{\partial}{\partial z}\left(-\overline{p} + \mu\left(\frac{\partial \overline{v_z}}{\partial z} + \frac{\partial \overline{v_z}}{\partial z}\right) - \rho\overline{(v_z' v_z')}\right). \end{aligned} \tag{3.19}$$

The terms of the form $-\overline{\rho(v_i' v_k')}$ are termed the Reynolds stresses. They are symmetric and describe the momentum flux of the random fluctuations and describe how these fluctuations will affect and interact with the mean flow [12, 26, 34].

It can be noted that we now have three equations (3.9, 3.18, 3.19) with six unknown quantities to solve within the system of governing equations. Thus, we need to relate some of the variables present to one another in order to close the system.

3.3.3 *Boussinesq's Closure Model*

Boussinesq proposed the following relation to close the system of equations [6, 39]:

$$-\overline{v_i' v_k'} = \nu_T \left(\frac{\partial \overline{v_i}}{\partial x_k} + \frac{\partial \overline{v_k}}{\partial x_i} \right). \tag{3.20}$$

Here, ν_T is kinematic eddy viscosity. The effective kinematic viscosity due to the turbulent flow is $\nu + \nu_T$.

As a result of this relation, the equations (3.9, 3.18, 3.19) can be re-written as

$$\begin{aligned} &\overline{v_x}\frac{\partial \overline{v_x}}{\partial x} + \overline{v_z}\frac{\partial \overline{v_x}}{\partial z} \\ &= \frac{\partial}{\partial x}\left(-\frac{1}{\rho}\overline{p} + 2(\nu + \nu_T)\frac{\partial \overline{v_x}}{\partial x} \right) \\ &+ \frac{\partial}{\partial z}\left((\nu + \nu_T)\left(\frac{\partial \overline{v_z}}{\partial x} + \frac{\partial \overline{v_x}}{\partial z} \right) \right), \end{aligned} \tag{3.21}$$

$$\begin{aligned} &\overline{v_x}\frac{\partial \overline{v_z}}{\partial x} + \overline{v_z}\frac{\partial \overline{v_z}}{\partial z} \\ &= \frac{\partial}{\partial x}\left((\nu + \nu_T)\left(\frac{\partial \overline{v_x}}{\partial z} + \frac{\partial \overline{v_z}}{\partial x} \right) \right) \\ &+ \frac{\partial}{\partial z}\left(-\frac{1}{\rho}\overline{p} + 2(\nu + \nu_T)\frac{\partial \overline{v_z}}{\partial z} \right), \end{aligned} \tag{3.22}$$

$$\frac{\partial \overline{v_x}}{\partial x} + \frac{\partial \overline{v_z}}{\partial z} = 0. \tag{3.23}$$

Unlike the kinematic viscosity, ν, which is a property of the fluid, the kinematic eddy viscosity, ν_T, is a property of the flow. It can depend on the spatial coordinates, the mean fluid velocity components, and on the spatial gradients of the mean flow velocity components.

3.3.4 *Implementation of the lubrication approximation*

We can take advantage of the geometry present in this problem, whereby the length scale is considerably larger than the width scale. As a result of this, the thin film approximation

$$\frac{H}{L} << 1, \qquad Re\left(\frac{H}{L}\right)^2 << 1, \tag{3.24}$$

Characteristic quantity	Description
L	The initial fracture length at time $t = 0$.
H	The half-width at time $t = 0$ and at $x = 0$, that is, one half of the initial fracture width.
U	The characteristic fluid velocity in the x-direction
V	The characteristic fluid velocity in the z-direction
P	The characteristic fluid pressure
E_0	The characteristic effective viscosity

Table 3.1: The characteristic quanitites selected in this problem.

can be implemented.

The characteristic quantities selected from this problem are presented in Table 3.1. A diagram illustrating the characteristic lengths in the problem is given in Figure 3.2.

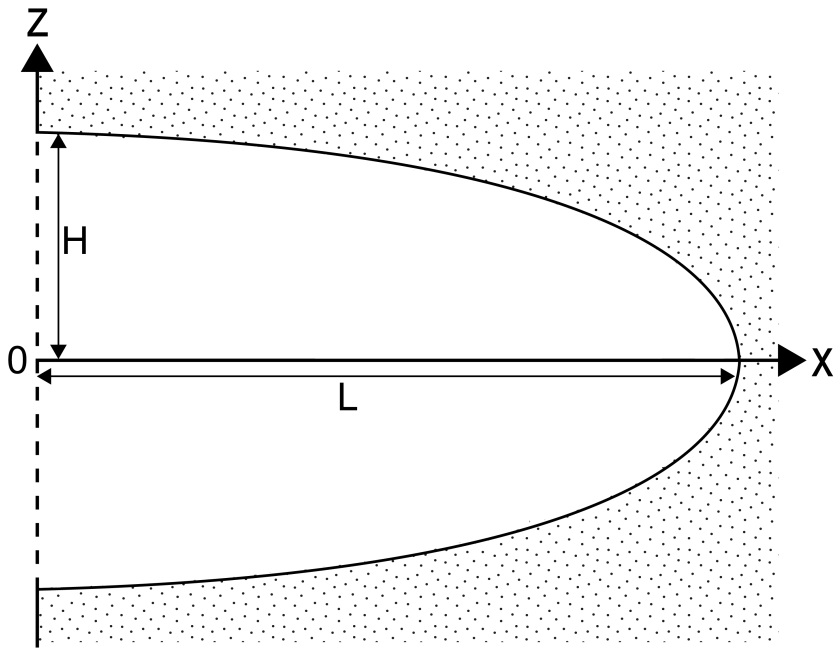


Figure 3.2: A simple diagram of the two-dimensional fracture at $t = 0$ illustrating the characteristic lengths L and H within the hydraulic fracture problem, whereby $H << L$.

The quantities V and P can be determined in terms of the other characteristic quantities.

By using the continuity equation (3.9), it can be seen that

$$\frac{U}{L} \sim \frac{V}{H}, \tag{3.25}$$

which results in

$$V \sim \frac{UH}{L}. \tag{3.26}$$

Similarly, by examining the x-component of the Navier-Stokes equation (3.21) and balancing the pressure gradient term with the most dominating term,

$$\frac{1}{\rho}\frac{\partial \overline{p}}{\partial x} \sim \frac{\partial}{\partial z}(\nu + \nu_T)\frac{\partial \overline{v_x}}{\partial z}, \tag{3.27}$$

we see

$$\frac{1}{\rho}\frac{P}{L} \sim \frac{1}{H}E_0\frac{U}{H}, \tag{3.28}$$

and thus,

$$P \sim \frac{\rho E_0 U L}{H^2}. \tag{3.29}$$

The characteristic velocity U will be specified later.

We can now define the following dimensionless variables:

$$x^* = \frac{x}{L}, \qquad z^* = \frac{z}{H}, \tag{3.30}$$

$$\bar{v_x^*} = \frac{\overline{v_x}}{U}, \qquad \bar{v_z^*} = \frac{L\overline{v_z}}{UH}, \tag{3.31}$$

$$\bar{p^*} = \frac{H^2\overline{p}}{\rho E_0 L U}, \qquad E^* = \frac{\nu + \nu_T}{E_0}. \tag{3.32}$$

Substituting these variables into equation (3.21) yields

$$\frac{U^2}{L}\left(\bar{v_x^*}\frac{\partial \bar{v_x^*}}{\partial x^*} + \bar{v_z^*}\frac{\partial \bar{v_z^*}}{\partial z^*}\right) = -\frac{E_0 U}{H^2}\frac{\partial \overline{p}^*}{\partial x^*} + 2\frac{E_0 U}{L^2}\frac{\partial}{\partial x^*}\left(E^*\frac{\partial \bar{v_x^*}}{\partial x^*}\right) + \frac{E_0 U}{H^2}\frac{\partial}{\partial z^*}\left(E^*\left(\frac{\partial \bar{v_x^*}}{\partial z^*} + \left(\frac{H}{L}\right)^2\frac{\partial \bar{v_z^*}}{\partial x^*}\right)\right). \tag{3.33}$$

Multiplying by $\frac{H^2}{E_0 U}$ and substituting the Reynolds number $Re = \frac{UL}{E_0}$ results in

$$Re\left(\frac{H}{L}\right)^2\left(\bar{v_x^*}\frac{\partial \bar{v_x^*}}{\partial x^*} + \bar{v_z^*}\frac{\partial \bar{v_z^*}}{\partial z^*}\right) = -\frac{\partial \overline{p}^*}{\partial x^*} + 2\frac{H^2}{L^2}\frac{\partial}{\partial x^*}\left(E^*\frac{\partial \bar{v_x^*}}{\partial x^*}\right) + \frac{\partial}{\partial z^*}\left(E^*\left(\frac{\partial \bar{v_x^*}}{\partial z^*} + \left(\frac{H}{L}\right)^2\frac{\partial \bar{v_z^*}}{\partial x^*}\right)\right). \tag{3.34}$$

However, as approximation (3.24) holds, we can neglect all terms of $\mathcal{O}\left(\frac{H}{L}\right)$, $\mathcal{O}\left(\mathrm{Re}\frac{H^2}{L^2}\right)$ or smaller.

Suppressing the stars for notational convenience, we thus obtain the equation

$$\frac{\partial \overline{p}}{\partial x} = \frac{\partial}{\partial z}\left(E\frac{\partial \overline{v_x}}{\partial z}\right). \tag{3.35}$$

Similarly, substituting these dimensionless variables into equation (3.22) gives

$$\begin{aligned}\frac{U^2 H}{L^2}\left(\bar{v}_x^*\frac{\partial \bar{v}_z^*}{\partial x^*} + \bar{v}_z^*\frac{\partial \bar{v}_z^*}{\partial z^*}\right) = -\frac{E_0 U L}{H^3}\frac{\partial \overline{p}^*}{\partial z^*} + 2\frac{E_0 U}{LH}\frac{\partial}{\partial z^*}\left(E^*\frac{\partial \bar{v}_z^*}{\partial z^*}\right)\\ + \frac{E_0 U}{LH}\frac{\partial}{\partial x^*}\left(E^*\left(\frac{\partial \bar{v}_x^*}{\partial z^*} + \left(\frac{H}{L}\right)^2\frac{\partial \bar{v}_z^*}{\partial x^*}\right)\right).\end{aligned} \tag{3.36}$$

Multiplying by $\frac{H^3}{E_0 U L}$ and substituting the Reynolds number $\mathrm{Re}=\frac{UL}{E_0}$ yields

$$\begin{aligned}\mathrm{Re}\left(\frac{H}{L}\right)^4\left(\bar{v}_x^*\frac{\partial \bar{v}_z^*}{\partial x^*} + \bar{v}_z^*\frac{\partial \bar{v}_z^*}{\partial z^*}\right) = -\frac{\partial \overline{p}^*}{\partial z^*} + 2\left(\frac{H}{L}\right)^2\frac{\partial}{\partial z^*}\left(E^*\frac{\partial \bar{v}_z^*}{\partial z^*}\right)\\ + \left(\frac{H}{L}\right)^2\frac{\partial}{\partial x^*}\left(E^*\left(\frac{\partial \bar{v}_x^*}{\partial z^*} + \left(\frac{H}{L}\right)^2\frac{\partial \bar{v}_z^*}{\partial x^*}\right)\right).\end{aligned} \tag{3.37}$$

Once again, due to approximation (3.24), we can neglect all terms of $\mathcal{O}\left(\frac{H}{L}\right)$, $\mathcal{O}\left(\mathrm{Re}\left(\frac{H}{L}\right)^2\right)$ or smaller.

Suppressing the stars for notational convenience, we thus obtain the equation

$$\frac{\partial \overline{p}}{\partial z} = 0. \tag{3.38}$$

It is trivial to verify that the continuity equation under this transformation, with the stars suppressed, yields

$$\frac{\partial \overline{v_x}}{\partial x} + \frac{\partial \overline{v_z}}{\partial z} = 0. \tag{3.39}$$

Thus, we have equations (3.35), (3.38), (3.39) governing the mean fluid flow within the fracture and these can be used to solve for the variables $\overline{v_x}(x,z)$, $\overline{v_z}(x,z)$, $\overline{p}(x,z)$.

As the problem is symmetric, we need only examine the upper half of the fracture, given by $0 \leqslant z \leqslant h(t,x)$.

3.3.5 *Prandtl's mixing length hypothesis*

Prandtl's mixing length hypothesis is a popular way of closing the turbulent fluid flow equations, by creating a relationship between the eddy viscosity ν_T and the mean fluid velocity [36].

In order to formulate this relation, Prandtl assumed that a fluid lump has a certain length, $l(x)$, over which it remains intact before losing momentum and dissipating [13, 36, 39]. Concise derivations of the mixing length hypothesis are given in [36, 39].

Prandtl's mixing length hypothesis is given by [3, 12, 26],

$$\nu_T = l^2(x) \left| \frac{\partial \overline{v_x}}{\partial z} \right|, \tag{3.40}$$

where the function $l(x)$ is called Prandtl's mixing length. It can now be used to close the system of equations. As we will be working in the upper half of the fracture, we see that

$$\nu_T = -l^2(x) \frac{\partial \overline{v_x}}{\partial z}, \tag{3.41}$$

as $\overline{v_x}(x, z)$ is a decreasing function for $0 \leqslant z \leqslant h(t, x)$.

While Prandtl's mixing length hypothesis has been criticized for being a simplification of what actually happens in turbulent flow, it still captures the broader behaviour of the mean fluid flow. It is also very important in practical engineering as it is still one of the best means of closing the turbulent flow equations while still keeping calculations practical, and the level of detail lost low [13].

3.3.6 *Boundary and initial conditions*

The following boundary conditions for the upper half of the fracture are applicable to the problem:

- *No-slip condition at the boundary:*

  Due to the fluid being viscous, the fluid will stick to the boundary $z = h(t, x)$. Thus

  $$v_x(t, x, h(t, x)) = 0. \tag{3.42}$$

  Upon taking a time average of the mean flow and random fluctuation components of this variable,

  $$\overline{v_x}(x, h(t, x)) = 0. \tag{3.43}$$

- *Mean fluid velocity in the x-direction is maximal at $z = 0$:*

The x-component of the mean fluid velocity has its maximum value for a given x at $z = 0$, corresponding to an extremum there. Thus,

$$\frac{\partial \overline{v_x}}{\partial z}(x, 0) = 0. \tag{3.44}$$

- *The z-component of the mean fluid velocity at the boundary must equal the velocity of the boundary:*

  This condition can be given mathematically as

  $$\overline{v_z}(t, x, h(t, x)) = \frac{Dh}{Dt}, \tag{3.45}$$

  where $\frac{D}{Dt}$ is the time change following the mean flow.

  Expanding this results in

  $$\overline{v_z}(x, h(t, x)) = \frac{Dh}{Dt} = \frac{\partial h}{\partial t} + \overline{v_x}(x, h(t, x))\frac{\partial h}{\partial x}. \tag{3.46}$$

  Using the no-slip boundary condition (3.43), this is simply

  $$\overline{v_z}(x, h(t, x)) = \frac{\partial h}{\partial t}. \tag{3.47}$$

- *No mean velocity component in the z-direction at $z = 0$:*

  The mean flow is symmetric about $z = 0$. As a result,

  $$\overline{v_z}(x, 0) = 0. \tag{3.48}$$

- *The fracture half-width vanishes at the fracture tip:*

  For all time t,

  $$h(t, L(t)) = 0, \tag{3.49}$$

  where $L(t)$ is the length of the fracture at time t.

The following initial conditions are also imposed on the model:

- *The fracture boundary has an initial profile:*

  There is a function $h_0(x)$ that describes the fracture boundary's initial shape. Thus,

  $$h(0, x) = h_0(x). \tag{3.50}$$

  It may not be possible to satisfy this condition for arbitrary $h_0(x)$ by a similarity solution.

- *Initially the dimensionless half-width at the fracture entry has a value of 1:*

  Thus,

  $$h(0, 0) = 1. \tag{3.51}$$

- *Initially, the dimensionless fracture length is 1:*

  Thus,

$$L(0) = 1. \tag{3.52}$$

3.3.7 *Final equation*

As a result of equation (3.38), we see $\overline{p} = \overline{p}(x)$.

We now take the continuity equation (3.39) and integrate it across the fracture half-width,

$$\int_0^{h(t,x)} \frac{\partial \overline{v_x}}{\partial x} dz + \overline{v_z}(x, h(t,x)) - \overline{v_z}(x, 0) = 0. \tag{3.53}$$

Using the boundary conditions (3.47) and (3.48), this becomes

$$\frac{\partial h}{\partial t} + \int_0^{h(t,x)} \frac{\partial \overline{v_x}}{\partial x} dz = 0. \tag{3.54}$$

We can make use of the formula for differentiation under an integral sign for the term [19] below,

$$\frac{d}{dx} \int_{\phi_1(x)}^{\phi_2(x)} f(x,z)dz = \int_{\phi_1(x)}^{\phi_2(x)} \frac{\partial f}{\partial x}(x,z)dz + f(x,\phi_2(x))\phi_2'(x) - f(x,\phi_1(x))\phi_1'(x). \tag{3.55}$$

Using this in conjunction with the boundary conditions (3.43) and (3.44) results in

$$\int_0^{h(t,x)} \frac{\partial \overline{v_x}}{\partial x} dz = \frac{\partial}{\partial x} \int_0^{h(t,x)} \overline{v_x}(x,z)dz. \tag{3.56}$$

Thus, equation (3.54) becomes:

$$\frac{\partial h}{\partial t} + \frac{\partial}{\partial x} \int_0^{h(t,x)} \overline{v_x}(x,z)dz = 0. \tag{3.57}$$

This equation is in the form of a conservation law. It relates the mean flux of the fluid across the half-width of the fracture at any point to the time rate of change of the half-width at that point.

Now, implementing Prandtl's mixing length hypothesis [3, 12, 26], as well as integrating once, equation (3.35) becomes

$$\frac{1}{E_0}\left(\nu - l(x)^2\frac{\partial\overline{v_x}}{\partial z}\right)\frac{\partial\overline{v_x}}{\partial z} = z\frac{\partial\overline{p}}{\partial x} + A(x), \tag{3.58}$$

where $A(x)$ is an arbitrary function. However, due to boundary condition (3.44), $A(x) = 0$. Thus,

$$l(x)^2\left(\frac{\partial\overline{v_x}}{\partial z}\right)^2 - \nu\frac{\partial\overline{v_x}}{\partial z} + E_0 z\frac{\partial\overline{p}}{\partial x} = 0. \tag{3.59}$$

3.3.7.1 *Equation with fully developed turbulence*

In this subsection, we will continue the governing equation derivation for fully developed turbulence, where the eddy viscosity is significantly larger than the kinematic viscosity.

As a result of the assumption, we note that $\nu << l(x)^2\frac{\partial\overline{v_x}}{\partial z}$ and so we can neglect this term in equation (3.59). While this makes the solution inaccurate near $z \approx 0$, it introduces a very marginal error on the rest of the domain.

Thus, equation (3.59) becomes

$$\left(\frac{\partial\overline{v_x}}{\partial z}\right)^2 = \frac{zE_0}{l(x)^2}\left(-\frac{\partial\overline{p}}{\partial x}\right). \tag{3.60}$$

It can be noted that $\frac{\partial\overline{p}}{\partial x} < 0$, for $0 \leqslant x \leqslant L(t)$. So, the mean pressure decreases as the fluid moves along the fracture.

Taking the negative root (because $\frac{\partial\overline{v_x}}{\partial z} < 0$ for $0 \leqslant z \leqslant h(t,x)$), integrating and using boundary condition (3.43) results in

$$\overline{v_x}(x,z) = \frac{2}{3}\frac{E_0^{\frac{1}{2}}}{l(x)}\left(-\frac{\partial\overline{p}}{\partial x}\right)^{\frac{1}{2}}\left[h^{\frac{3}{2}} - z^{\frac{3}{2}}\right]. \tag{3.61}$$

This expression can be placed into equation (3.57), giving

$$\frac{\partial h}{\partial t} + \frac{2}{5}E_0^{\frac{1}{2}}\frac{\partial}{\partial x}\left[\frac{1}{l(x)}\left(-\frac{\partial\overline{p}}{\partial x}\right)^{\frac{1}{2}}h^{\frac{5}{2}}\right] = 0. \tag{3.62}$$

At this point, we can now consider the Perkins-Kern-Nordgren (PKN) approximation to close the equations. This approximation assumes that the net mean pressure is proportional to the fracture half-width [2, 15, 32, 35, 37]:

$$\overline{p}(t,x) + \sigma_{zz}^{\infty} = \Lambda h(t,x), \tag{3.63}$$

where σ_{zz}^{∞} is the normal stress at infinity, and

$$\Lambda = \frac{E}{(1-\sigma^2)B}, \tag{3.64}$$

where E is Young's modulus of the rock mass, σ is Poisson's ratio of the rock mass, and B is the breadth of the fracture.

Implementing this approximation and letting $K = (E_0\Lambda)^{\frac{1}{2}}$ thus results in the equation that will be used within this research:

$$\frac{\partial h}{\partial t} + \frac{2}{5}K\frac{\partial}{\partial x}\left[\frac{1}{l(x)}h^{\frac{5}{2}}\left(-\frac{\partial h}{\partial x}\right)^{\frac{1}{2}}\right] = 0. \tag{3.65}$$

3.3.7.2 *Equation with light turbulence*

In this subsection, we consider lighter, transitional turbulence where the kinematic viscosity is sufficiently large in comparison to the eddy viscosity so that it cannot be completely neglected. This model may be more appropriate to model turbulent magma flows with larger kinematic viscosities, as suggested by [14].

We resume this derivation from equations (3.57) and (3.59) as no approximations relating to the viscosity had been implemented at this point.

Equation (3.59) may be viewed as a quadratic equation in $\frac{\partial \overline{v_x}}{\partial z}$. The roots of the quadratic equation are

$$\frac{\partial \overline{v_x}}{\partial z} = \frac{\nu \pm \sqrt{\nu^2 + 4l(x)^2 E_0 z\left(-\frac{\partial \overline{p}}{\partial x}\right)}}{2l(x)^2}, \qquad 0 \leqslant z \leqslant h(t,x). \tag{3.66}$$

Since $\frac{\partial \overline{p}}{\partial x} < 0$ and $z \geqslant 0$, the discriminant is positive and both roots are therefore real. Also, since $\frac{\partial \overline{v_x}}{\partial z} < 0$ for $z \geqslant 0$, we take the negative branch of (3.66). We can now make an approximation that ensures the kinematic viscosity is still present in the equation, while resulting in a simpler equation.

Consider the square root term in (3.66). It may be re-written as

$$2l(x)E_0^{\frac{1}{2}}z^{\frac{1}{2}}\left(-\frac{\partial \overline{p}}{\partial x}\right)^{\frac{1}{2}}\left(1 + \frac{\nu^2}{4l(x)^2 E_0 z\left(-\frac{\partial \overline{p}}{\partial x}\right)}\right)^{\frac{1}{2}}. \tag{3.67}$$

By the generalized binomial theorem,

$$(1+x)^{\frac{1}{2}} = 1 + \frac{1}{2}x - \frac{1}{8}x^2 + \frac{1}{16}x^3 - \ldots, \tag{3.68}$$

for any $x \in \mathbb{R}$. Thus, letting

$$x = \frac{\nu^2}{4l(x)^2 E_0 z\left(-\frac{\partial \overline{p}}{\partial x}\right)}, \tag{3.69}$$

the square root term in equation (3.67) can be expanded in the form

$$2l(x)E_0^{\frac{1}{2}}z^{\frac{1}{2}}\left(-\frac{\partial\overline{p}}{\partial x}\right)^{\frac{1}{2}}\left(1+\frac{1}{2}x-\frac{1}{8}x^2+\dots\right). \tag{3.70}$$

Taking a first order approximation results in

$$\begin{aligned}&\left(\nu^2+4l(x)^2E_0z\left(-\frac{\partial\overline{p}}{\partial x}\right)\right)^{\frac{1}{2}}+\mathcal{O}(\nu^2)\\&=2l(x)E_0^{\frac{1}{2}}z^{\frac{1}{2}}\left(-\frac{\partial\overline{p}}{\partial x}\right)^{\frac{1}{2}}+\mathcal{O}(\nu^2),\qquad \nu\to 0,\end{aligned} \tag{3.71}$$

and thus

$$\frac{\partial\overline{v_x}}{\partial z}=\frac{\nu}{2l(x)^2}-\frac{z^{\frac{1}{2}}E_0^{\frac{1}{2}}}{l(x)}\left(-\frac{\partial\overline{p}}{\partial x}\right)^{\frac{1}{2}}+\mathcal{O}(\nu^2),\qquad \nu\to 0. \tag{3.72}$$

Neglecting terms of order ν^2 and integrating (3.72) with respect to z and implementing boundary condition (3.43) results in

$$\overline{v_x}(x,z)=\frac{2}{3}\frac{E_0^{\frac{1}{2}}}{l(x)}\left(-\frac{\partial\overline{p}}{\partial x}\right)^{\frac{1}{2}}\left(h^{\frac{3}{2}}-z^{\frac{3}{2}}\right)+\frac{\nu}{2l(x)^2}(z-h). \tag{3.73}$$

Substituting equation (3.73) into equation (3.57) and implementing the PKN approximation (3.63) with $K=(E_0\Lambda)^{\frac{1}{2}}$ results in the equation

$$\frac{\partial h}{\partial t}+\frac{2}{5}K\frac{\partial}{\partial x}\left[\frac{1}{l(x)}h^{\frac{5}{2}}\left(-\frac{\partial h}{\partial x}\right)^{\frac{1}{2}}\right]-\frac{\nu}{4}\frac{\partial}{\partial x}\left[\frac{1}{l(x)^2}h^2\right]=0. \tag{3.74}$$

3.3.7.3 *Characteristic velocity* U

Because of the PKN approximation the characteristic velocity U can now be specified as it gives a second expression for the characteristic pressure P. From (3.63),

$$P=\Lambda H, \tag{3.75}$$

and using the first expression for P, (3.29), we obtain for the characteristic velocity,

$$U=\frac{\Lambda H^3}{\rho E_0 L}. \tag{3.76}$$

3.3.8 *Comparison with other models for a turbulent fracture*

Anthonyrajah et al. [2] made the PKN approximation in the wall shear stress model for a turbulent fluid fracture, introduced by Emerman et al. [14]. Anthonyrajah et al. obtained the general non-linear diffusion equation

$$\frac{\partial h}{\partial t} + D\frac{\partial}{\partial x}\left[\left(-h^3\frac{\partial h}{\partial x}\right)^{\frac{1}{m+2}}\right] = 0. \tag{3.77}$$

For laminar flow, $m = -1$, and

$$\frac{\partial h}{\partial t} + D\frac{\partial}{\partial x}\left(-h^3\frac{\partial h}{\partial x}\right) = 0, \tag{3.78}$$

while $m = -\frac{1}{4}$ corresponds to smooth wall turbulence,

$$\frac{\partial h}{\partial t} + D\frac{\partial}{\partial x}\left(h^{\frac{12}{7}}\left(-\frac{\partial h}{\partial x}\right)^{\frac{4}{7}}\right) = 0. \tag{3.79}$$

Rough wall turbulence is modelled when $m = 0$, giving

$$\frac{\partial h}{\partial t} + D\frac{\partial}{\partial x}\left(h^{\frac{3}{2}}\left(-\frac{\partial h}{\partial x}\right)^{\frac{1}{2}}\right) = 0. \tag{3.80}$$

These equations compare to (3.65) for Prandtl's mixing length model with $\nu = 0$.

4

FULL TURBULENCE MODEL ANALYSIS

In this chapter, equation (3.65) will be considered. Conservation laws will be calculated to give insight into the problem. Lie symmetry analysis will be carried out and a group invariant solution will be obtained. Both analytical and numerical solutions will be found and a thorough discussion of the results will be provided.

4.1 Conservation laws

Consider equation (3.65). It can be expanded in the form

$$\begin{aligned} F(t,x,h,h_t,h_x,h_{xx}) =& h_t - K\left(\frac{2}{5}\frac{l'(x)}{l(x)^2}h^{\frac{5}{2}}(-h_x)^{\frac{1}{2}}\right. \\ &\left. + \frac{1}{l(x)}h^{\frac{3}{2}}(-h_x)^{\frac{3}{2}} + \frac{1}{5}\frac{1}{l(x)}h^{\frac{5}{2}}(-h_x)^{-\frac{1}{2}}h_{xx}\right) = 0. \end{aligned} \tag{4.1}$$

When investigating conservation laws, t, x, h, h_t, h_x, h_{tt}, h_{tx}, h_{xx} ..., and all the partial derivatives of h are treated as independent variables. The suffix notation is then used to denote partial differentiation.

A conserved vector $\underline{\mathbf{T}} = (T^1,\ T^2)$ for equation (3.65) must satisfy the conservation law

$$D_t T^1 + D_x T^2_{|((3.65)=0)} = 0, \tag{4.2}$$

where

$$D_t = \frac{\partial}{\partial t} + h_t\frac{\partial}{\partial h} + h_{tt}\frac{\partial}{\partial h_t} + h_{tx}\frac{\partial}{\partial h_x} + \ldots, \tag{4.3}$$

$$D_x = \frac{\partial}{\partial x} + h_x\frac{\partial}{\partial h} + h_{tx}\frac{\partial}{\partial h_t} + h_{xx}\frac{\partial}{\partial h_x} + \ldots. \tag{4.4}$$

The method of characteristics will be utilized to find the conserved vector of equation (3.65).

Consider a multiplier of the form $\Lambda = \Lambda(t,x,h)$ and conserved vector components $T^i = T^i(t,x,h,h_t,h_x)$, $i = 1,\ 2$. Note that the multiplier Λ should not be confused with the PKN approximation constant also denoted by Λ.

Here, equation (4.2) is equivalent to finding T^1, T^2 and multiplier Λ which satisfy the equation

$$D_t T^1 + D_x T^2 = \Lambda F(t, x, h, h_t, h_x, h_{xx}). \tag{4.5}$$

Equation (4.5) is satisfied by all functions $h(t, x)$ and not only by solutions of the PDE (4.1).

Expanding (4.5) results in

$$\begin{aligned}
&\frac{\partial T^1}{\partial t} + h_t \frac{\partial T^1}{\partial h} + h_{tt} \frac{\partial T^1}{\partial h_t} + h_{tx} \frac{\partial T^1}{\partial h_x} + \frac{\partial T^2}{\partial x} + h_x \frac{\partial T^2}{\partial h} + h_{tx} \frac{\partial T^2}{\partial h_t} \\
&+ h_{xx} \frac{\partial T^2}{\partial h_x} - \Lambda(t, x, h) \left[h_t - K \left(\frac{2l'(x)}{5l(x)^2} h^{\frac{5}{2}} (-h_x)^{\frac{1}{2}} + \frac{1}{l(x)} h^{\frac{3}{2}} (-h_x)^{\frac{3}{2}} \right.\right. \\
&\qquad \left.\left. + \frac{1}{5l(x)} h^{\frac{5}{2}} (-h_x)^{-\frac{1}{2}} h_{xx} \right) \right] = 0.
\end{aligned} \tag{4.6}$$

Since equation (4.6) is satisfied by all functions $h(t, x)$, the partial derivatives of $h(t, x)$ are independent. The coefficients of the partial derivatives in h in (4.6) must therefore separately vanish. Since T^1 and T^2 are not dependent on the second order derivatives of h, equation (4.6) can be separated according to these derivatives. This results in:

$$h_{tt}: \quad \frac{\partial T^1}{\partial h_t} = 0, \tag{4.7}$$

$$h_{tx}: \quad \frac{\partial T^1}{\partial h_x} + \frac{\partial T^2}{\partial h_t} = 0, \tag{4.8}$$

$$h_{xx}: \quad \frac{\partial T^2}{\partial h_x} + \frac{K\Lambda}{5l(x)} h^{\frac{5}{2}} (-h_x)^{-\frac{1}{2}} = 0, \tag{4.9}$$

$$\begin{aligned}
\text{Remainder}: \quad &\frac{\partial T^1}{\partial t} + h_t \frac{\partial T^1}{\partial h} + \frac{\partial T^2}{\partial x} + h_x \frac{\partial T^2}{\partial h} - h_t \Lambda(t, x, h) \\
&+ \frac{K\Lambda}{l(x)} h^{\frac{3}{2}} (-h_x)^{\frac{3}{2}} + \frac{2K\Lambda}{5} \frac{l'(x)}{l(x)^2} h^{\frac{5}{2}} (-h_x)^{\frac{1}{2}} = 0.
\end{aligned} \tag{4.10}$$

Equation (4.9) allows for T^2 to be solved, giving

$$T^2(t, x, h, h_t, h_x) = \frac{2K}{5l(x)} \Lambda h^{\frac{5}{2}} (-h_x)^{\frac{1}{2}} + A(t, x, h, h_t), \tag{4.11}$$

where $A(t, x, h, h_t)$ is a function to be determined.

Similarly, from equations (4.7) and (4.8), it can be seen that

$$T^1(t, x, h, h_x) = -\frac{\partial A}{\partial h_t} h_x + B(t, x, h). \tag{4.12}$$

Since T^1 is independent of h_t, this implies that

$$\frac{\partial A}{\partial h_t} = C(t, x, h). \tag{4.13}$$

This is a differential equation that allows for the determination of the function A as

$$A(t, x, h, h_t) = C(t, x, h)h_t + D(t, x, h). \tag{4.14}$$

Thus,

$$T^1(t, x, h, h_x) = -C(t, x, h)h_x + B(t, x, h), \tag{4.15}$$

$$T^2(t, x, h, h_t, h_x) = \frac{2K}{5l(x)}\Lambda h^{\frac{5}{2}}(-h_x)^{\frac{1}{2}} + C(t, x, h)h_t + D(t, x, h), \tag{4.16}$$

with the remaining terms of the determining equation given by

$$-\frac{\partial C}{\partial t}h_x + \frac{\partial B}{\partial t} + \frac{\partial B}{\partial h}h_t + \frac{2K}{5l(x)}\frac{\partial \Lambda}{\partial x}h^{\frac{5}{2}}(-h_x)^{\frac{1}{2}} + \frac{\partial C}{\partial x}h_t + \frac{\partial D}{\partial x}$$

$$-\frac{2K}{5l(x)}\frac{\partial \Lambda}{\partial h}h^{\frac{5}{2}}(-h_x)^{\frac{3}{2}} + \frac{\partial D}{\partial h}h_x - h_t\Lambda = 0. \tag{4.17}$$

The variables h_t and h_x are explicit in this equation, and thus we separate by those powers:

$$h_x: \qquad \frac{\partial D}{\partial h} - \frac{\partial C}{\partial t} = 0, \tag{4.18}$$

$$(-h_x)^{\frac{3}{2}}: \qquad -\frac{2K}{5l(x)}\frac{\partial \Lambda}{\partial h}h^{\frac{5}{2}} = 0, \tag{4.19}$$

$$(-h_x)^{\frac{1}{2}}: \qquad \frac{2K}{5l(x)}\frac{\partial \Lambda}{\partial x}h^{\frac{5}{2}} = 0, \tag{4.20}$$

$$h_t: \qquad \frac{\partial B}{\partial h} + \frac{\partial C}{\partial x} - \Lambda = 0, \tag{4.21}$$

$$1: \qquad \frac{\partial B}{\partial t} + \frac{\partial D}{\partial x} = 0. \tag{4.22}$$

From equations (4.19) and (4.20), it can be seen that $\Lambda = \Lambda(t)$ only. The equations reduce to:

$$h_x: \qquad \frac{\partial D}{\partial h} - \frac{\partial C}{\partial t} = 0, \tag{4.23}$$

$$h_t: \qquad \Lambda(t) = \frac{\partial B}{\partial h} + \frac{\partial C}{\partial x}, \tag{4.24}$$

$$1: \qquad \frac{\partial B}{\partial t} + \frac{\partial D}{\partial x} = 0. \tag{4.25}$$

Differentiating equation (4.23) with respect to x and differentiating equation (4.25) by h results in

$$\frac{\partial^2 D}{\partial x \partial h} - \frac{\partial^2 C}{\partial t \partial x} = 0, \tag{4.26}$$

and

$$\frac{\partial^2 D}{\partial x \partial h} + \frac{\partial^2 B}{\partial t \partial h} = 0, \tag{4.27}$$

respectively.

Subtracting equation (4.27) from (4.26) results in

$$\frac{\partial^2 B}{\partial t \partial h} + \frac{\partial^2 C}{\partial t \partial x} = 0. \tag{4.28}$$

Differentiating equation (4.21) with respect to t gives

$$\frac{\partial^2 B}{\partial t \partial h} + \frac{\partial^2 C}{\partial t \partial x} = \Lambda'(t). \tag{4.29}$$

Thus, it can be concluded that $\Lambda'(t) = 0$ and thus $\Lambda = c_1$, where c_1 is a constant. This simplifies the components of the conserved vector to:

$$T^1(t, x, h, h_x) = -C(t, x, h)h_x + B(t, x, h), \tag{4.30}$$

$$T^2(t, x, h, h_t, h_x) = \frac{2K}{5l(x)} c_1 h^{\frac{5}{2}} (-h_x)^{\frac{1}{2}} + C(t, x, h)h_t + D(t, x, h), \tag{4.31}$$

where

$$\frac{\partial D}{\partial h} - \frac{\partial C}{\partial t} = 0, \tag{4.32}$$

$$c_1 = \frac{\partial B}{\partial h} + \frac{\partial C}{\partial x}, \tag{4.33}$$

$$\frac{\partial B}{\partial t} + \frac{\partial D}{\partial x} = 0. \tag{4.34}$$

From these equations, we can solve for $B(t, x, h)$ and $D(t, x, h)$ to obtain

$$B(t, x, h) = c_1 h + E(t, x) - \frac{\partial}{\partial x} F(t, x, h), \tag{4.35}$$

$$D(t, x, h) = \frac{\partial}{\partial t} F(t, x, h) + G(t, x), \tag{4.36}$$

where

$$F(t, x, h) = \int^{h} C(t, x, \bar{h}) d\bar{h}. \tag{4.37}$$

It can easily be verified that the conserved vector is thus given by

$$T^1(t,x,h,h_x) = c_1 h - C(t,x,h)h_x + E(t,x) - \frac{\partial F(t,x,h)}{\partial x}, \tag{4.38}$$

$$T^2(t,x,h,h_t,h_x) = \frac{2K}{5l(x)} c_1 h^{\frac{5}{2}} (-h_x)^{\frac{1}{2}} + C(t,x,h)h_t + \frac{\partial F(t,x,h)}{\partial t} + G(t,x), \tag{4.39}$$

provided that

$$\frac{\partial E}{\partial t} + \frac{\partial G}{\partial x} = 0. \tag{4.40}$$

The components of (4.38) and (4.39) are of the form

$$T^1(t,x,h,h_x) = c_1 h + T^1_*(t,x,h,h_x), \tag{4.41}$$

$$T^2(t,x,h,h_t,h_x) = c_1 \frac{2K}{5l(x)} h^{\frac{5}{2}} (-h_x)^{\frac{1}{2}} + T^2_*(t,x,h,h_t), \tag{4.42}$$

where

$$T^1_*(t,x,h,h_x) = -C(t,x,h)h_x + E(t,x) - \frac{\partial F}{\partial x}(t,x,h), \tag{4.43}$$

$$T^2_*(t,x,h,h_t) = C(t,x,h)h_t + \frac{\partial F}{\partial t}(t,x,h) + G(t,x). \tag{4.44}$$

But, it can be verified that

$$D_1 T^1_* + D_2 T^2_* \equiv 0, \tag{4.45}$$

without using the partial differential equation (4.1). Thus, $\underline{\mathbf{T}}_* = (T^1_*, T^2_*)$ is a trivial conserved vector and we can set

$$T^1_* = 0, \qquad T^2_* = 0. \tag{4.46}$$

Thus, (4.41) and (4.42) reduce to

$$T^1(t,x,h,h_x) = c_1 h \tag{4.47}$$

$$T^2(t,x,h,h_t,h_x) = c_1 \frac{2K}{5l(x)} h^{\frac{5}{2}} (-h_x)^{\frac{1}{2}}, \tag{4.48}$$

which is the elementary conserved vector. Thus with a multiplier of the form $\Lambda(t,x,h)$ and a conserved vector $T^i = T^i(t,x,h,h_t,h_x)$, the only conserved vector is the elementary conserved vector.

4.2 Lie point symmetries and group invariant solution

We derive the Lie point symmetries of equation (3.65) in order to obtain a group invariant solution of the equation. The full calculation of the Lie point symmetries is presented in Appendix A.1. It yields the symmetry generator

$$X = (c_1 t + c_2)\frac{\partial}{\partial t} + (c_3 x + c_4)\frac{\partial}{\partial x} + c_5 h\frac{\partial}{\partial h}, \tag{4.49}$$

where the mixing length takes the form

$$l(x) = l_0 \left(c_3 x + c_4\right)^{2\frac{c_5}{c_3} + \frac{c_1}{c_3} - \frac{3}{2}}, \tag{4.50}$$

where l_0 is a constant.

Now, $h(t,x) = \psi(t,x)$ is a group invariant solution of equation (3.65) provided

$$X\left(h(t,x) - \psi(t,x)\right)_{|_{h(t,x)=\psi(t,x)}} = 0. \tag{4.51}$$

This results in the partial differential equation

$$(c_1 t + c_2)\frac{\partial \psi}{\partial t} + (c_3 x + c_4)\frac{\partial \psi}{\partial x} = c_5 \psi. \tag{4.52}$$

We first consider the general case in which $c_1 \neq 0$, $c_2 \neq 0$, $c_3 \neq 0$, $c_4 \neq 0$ and $c_5 \neq 0$. We will choose $c_4 = 0$ during the analysis. Later, we will consider the special case in which only c_2 and c_4 are non-zero.

The differential equations of the characteristic curves are

$$\frac{dt}{c_1 t + c_2} = \frac{dx}{c_3 x + c_4} = \frac{d\psi}{c_5 \psi}. \tag{4.53}$$

Equating the first two expressions

$$\frac{dt}{c_1 t + c_2} = \frac{dx}{c_3 x + c_4}, \tag{4.54}$$

and solving results in the invariant

$$I_1 = \frac{c_3 x + c_4}{(c_1 t + c_2)^{\frac{c_3}{c_1}}}. \tag{4.55}$$

Similarly, equating the first and last expressions

$$\frac{dt}{c_1 t + c_2} = \frac{d\psi}{c_5 \psi}, \tag{4.56}$$

and solving results in the invariant

$$I_2 = \frac{\psi(t,x)}{(c_1 t + c_2)^{\frac{c_5}{c_1}}}. \tag{4.57}$$

A group invariant solution of the PDE (4.52) for ψ is of the form $I_2 = F(I_1)$ [7, 24]. Thus, using this solution form and remembering that $h(t,x) = \psi(t,x)$, we obtain

$$h(t,x) = (c_1 t + c_2)^{\frac{c_5}{c_1}} F(\gamma), \tag{4.58}$$

where

$$\gamma = \frac{c_3 x + c_4}{(c_1 t + c_2)^{\frac{c_3}{c_1}}}. \tag{4.59}$$

We substitute the group invariant solution into PDE (3.65). It reduces the PDE to an ODE, given by

$$\frac{2K}{5l_0} c_3^{\frac{3}{2}} \frac{d}{d\gamma}\left[\gamma^{\frac{3}{2}-2\frac{c_5}{c_3}-\frac{c_1}{c_3}} F(\gamma)^{\frac{5}{2}} \left(-\frac{dF}{d\gamma}\right)^{\frac{1}{2}}\right] - c_3 \frac{d}{d\gamma}\left(\gamma F(\gamma)\right) + (c_3 + c_5) F(\gamma) = 0. \tag{4.60}$$

Now, the property that $\gamma(t,0) = 0$ is desired. To achieve this result, $c_4 = 0$. As the ODE (4.60) is independent of this parameter, we can implement $c_4 = 0$ without affecting the obtained ODE.

Using the group invariant solution, expressions for the length of the fracture, $L(t)$, and the volume of a fracture, $V(t)$, at a given time can be obtained.

We make use of the boundary condition $h(t, L(t)) = 0$. Implementing this boundary condition results in

$$F\left(\frac{c_3 L(t)}{(c_1 t + c_2)^{\frac{c_3}{c_1}}}\right) = 0. \tag{4.61}$$

If we define

$$g(t) = \frac{c_3 L(t)}{(c_1 t + c_2)^{\frac{c_3}{c_1}}}, \tag{4.62}$$

equation (4.61) can be rewritten as

$$F(g(t)) = 0. \tag{4.63}$$

Differentiating (4.63) with respect to t gives

$$\frac{dF}{dg}\frac{dg}{dt} = 0. \tag{4.64}$$

But, $F(\gamma)$ is not a constant function of γ since the half-width in (4.58) depends on x, and therefore $\frac{dF}{dg} \neq 0$. As a result, (4.64) shows that $g(t) = c^*$, where c^* is a constant. We also have the condition that $L(0) = 1$, and so the fracture length can be expressed by

$$L(t) = \left(1 + \frac{c_1}{c_2} t\right)^{\frac{c_3}{c_1}}. \tag{4.65}$$

As a result of this, the boundary condition $h(t, L(t)) = 0$ given by (4.61) reduces to

$$F\left(c_3 \cdot c_2^{-\frac{c_3}{c_1}}\right) = 0. \tag{4.66}$$

The total volume of the fracture per unit breadth is

$$V(t) = 2\int_0^{L(t)} h(t,x)\,dx, \tag{4.67}$$

which becomes

$$V(t) = V_0\left(1 + \frac{c_1}{c_2}t\right)^{\frac{c_5}{c_1}+\frac{c_3}{c_1}}, \tag{4.68}$$

where

$$V_0 = \frac{2}{c_3}c_2^{\frac{c_5}{c_1}+\frac{c_3}{c_1}}\int_0^{c_3\cdot c_2^{-\frac{c_3}{c_1}}} F(\gamma)\,d\gamma. \tag{4.69}$$

The final expression that can be obtained is the balance law. Since the rate of change of the volume of the fracture with time must equal the rate of fluid flow into the fracture at the entry, the expression

$$\frac{dV}{dt} = 2\int_0^{h(t,0)} \overline{v_x}(0,z)\,dz, \tag{4.70}$$

is obtained. Differentiating (4.68) with respect to t, using (3.61) for $\overline{v_x}(0,z)$ with the PKN approximation (3.63), and substituting $h(t,0)$ given by (4.58), the balance law (4.70) becomes

$$2\left(1+\frac{c_5}{c_3}\right)\int_0^{c_3\cdot c_2^{-\frac{c_3}{c_1}}} F(\gamma)\,d\gamma = \frac{4}{5}\frac{K}{l_0}c_3^{\frac{1}{2}}F(0)^{\frac{5}{2}}\left(-\frac{dF}{d\gamma}(0)\right)^{\frac{1}{2}}\gamma_{|_{\gamma=0}}^{-\left(2\frac{c_5}{c_3}+\frac{c_1}{c_3}-\frac{3}{2}\right)}. \tag{4.71}$$

Since the left hand side of (4.71) is finite, the right hand side of (4.71) must also be finite. Since the half-width and the slope of the half-width at the fracture entry are finite, it follows that $F(0)$ and $\frac{dF(0)}{d\gamma}$ are finite as well. Thus, the right hand side of (4.71) is finite provided

$$-\frac{3}{2} + 2\frac{c_5}{c_3} + \frac{c_1}{c_3} \leqslant 0. \tag{4.72}$$

When

$$-\frac{3}{2}+2\frac{c_5}{c_3}+\frac{c_1}{c_3}<0, \tag{4.73}$$

we observe that the right hand side of (4.71) vanishes, and so the left hand side must vanish resulting in

$$\frac{c_5}{c_3}=-1. \tag{4.74}$$

When (4.74) is satisfied, (4.68) shows that the total volume of the fracture per unit breadth remains constant as the fracture evolves.

Further information on the ratio of the constants is obtained from the mixing length (4.50) which, when $c_4=0$, reduces to

$$l(x)=l_0 x^{2\frac{c_5}{c_3}+\frac{c_1}{c_3}-\frac{3}{2}}. \tag{4.75}$$

For the mixing length to remain finite as $x\to 0$, it is necessary that

$$-\frac{3}{2}+2\frac{c_5}{c_3}+\frac{c_1}{c_3}\geqslant 0. \tag{4.76}$$

Combining (4.72) and (4.76) results in

$$-\frac{3}{2}+2\frac{c_5}{c_3}+\frac{c_1}{c_3}=0, \tag{4.77}$$

giving in a constant mixing length and the condition

$$c_5=\frac{3}{4}c_3-\frac{1}{2}c_1. \tag{4.78}$$

4.2.1 *Constant Mixing Length*

By implementing (4.78), we see that

$$\xi^1=c_1t+c_2,\quad \xi^2=c_3x+c_4,\quad \eta=\left(\frac{3}{4}c_3-\frac{1}{2}c_1\right)h, \tag{4.79}$$

where

$$l(x)=l_0. \tag{4.80}$$

We define $\alpha=\frac{c_3}{c_1}$ and introduce the variable

$$u=\frac{x}{L(t)}. \tag{4.81}$$

Thus, we make the transformation

$$\gamma=c_3\cdot c_2^{-\alpha}u, \tag{4.82}$$

and

$$F(\gamma) = \left(\frac{5L_0}{2k}\right)^{\frac{1}{2}} c_3^{\frac{1}{2}} c_2^{-\frac{3}{4}\alpha} G(u). \tag{4.83}$$

In doing so, the problem can be summarized into the following statements:

$$\gamma = c_3 \cdot c_2^{-\alpha} u, \qquad u = \frac{x}{L(t)}, \tag{4.84}$$

$$\alpha = \frac{c_3}{c_1}, \qquad \frac{c_5}{c_1} = \frac{3}{4}\alpha - \frac{1}{2}, \tag{4.85}$$

$$\frac{d}{du}\left[G(u)^{\frac{5}{2}}\left(-\frac{dG}{du}\right)^{\frac{1}{2}}\right] - \frac{d}{du}\left(uG(u)\right) + \left(\frac{7}{4} - \frac{1}{2\alpha}\right) G(u) = 0, \tag{4.86}$$

$$G(1) = 0, \tag{4.87}$$

$$\left(\frac{7}{4} - \frac{1}{2\alpha}\right) \int_0^1 G(u)du = G(0)^{\frac{5}{2}} \left(-\frac{dG}{du}(0)\right)^{\frac{1}{2}}, \tag{4.88}$$

$$G(u)^{\frac{5}{2}} \left(-\frac{dG}{du}\right)^{\frac{1}{2}} \Big|_{u=1} = 0, \tag{4.89}$$

$$L(t) = \left(1 + \frac{c_1}{c_2} t\right)^{\alpha}, \tag{4.90}$$

$$V(t) = \left(1 + \frac{c_1}{c_2} t\right)^{\frac{7}{4}\alpha - \frac{1}{2}} V_0, \tag{4.91}$$

$$V_0 = 2\left(\frac{c_3}{c_2}\right)^{\frac{1}{2}} \left(\frac{5l_0}{2K}\right)^{\frac{1}{2}} \cdot \int_0^1 G(u)du, \tag{4.92}$$

$$h(t,x) = \left(\frac{c_3}{c_2}\right)^{\frac{1}{2}} \left(\frac{5l_0}{2K}\right)^{\frac{1}{2}} \left(1 + \frac{c_1}{c_2} t\right)^{\frac{3}{4}\alpha - \frac{1}{2}} G(u). \tag{4.93}$$

The final condition to be imposed on this system is that $h(0,0) = 1$. In doing so, it can be determined that

$$\frac{c_3}{c_2} = \frac{1}{G^2(0)} \left(\frac{2K}{5l_0}\right), \tag{4.94}$$

and as a result

$$\frac{c_1}{c_2} = \frac{c_3}{c_2} \cdot \frac{c_1}{c_3} = \frac{1}{\alpha} \frac{1}{G^2(0)} \left(\frac{2K}{5l_0}\right). \tag{4.95}$$

Thus, the system of equations can be summarised as

$$\gamma = c_3 \cdot c_2^{-\alpha} u, \qquad u = \frac{x}{L(t)}, \tag{4.96}$$

$$\alpha = \frac{c_3}{c_1}, \qquad \frac{c_5}{c_1} = \frac{3}{4}\alpha - \frac{1}{2}, \tag{4.97}$$

$$\frac{c_3}{c_2} = \frac{1}{G^2(0)}\left(\frac{2K}{5l_0}\right), \quad \frac{c_1}{c_2} = \frac{1}{\alpha}\frac{1}{G^2(0)}\left(\frac{2K}{5l_0}\right), \tag{4.98}$$

$$\frac{c_5}{c_2} = \left(\frac{3}{4}\alpha - \frac{1}{2}\right)\frac{1}{G^2(0)}\frac{2K}{5l_0}, \tag{4.99}$$

$$\frac{d}{du}\left[G(u)^{\frac{5}{2}}\left(-\frac{dG}{du}\right)^{\frac{1}{2}}\right] - \frac{d}{du}\left(uG(u)\right) + \left(\frac{7}{4} - \frac{1}{2\alpha}\right)G(u) = 0, \tag{4.100}$$

$$G(1) = 0, \tag{4.101}$$

$$\left(\frac{7}{4} - \frac{1}{2\alpha}\right)\int_0^1 G(u)du = G(0)^{\frac{5}{2}}\left(-\frac{dG}{du}(0)\right)^{\frac{1}{2}}, \tag{4.102}$$

$$G(u)^{\frac{5}{2}}\left(-\frac{dG}{du}\right)^{\frac{1}{2}}\Bigg|_{u=1} = 0, \tag{4.103}$$

$$L(t) = \left(1 + \frac{1}{\alpha}\frac{1}{G^2(0)}\left(\frac{2K}{5l_0}\right)t\right)^{\alpha}, \tag{4.104}$$

$$V(t) = \left(1 + \frac{1}{\alpha}\frac{1}{G^2(0)}\left(\frac{2K}{5l_0}\right)t\right)^{\frac{7}{4}\alpha - \frac{1}{2}} V_0, \tag{4.105}$$

$$V_0 = \frac{2}{G(0)}\int_0^1 G(u)du, \tag{4.106}$$

$$h(t,u) = \left(1 + \frac{1}{\alpha}\frac{1}{G^2(0)}\left(\frac{2K}{5l_0}\right)t\right)^{\frac{3}{4}\alpha - \frac{1}{2}} \frac{G(u)}{G(0)}. \tag{4.107}$$

4.3 Solutions

4.3.1 *Exact analytical solutions*

There are two exact analytical solutions to equation (4.100) for the boundary conditions (4.101), (4.102) and (4.103). These will be presented and discussed below.

4.3.1.1 *First exact analytical solution*

When the parameter α takes on the value $\frac{2}{7}$, equation (4.100) becomes integrable. Setting $\alpha = \frac{2}{7}$, equation (4.100) and its boundary conditions (4.101-4.103) reduce to,

$$\frac{d}{du}\left[G(u)^{\frac{5}{2}}\left(-\frac{dG}{du}\right)^{\frac{1}{2}} - uG(u)\right] = 0, \tag{4.108}$$

$$G(1) = 0, \tag{4.109}$$

$$G(0)^{\frac{5}{2}}\left(-\frac{dG}{du}(0)\right)^{\frac{1}{2}} = 0, \tag{4.110}$$

$$G(u)^{\frac{5}{2}}\left(-\frac{dG}{du}\right)^{\frac{1}{2}}\Bigg|_{u=1} = 0. \tag{4.111}$$

Integrating (4.108) once with respect to u results in

$$G(u)^{\frac{5}{2}}\left(-\frac{dG}{du}\right)^{\frac{1}{2}} - uG(u) = A, \tag{4.112}$$

where A is a constant to be determined.

The boundary conditions at either $u = 0$, (4.110), or at $u = 1$, (4.109) and (4.111), can be utilised to solve for A, both resulting in $A = 0$. Solving ODE (4.112) with $A = 0$ results in

$$G(u) = \left(B - \frac{4}{3}u^3\right)^{\frac{1}{4}}, \tag{4.113}$$

where B is a constant to be determined.

Imposing boundary condition (4.109), it is found that $B = \frac{4}{3}$ and therefore,

$$G(u) = \left(\frac{4}{3}\right)^{\frac{1}{4}}\left(1 - u^3\right)^{\frac{1}{4}}. \tag{4.114}$$

It can be verified that by using boundary conditions (4.109) and (4.111) to obtain $G(u)$, boundary condition (4.110) is automatically satisfied. Likewise, boundary condition (4.111) holds if the conditions (4.109) and (4.110) were used in obtaining the solution.

Now, substituting $\alpha = \frac{2}{7}$ and (4.114) into the general expressions of the half-width (4.107), length (4.104) and volume (4.105), results in

$$h(t,u) = \left(1 + \frac{7\sqrt{3}K}{10l_0}t\right)^{-\frac{2}{7}} (1-u^3)^{\frac{1}{4}}, \tag{4.115}$$

$$L(t) = \left(1 + \frac{7\sqrt{3}K}{10l_0}t\right)^{\frac{2}{7}}, \tag{4.116}$$

$$V(t) = V_0 = 2\int_0^1 (1-u^3)^{\frac{1}{4}}\,du = 1.81531. \tag{4.117}$$

From (4.117), it can be noted that this analytical solution obtained by setting $\alpha = \frac{2}{7}$ corresponds to the case where the fracture volume remains constant over time.

4.3.1.2 *Second exact analytical solution*

An exact analytic solution to equation (4.100) can be found by looking for a solution of the form

$$G(u) = A(1-u)^n, \tag{4.118}$$

where A and n are constants to be determined.

Substituting (4.118) into equation (4.100) results in

$$nA(1-u)^{n-1} - A^3 n^{\frac{1}{2}}\left(3n - \frac{1}{2}\right)(1-u)^{3n-\frac{3}{2}} + \left(\frac{3}{4} - n - \frac{1}{2\alpha}\right)A(1-u)^n = 0. \tag{4.119}$$

Equation (4.119) will be satisfied if

$$nA(1-u)^{n-1} - A^3 n^{\frac{1}{2}}\left(3n - \frac{1}{2}\right)(1-u)^{3n-\frac{3}{2}} = 0, \tag{4.120}$$

and

$$\left(\frac{3}{4} - n - \frac{1}{2\alpha}\right)A(1-u)^n = 0. \tag{4.121}$$

By equating the powers of $(1-u)$ in (4.120), it is found that $n = \frac{1}{4}$. Substituting this value for n into (4.120) and (4.121) results in

$$A(1-u)^{-\frac{3}{4}}\left(\frac{1}{4} - \frac{A^2}{8}\right) = 0, \tag{4.122}$$

and

$$\left(\frac{1}{2}-\frac{1}{2\alpha}\right)A(1-u)^{\frac{1}{4}}=0, \tag{4.123}$$

respectively.

From (4.123), since we do not want a trivial solution, we impose $A \neq 0$ and thus for (4.123) to vanish, $\alpha = 1$. Solving for A in equation (4.122) results in $A = \sqrt{2}$.

Thus, an exact analytic solution of equation (4.100) for $\alpha = 1$ is given by

$$G(u) = \sqrt{2}(1-u)^{\frac{1}{4}}. \tag{4.124}$$

This solution satisfies boundary conditions (4.101)-(4.103).

Substituting $\alpha = 1$ and (4.124) into the general expressions of the half-width (4.107), length (4.104) and volume (4.105), gives

$$h(t,x) = \left(1+\frac{K}{5l_0}t\right)^{\frac{1}{4}}(1-u)^{\frac{1}{4}} = L(t)^{\frac{1}{4}}(1-u)^{\frac{1}{4}}, \tag{4.125}$$

$$L(t) = 1+\frac{K}{5l_0}t, \tag{4.126}$$

$$V(t) = \frac{8}{5}\left(1+\frac{K}{5l_0}t\right)^{\frac{5}{4}}. \tag{4.127}$$

It can be noted that the fracture length, (4.126), is linear in time. As a result, its derivative with respect to t is constant, implying that $\alpha = 1$ corresponds to a constant speed of propagation of the fracture length.

4.3.2 *Asymptotic solutions*

We can approximate the behaviour of $G(u)$ as $u \to 1$ by an asymptotic solution. We look for a solution of the form

$$G(u) \sim C(1-u)^n, \quad \text{as} \quad u \to 1, \tag{4.128}$$

where C and n are constants to be determined, since it satisfies the boundary condition (4.101).

Substituting (4.128) into equation (4.100) gives

$$\left(\frac{1}{2}-3n\right)n^{\frac{1}{2}}C^3(1-u)^{3n-\frac{3}{2}} + Cn(1-u)^{n-1} - C(n+1)(1-u)^n + C\left(\frac{7}{4}-\frac{1}{2\alpha}\right)(1-u)^n = 0, \tag{4.129}$$

as $u \to 1$. By balancing the dominant terms, which are of order $(1-u)^{3n-\frac{3}{2}}$ and $(1-u)^{n-1}$, we see that $n = \frac{1}{4}$. Thus,

$$-\frac{1}{8}C^3 + \frac{1}{4}C - \frac{5}{4}C(1-u) + C(1-u)\left(\frac{7}{4} - \frac{1}{2\alpha}\right) = 0, \quad \text{as} \quad u \to 1. \tag{4.130}$$

Let $u \to 1$, then (4.130) tends to

$$\frac{C}{4} - \frac{C^3}{8} = 0. \tag{4.131}$$

Thus, either $C = 0$ (which we will not consider), or $C = \sqrt{2}$, and so

$$G(u) = \sqrt{2}(1-u)^{\frac{1}{4}}, \quad \text{as} \quad u \to 1, \tag{4.132}$$

which is the asymptotic solution. It can be noted that this solution is valid for all values of α.

4.3.3 *Numerical solution using the shooting method*

The boundary value problem to be solved is given by

$$\frac{d}{du}\left[G(u)^{\frac{5}{2}}(-G'(u))^{\frac{1}{2}}\right] - \frac{d}{du}\left[uG(u)\right] + \left(\frac{7}{4} - \frac{1}{2\alpha}\right)G(u) = 0, \tag{4.133}$$

subject to the conditions

$$G(1) = 0, \tag{4.134}$$

$$\left(\frac{7}{4} - \frac{1}{2\alpha}\right)\int_0^1 G(u)du = G(0)^{\frac{5}{2}}(-G'(0))^{\frac{1}{2}}. \tag{4.135}$$

The flux of the fluid must also vanish at the fracture tip,

$$G(u)^{\frac{5}{2}}\left(-\frac{dG}{du}\right)^{\frac{1}{2}}\Bigg|_{u=1} = 0. \tag{4.136}$$

If this problem is solved for G'' and split into a system of first order equations, it can be seen that the Jacobian is both singular and non-constant at certain points in the domain. This makes it a particularly challenging problem to solve, as most standard numerical methods are simply not applicable to this problem.

The most accessible way of solving this problem is by using the shooting method and converting the problem into a set of two initial value problems, rather than solving the boundary value problem directly.

The Lie point symmetries of the equation of interest can assist in this conversion if they are scaling symmetries. The Lie point symmetries of ODE (4.133) are generated by

$$X = 4u\frac{\partial}{\partial u} + 3G\frac{\partial}{\partial u}. \tag{4.137}$$

From Lie's equations [24], a transformation that leaves equation (4.133) invariant is given by

$$\overline{u} = e^{4p}u, \qquad \overline{G}(\overline{u}) = e^{3p}G(u), \tag{4.138}$$

where p is the group parameter. By defining $\lambda = e^{4p}$, the transformation (4.138) may be rewritten as

$$\overline{u} = \lambda u, \qquad \overline{G}(\overline{u}) = \lambda^{\frac{3}{4}}G(u). \tag{4.139}$$

Using the transformation (4.139) on the boundary value problem (4.133) and conditions (4.134), (4.135), results in

$$\frac{d}{d\overline{u}}\left[\overline{G}(\overline{u})^{\frac{5}{2}}(-\overline{G}'(\overline{u}))^{\frac{1}{2}}\right] - \frac{d}{d\overline{u}}\left[\overline{u}\overline{G}(\overline{u})\right] + \left(\frac{7}{4} - \frac{1}{2\alpha}\right)\overline{G}(\overline{u}) = 0, \tag{4.140}$$

$$\overline{G}(\lambda) = 0, \tag{4.141}$$

$$\overline{G}(0)^{\frac{5}{2}}(-\overline{G}'(0))^{\frac{1}{2}} = \left(\frac{7}{4} - \frac{1}{2\alpha}\right)\int_0^\lambda \overline{G}(\overline{u})d\overline{u}. \tag{4.142}$$

We may select

$$\overline{G}(0) = 1 \tag{4.143}$$

and thus

$$G(0) = \lambda^{-\frac{3}{4}}. \tag{4.144}$$

As a result of this transformation and solving the equations for the highest order derivatives, we thus have a set of two initial value problems.

Initial Value Problem 1

$$\overline{G}''(\overline{u}) = 2\overline{u}\overline{G}(\overline{u})^{-\frac{5}{2}}(-\overline{G}'(\overline{u}))^{\frac{3}{2}} - 5\overline{G}(\overline{u})^{-1}\overline{G}'(\overline{u})^2 + \overline{G}(\overline{u})^{-\frac{3}{2}}(-\overline{G}'(\overline{u}))^{\frac{1}{2}}\left(\frac{3}{2} - \frac{1}{\alpha}\right), \tag{4.145}$$

$$\overline{G}(0) = 1, \tag{4.146}$$

$$\overline{G}'(0) = -\left(\frac{7}{4} - \frac{1}{2\alpha}\right)^2\left[\int_0^\lambda \overline{G}(\overline{u})d\overline{u}\right]^2, \tag{4.147}$$

where λ is the value that results in $\overline{G}(\lambda) = 0$, and $\overline{u} \in [0, \lambda]$.

Integration of this problem must be done backwards, from $\overline{u} = \lambda$ to $\overline{u} = 0$, in order to avoid the problems the singularity in boundary condition (4.134) introduces in the numerical scheme. Taking this approach greatly reduces the complexity of solving this problem and also increases the accuracy.

The asymptotic solution as $\overline{u} \to \lambda$ is used to derive both an approximate value for $\overline{G}(\lambda)$ and $\overline{G}'(\lambda)$, to aid in overcoming the singularity at the end point $u = \lambda$. From equations (4.132) and (4.139),

$$\overline{G}^*(\overline{u}) = \sqrt{2}\lambda^{\frac{1}{2}}(\lambda - \overline{u})^{\frac{1}{4}}, \quad \text{as} \quad \overline{u} \to \lambda, \tag{4.148}$$

and so

$$\overline{G}'^*(\overline{u}) = -\frac{\sqrt{2}}{4}\lambda^{\frac{1}{2}}(\lambda - \overline{u})^{-\frac{3}{4}}, \quad \text{as} \quad \overline{u} \to \lambda. \tag{4.149}$$

Taking the values of $\overline{G}^*$, $\overline{G}'^*$ at $\overline{u} = \lambda - \epsilon$ where ϵ is very small (i.e. $\mathcal{O}(10^{-10})$) gives the approximate boundary conditions required, while avoiding the singularity at $\overline{u} = \lambda$.

Upon obtaining these new approximate 'initial' values at the end point of the domain, a standard ODE solver can be used iteratively in a binary search for an adequate value of λ. ODE45 in Matlab was chosen to perform the numerical solution in this research. It is a fourth-order Runge-Kutta method with variable step sizes adjusted accordingly at each step. It offers a good balance between accuracy and computational time and performed well on this particular problem set.

Upon finding a value of λ for which the original initial condition is satisfied, that is,

$$\|\overline{G}_\lambda(0) - 1\| \leqslant \epsilon_\lambda, \tag{4.150}$$

for some small value ϵ_λ, the solution of this problem is complete.

The boundary condition (4.135) will generally also be satisfied within a similar error tolerance; otherwise, a similar binary search can be undertaken to find a λ value satisfying boundary condition (4.135).

The value of λ and the slope at $\overline{u} = 0$ must be returned from the algorithm and noted, in order to solve the second initial value problem.

Initial Value Problem 2

$$G''(u) = 2uG(u)^{-\frac{5}{2}}(-G'(u))^{\frac{3}{2}} - 5G(u)^{-1}G'(u)^2 + G(u)^{-\frac{3}{2}}(-G'(u))^{\frac{1}{2}}\left(\frac{3}{2} - \frac{1}{\alpha}\right), \tag{4.151}$$

$$G(0) = \lambda^{-\frac{3}{4}}, \tag{4.152}$$

$$G'(0) = \lambda^{\frac{1}{4}}\overline{G}'(0). \tag{4.153}$$

Using the values obtained from solving the first initial value problem, this problem can easily be solved using in-built solvers in any mathematical programming language.

4.3.3.1 *Algorithm*

Algorithm 1 gives a suggested high-level algorithm of how to approach solving IVP 1 in a mathematical programming language, such as Matlab.

The inputs required to algorithmically solve IVP 1 numerically will be explained below:

- $[\lambda_a, \lambda_b]$:
  This is an initial interval in which we search for a λ that results in the boundary condition (4.146) being satisfied, correct to an error tolerance. For this problem, often $[\lambda_a, \lambda_b] = (0, 2]$ is sufficient.

- *Initial Value Problem 1 (IVP 1)*:
  Assuming this equation has been non-dimensionalized, this will involve an ODE to solve for a function $\overline{G}(\overline{u})$, where $\overline{u} \in [0, \lambda]$. This must be given in the form of a first-order system of equations if using in-built solvers such as ODE45 (Matlab) and other similar programs.

- λ_0:
  This is an initial guess of the value of λ, and it lies within the interval $[\lambda_a, \lambda_b]$. The algorithm, provided it is allowed to run for a sufficiently large number of iterations, will correct the value of λ to one that satisfies the boundary conditions. As a result, an arbitrary $\lambda_0 \in [\lambda_a, \lambda_b]$ can generally be picked without affecting the results.

- *An asymptotic solution,* $\overline{G}^*(\overline{u})$*, as* $\overline{u} \to \lambda$:
  This will be utilized to obtain approximate values for the numerical solution as $\overline{u}$ nears λ, because problems of this nature have singularities near the fracture tip [2, 15, 17].

- *Maximum iterations number (*i_{max}*)*:
  This will be used to control the maximum number of iterations an algorithm should be permitted to perform before termination, if it has not already converged. This is important as these equations are exceptionally parameter sensitive and have a relatively long computation time per iteration. In the unlikely event that the algorithm has not converged within a sensible amount of iterations, picking a smaller λ_0 often assists.

- *Error tolerance (*ϵ_λ*)*:
  This is an error size that is deemed acceptable by the programmer in the calculation of the lambda value. This will give a criteria that allows termination of the algorithm, based on finding some interval $[\lambda_a^{(n)}, \lambda_b^{(n)}]$

on the n^{th} algorithm iteration, whereby both $\lambda_a^{(n)}$ and $\lambda_b^{(n)}$ result in a value of $\overline{G}(0)$ where $|\overline{G}_\lambda(0) - 1| \leqslant \epsilon$.

Algorithm 1 Algorithm to numerically solve IVP 1

procedure IVP1SOLVER(α, λ_0, λ_a, λ_b, ϵ_λ, i_{max}, $\overline{G}^*(\overline{u})$, IVP 1)
  $i \leftarrow 0$
  $\overline{G}_{\lambda_c}(0) \leftarrow \infty$
  $\lambda \leftarrow \lambda_0$
  while $(i < i_{max})$ and $(\|\overline{G}_{\lambda_c}(0) - 1\| > \epsilon_\lambda)$ **do**
    $i \leftarrow i + 1$
    $\lambda_c \leftarrow (\lambda_a + \lambda_b)/2$
    $\epsilon \leftarrow 10^{-10}$
    $G_{end} \leftarrow \overline{G}^*(\lambda - \epsilon)$
    $dG_{end} \leftarrow \overline{G}'^*(\lambda - \epsilon)$
    Solve $\{$IVP 1 , $G_{end}, dG_{end}\}$ for $\overline{u} \in [\lambda, 0]$ for λ_a, λ_b and λ_c
    Extract $\overline{G}_{\lambda_a}(0), \overline{G}_{\lambda_b}(0)$ and $\overline{G}_{\lambda_c}(0)$ from the solutions
    $\Delta_1 \leftarrow \|\overline{G}_{\lambda_a}(0) - 1\|$
    $\Delta_2 \leftarrow \|\overline{G}_{\lambda_b}(0) - 1\|$
    if $\Delta_2 < \Delta_1$ **then**
      $\lambda_a \leftarrow \lambda_c$
    else
      $\lambda_b \leftarrow \lambda_c$
    end if
    $\lambda \leftarrow \lambda_c$
  end while
  $\text{rhs} \leftarrow -\left(\frac{7}{4} - \frac{1}{2\alpha}\right)^2 \left[\int_0^{\lambda-\epsilon} \overline{G}_{\lambda_c}(\overline{u})\, d\overline{u}\right]^2$
  errMargin$\leftarrow \|\overline{G}_{\lambda_c}(0) - \text{rhs}\|$
  return λ, $\overline{G}'_{\lambda_c}(0)$, errMargin
end procedure

4.3.3.2 *Algorithm accuracy benchmark*

A simple way to determine the accuracy of the numerical method employed in this research is to make use of the exact analytic solutions obtained for $\alpha = \frac{2}{7}$, given by (4.114), and for $\alpha = 1$, given by (4.124).

Table 4.1 shows the values of the analytic and numerical solution for $\alpha = \frac{2}{7}$ at a range of values of u. It can be calculated that the average error between the numerical solution and analytical solution is 0.0000308417. Likewise, Table 4.2 gives a comparison between the analytical and numerical solution for $\alpha = 1$, over varying u. The average error between the numerical and analytic solution in this case is 0.000820769.

u	$G^*(u)$	$G(u)$	Error
0	1.0746	1.07457	0.0000349263
0.05	1.07457	1.07454	0.0000348235
0.1	1.07434	1.0743	0.0000346404
0.15	1.0737	1.07366	0.0000343549
0.2	1.07245	1.07241	0.0000339861
0.25	1.07038	1.07035	0.0000335489
0.3	1.06728	1.06724	0.0000330619
0.35	1.06289	1.06286	0.0000325331
0.4	1.05698	1.05695	0.0000319736
0.45	1.04924	1.04921	0.0000313916
0.5	1.03932	1.03929	0.0000307978
0.55	1.02681	1.02678	0.0000301955
0.6	1.01118	1.01115	0.000029593
0.65	0.991718	0.991689	0.0000289922
0.7	0.967473	0.967444	0.000028398
0.75	0.937029	0.937001	0.0000278141
0.8	0.898158	0.898131	0.0000272443
0.85	0.846954	0.846928	0.000026692
0.9	0.775339	0.775313	0.0000261667
0.95	0.66039	0.660364	0.0000257008

Table 4.1: The values of the approximate numerical solution of ODE (4.133), $G^*(u)$, the analytic solution, $G(u)$, and the error between the two, for $\alpha = \frac{2}{7}$.

u	$G^*(u)$	$G(u)$	Error
0.	1.41506	1.41421	0.000845475
0.05	1.39704	1.39619	0.000842981
0.1	1.37829	1.37745	0.000840473
0.15	1.35874	1.35791	0.000837948
0.2	1.33832	1.33748	0.000835406
0.25	1.31691	1.31607	0.000832851
0.3	1.2944	1.29357	0.000830277
0.35	1.27065	1.26982	0.000827686
0.4	1.24549	1.24467	0.000825076
0.45	1.21871	1.21788	0.000822448
0.5	1.19003	1.18921	0.000819801
0.55	1.15911	1.15829	0.000817135
0.6	1.1255	1.12468	0.000814447
0.65	1.08857	1.08776	0.000811739
0.7	1.04744	1.04664	0.000809005
0.75	1.00081	1.	0.000806245
0.8	0.946545	0.945742	0.000803452
0.85	0.880912	0.880112	0.000800615
0.9	0.796068	0.795271	0.000797706
0.95	0.669535	0.66874	0.000794623

Table 4.2: The values of the approximate numerical solution of ODE (4.133), $G^*(u)$, the analytic solution, $G(u)$, and the error between the two, for $\alpha = 1$.

Figure 4.1 illustrates the numerical solution and exact analytical solution for $\alpha = \frac{2}{7}$ on the same set of axes. Similarly, Figure 4.2 shows the numerical solution and exact analytical solution for $\alpha = 1$ on the same axes.

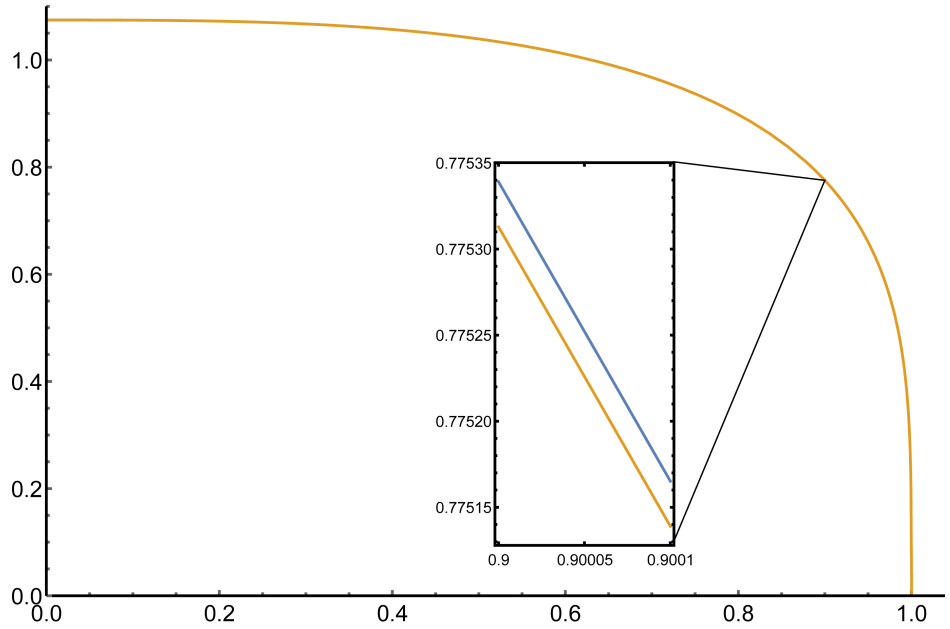


Figure 4.1: A graph illustrating the exact analytic solution for $\alpha = \frac{2}{7}$ (orange) and numerical solution (blue) on the same set of axes. The box within the graph is a zoomed up portion of the graph from $u = 0.9$ to $u = 0.9001$, to allow for closer inspection of the difference between the two graphs.

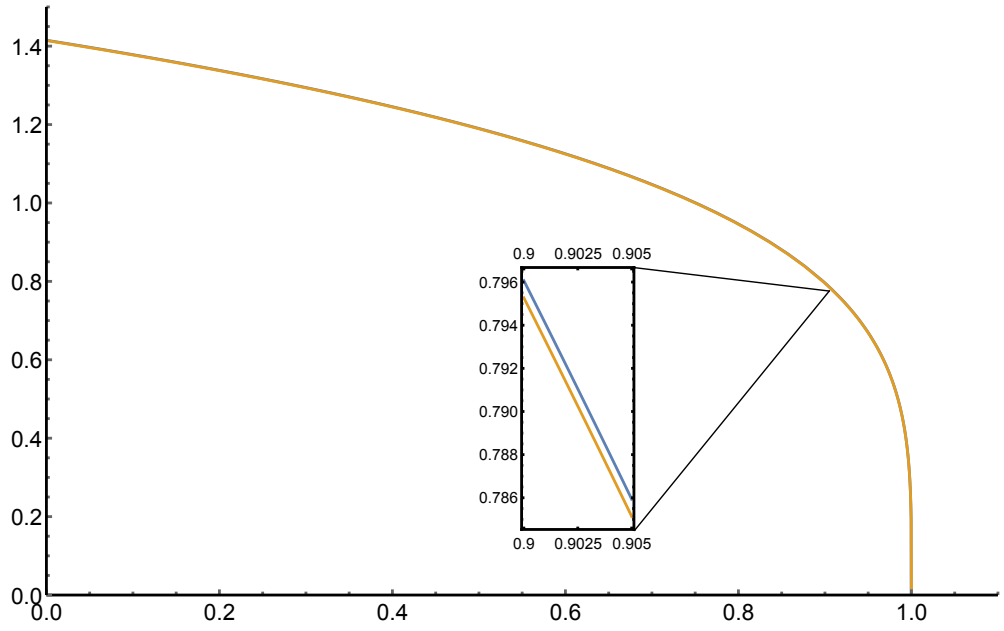


Figure 4.2: A graph illustrating the exact analytic solution for $\alpha = 1$ (orange) and numerical solution (blue) on the same set of axes. The box within the graph is a zoomed up portion of the graph from $u = 0.9$ to $u = 0.905$.

It can be noted that the average error between the numerical and analytic solution for $\alpha = \frac{2}{7}$ is of order $\mathcal{O}(10^{-5})$, whereas the average error between the $\alpha = 1$ solutions is of order $\mathcal{O}(10^{-4})$. This discrepancy can be explained by looking at the effect the α value has on the boundary condition (4.142) utilised in the numerical solution. For $\alpha = \frac{2}{7}$, the integral component of (4.142) vanishes, whereas it is still present in the numerical solution for $\alpha = 1$. As this integral relies on the calculated parameter λ, additional error is introduced into the solution, thus accounting for the difference in error orders between the two solutions.

4.3.4 *Numerical solution using quasi-linearization*

Applying the quasi-linearisation technique, as outlined in Section 2.7.2, equation (4.100) and its boundary conditions, (4.101) and (4.102), can be expressed as

$$G''_{(n+1)}(u) - \alpha_{(n)} G'_{(n+1)}(u) - \beta_{(n)} G_{(n+1)}(u) = \gamma_{(n)}, \tag{4.154}$$

where

$$G(1)_{(n+1)} = 0, \tag{4.155}$$

$$G(0)^{\frac{5}{2}}_{(n+1)}(-G'(0)_{(n+1)})^{\frac{1}{2}} = \left(\frac{7}{4} - \frac{1}{2\alpha}\right) \int_0^1 G(u)_{(n+1)}\, du, \tag{4.156}$$

and

$$\begin{aligned}\alpha_{(n)} =& -10 G_{(n)}(u)^{-1} G'_{(n)}(u) + 3u G_{(n)}(u)^{-\frac{5}{2}} (-G'_{(n)}(u))^{-\frac{5}{2}} \\ & - \frac{1}{2}\left(\frac{3}{2} - \frac{1}{\alpha}\right) G_{(n)}(u)^{-\frac{3}{2}} (-G'_{(n)}(u))^{-\frac{1}{2}},\end{aligned} \tag{4.157}$$

$$\begin{aligned}\beta_{(n)} =& 5 G_{(n)}(u)^{-2} (G'_{(n)}(u))^2 - 5u G_{(n)}(u)^{-\frac{7}{2}} (-G'_{(n)}(u))^{-\frac{3}{2}} \\ & - \frac{3}{2}\left(\frac{3}{2} - \frac{1}{\alpha}\right) G_{(n)}(u)^{-\frac{5}{2}} (-G'_{(n)}(u)),\end{aligned} \tag{4.158}$$

$$\begin{aligned}\gamma_{(n)} =& 10u G_{(n)}(u)^{-\frac{5}{2}} (-G'_{(n)}(u))^{-\frac{3}{2}} \\ & + \left(3 - \frac{2}{\alpha}\right) G_{(n)}(u)^{-\frac{3}{2}} (-G'_{(n)}(u))^{\frac{1}{2}}.\end{aligned} \tag{4.159}$$

Unfortunately, attempts to apply this numerical method to solve the ODE proved unsuccessful because the iterations did not converge. It may be a case as mentioned in [29] whereby some equations simply do not converge using this method.

4.3.5 *Graphical results*

This section will illustrate the fracture half-width, length and volume for varying parameter values. The ratio $\frac{2K}{5l_0}$ will be denoted by p. This constant p should not be confused with the mean pressure of the fluid flow, denoted by $\overline{p}$. It characterises the degree of turbulence present within the fracturing fluid flow. Small values of p imply that l_0 is very large and thus there is a great deal of turbulence in the fluid flow, whereas larger values of p indicate a small l_0, implying the flow is closer to laminar flow.

Figure 4.3 illustrates the effect of α on the initial fracture profile, as well as the fracture length and volume for fixed p. As α increases, the gradient at the fracture entrance increases negatively. It can also be noted that for larger α, the fracture length and volume are initially smaller. However, after a very short time, they increase rapidly, whereas smaller α values give a much more modest growth over time.

Figures 4.4 and 4.5 show how the fracture half-width evolves over time for $\alpha = 0.5$ and $\alpha = 2$. It can be noted that, due to the exponent in $h(t,u)$ (4.107), $\alpha = \frac{2}{3}$ is a transitional value. For $\alpha < \frac{2}{3}$, as in Figure 4.4, it can be observed that as t increases, the fracture half-width decreases. However, if $\alpha > \frac{2}{3}$, as in Figure 4.5, the fracture half-with increases over time. From the PKN approximation (3.63), when $\alpha = \frac{2}{3}$, the pressure at the fracture entry is constant. For $\alpha < \frac{2}{3}$, the pressure at the fracture entry decreases with time while for $\alpha > \frac{2}{3}$, it increases with time.

Figure 4.6 displays the fracture half-width at $t = 1$, as well as the fracture length and volume, for $\alpha = 0.5 < \frac{2}{3}$, for varying p. It can be observed that the larger p values (which imply less turbulence) result in smaller fracture half-widths. However, these larger p values yield significantly larger fracture lengths and volumes over time.

Figure 4.7 shows the fracture half-width at $t = 1$, and fracture length and volume, for $\alpha = 2 > \frac{2}{3}$, for varying p. Here, larger p values imply larger fracture half-widths, lengths and volumes.

Figures 4.8, 4.9 and 4.10 show a comprehensive view of how fractures evolve over t and u, for $p = 1$, at different α values. Figure 4.8 corresponds to $\alpha = \frac{2}{7}$ and, as expected, the half-width decreases over time. Figures 4.9 and 4.10 corresponding to $\alpha = 1$ and $\alpha = 2$ likewise show how the half-width increases over time.

4.3.6 *Solutions of physical importance*

The value of the ratio $\alpha = \frac{c_3}{c_1}$ plays an important role in determining hydraulic fracturing behaviour. Specific values of this ratio can correspond to

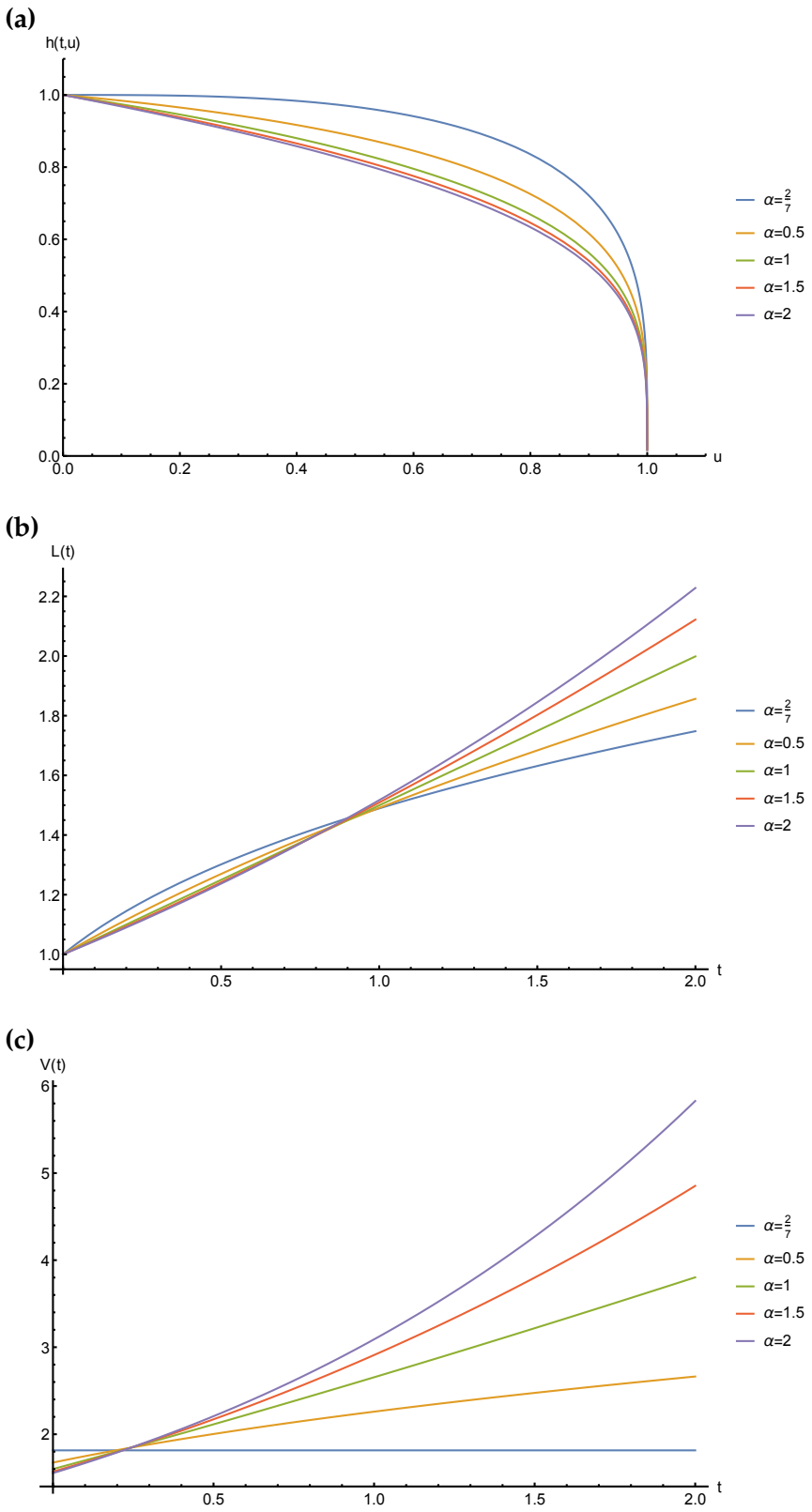


Figure 4.3: Graphs illustrating the effect of the parameter α on **(a)** the initial fracture profile, **(b)** the fracture length and **(c)** the fracture volume. Here, the parameters $\frac{2K}{5l_0} = 1$ and α takes on the values $\frac{2}{7}$, 0.5, 1, 1.5 and 2.

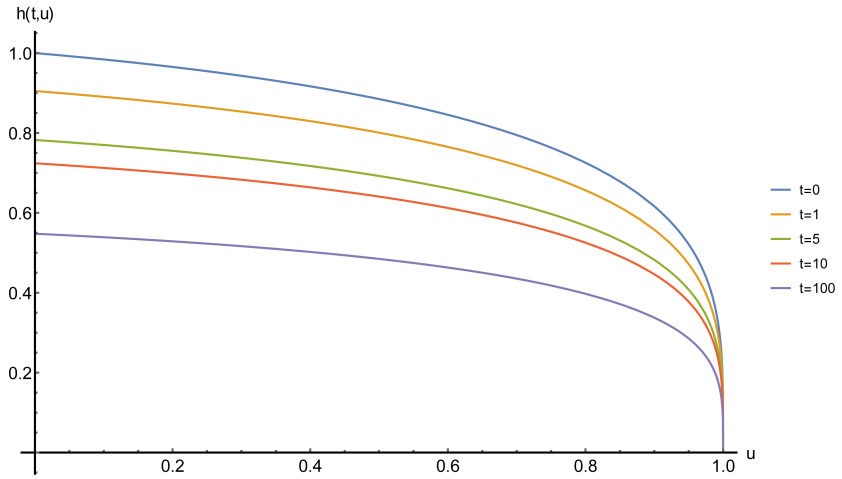


Figure 4.4: A graph showing the fracture half-width for $\alpha = 0.5$, at a fixed value of $p = \frac{2K}{5l_0} = 1$, where t varies, taking on the values $t = 0, 1, 5, 10$ and 100.

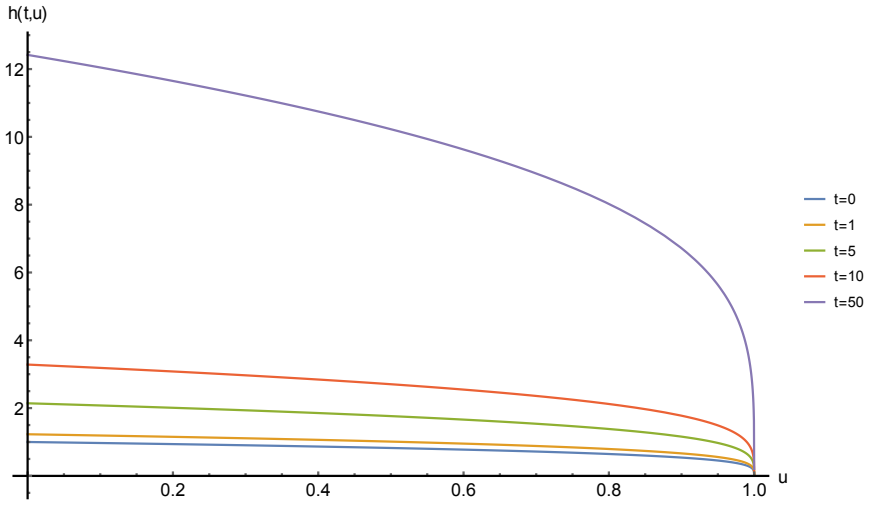


Figure 4.5: A graph showing the fracture half-width for $\alpha = 2$, at a fixed value of $p = \frac{2K}{5l_0} = 1$, where t varies, taking on the values $t = 0, 1, 5, 10$ and 50.

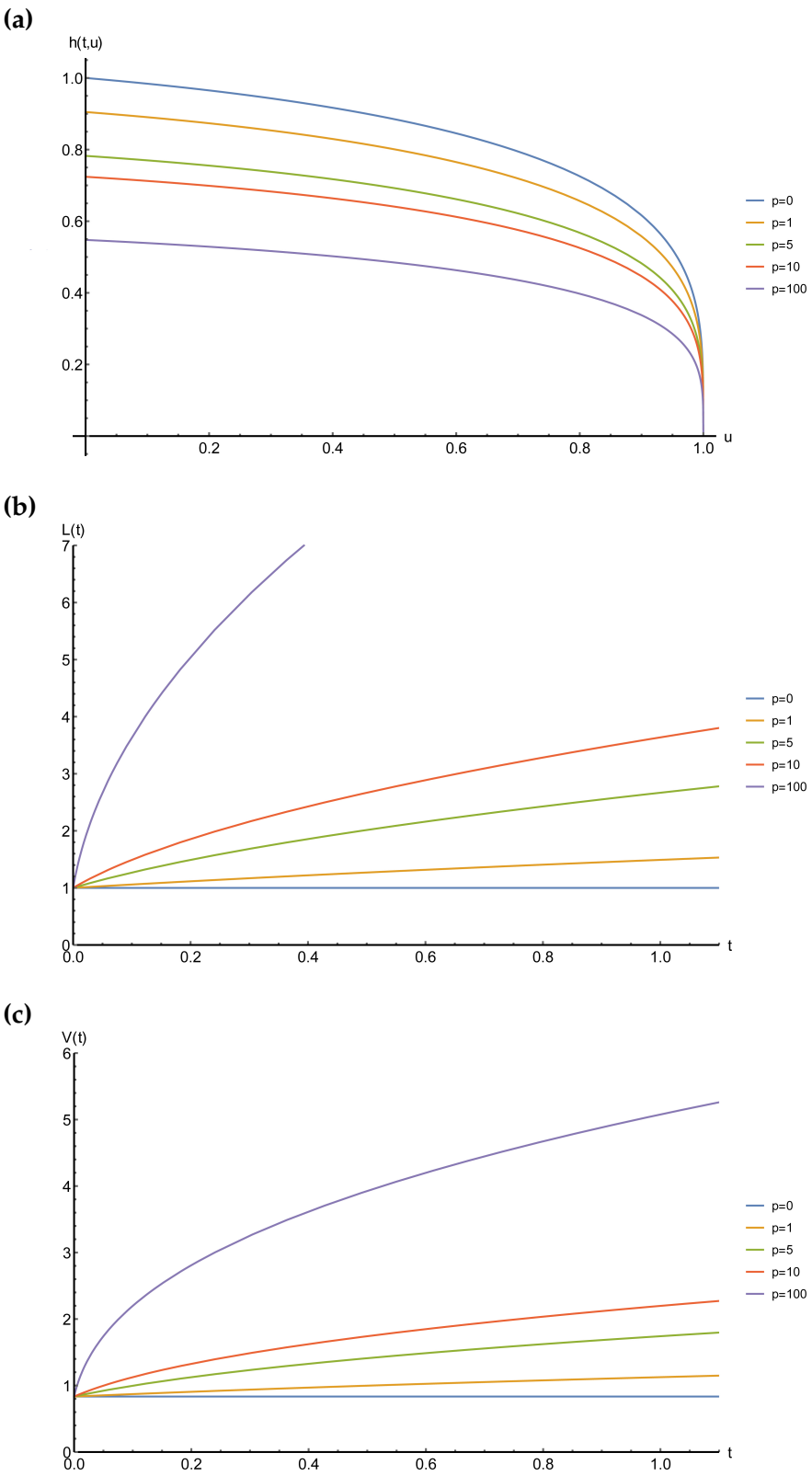


Figure 4.6: Graphs illustrating **(a)** the fracture half-width, **(b)** the fracture length and **(c)** the fracture volume, for $\alpha = 0.5$, at a fixed value of $t = 1$, where $p = \frac{2K}{5l_0}$ varies, taking on the values $p = 0, 1, 5, 10$, and 100.

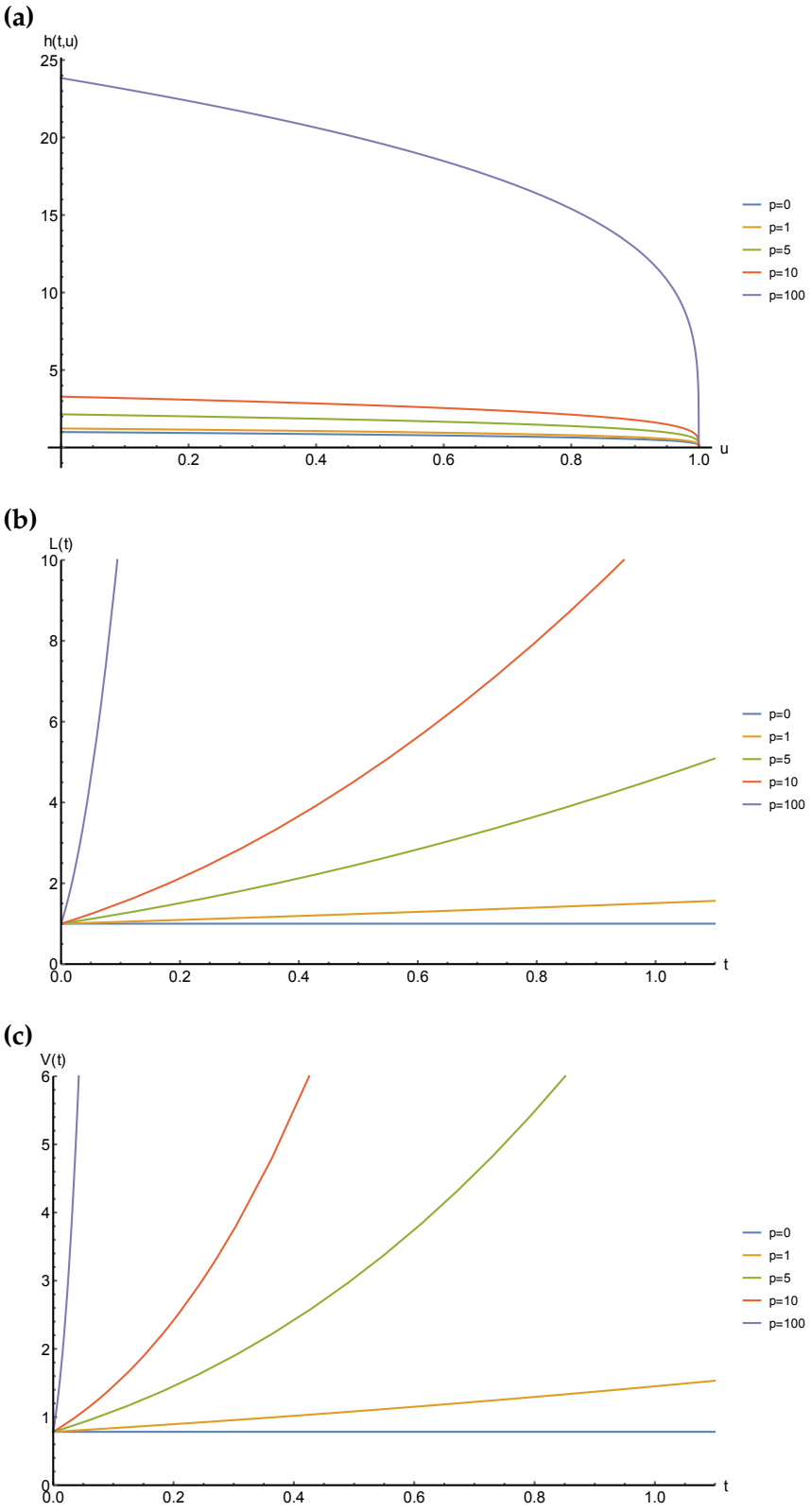


Figure 4.7: Graphs illustrating **(a)** the fracture half-width, **(b)** the fracture length and **(c)** the fracture volume, for $\alpha = 2$, at a fixed value of $t = 1$, where $p = \frac{2K}{5l_0}$ varies, taking on the values $p = 0, 1, 5, 10$ and 100.

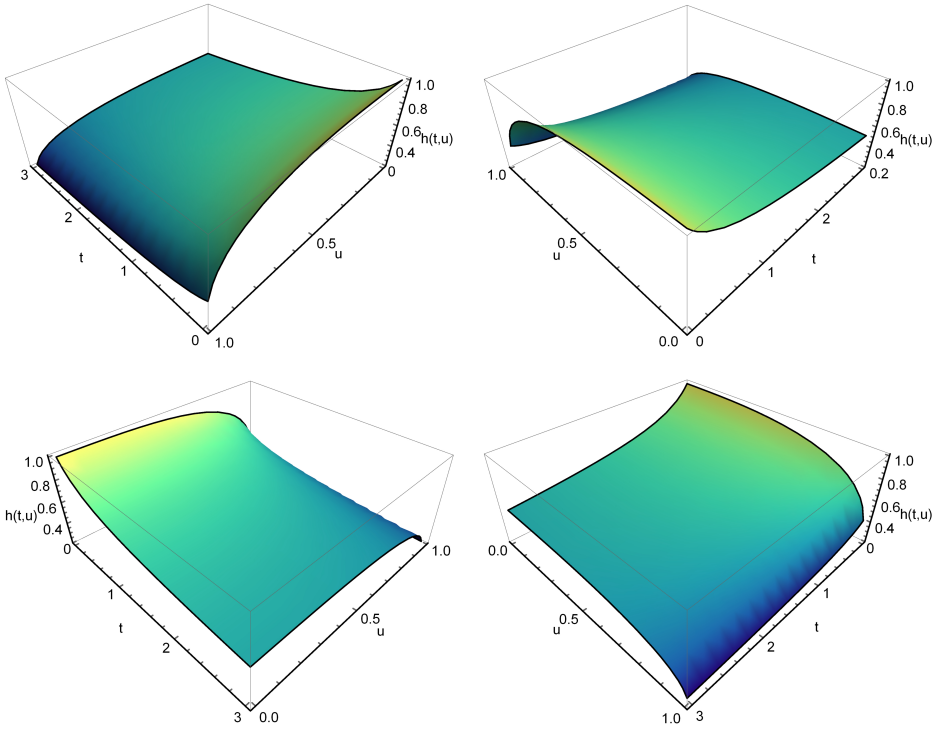


Figure 4.8: Graphs illustrating the fracture half-width varying across t and u for $\alpha = \frac{2}{7}$, at different view points. Here, the parameter $\frac{2K}{5l_0} = 1$.

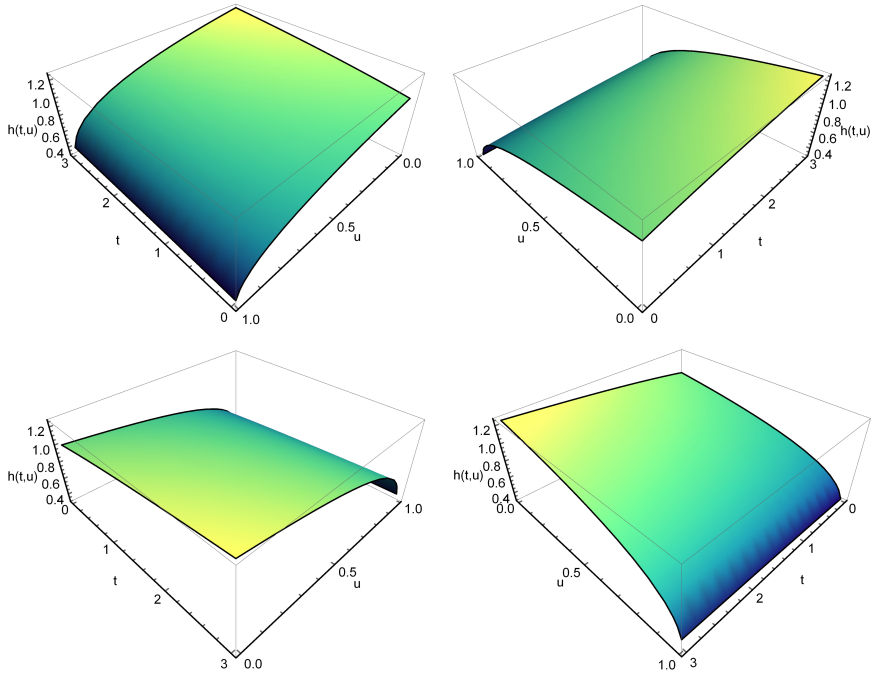


Figure 4.9: Graphs illustrating the fracture half-width varying across t and u for $\alpha = 1$, at different view points. Here, the parameter $\frac{2K}{5l_0} = 1$.

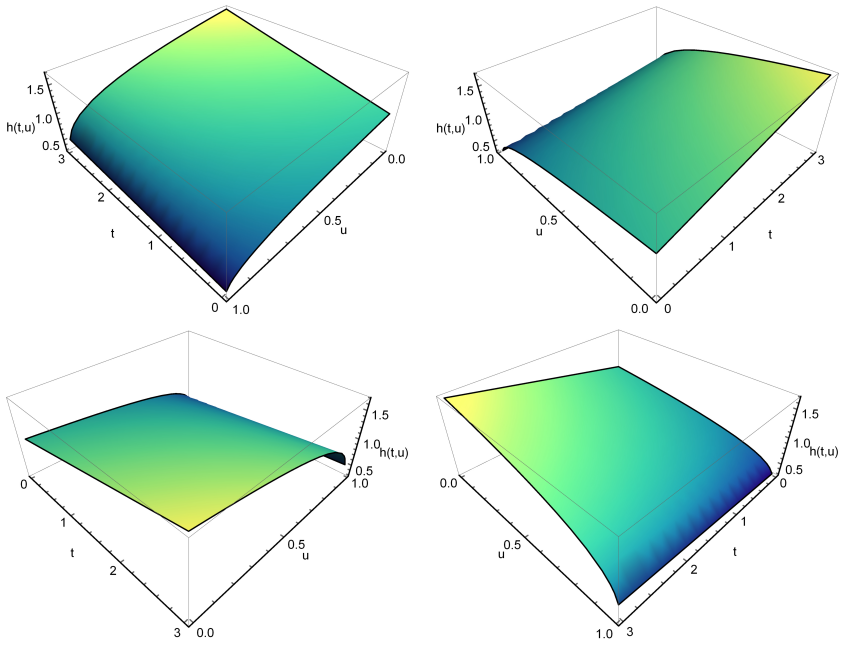


Figure 4.10: Graphs illustrating the fracture half-width varying across t and u for $\alpha = 2$, at different view points. Here, the parameter $\frac{2K}{5t_0} = 1$.

scenarios of important physical significance. This information is summarized in Table 4.3.

Scenario of physical significance	**Value of α**
Constant fracture volume	$\frac{2}{7} = 0.285714$
Constant rate of fracture volume change	$\frac{6}{7} = 0.857143$
Constant rate of fracture length change	1
Constant pressure at the fracture entry ($x = 0$)	$\frac{2}{3} = 0.666667$

Table 4.3: Table illustrating values of the parameter α that correspond to physically significant scenarios.

We assume that $\alpha > 0$. This assumption is made by examining the fracture length expression (4.104) and noting that in order for a fracture to extend over time this restriction needs to be enforced.

4.3.6.1 *Constant fracture volume change*

The general expression for the volume is given by (4.105). It can be observed that a constant fracture volume corresponds to $\alpha = \frac{2}{7}$. A constant fracture volume implies that as the fracture length extends, the fracture width narrows.

Values of $\alpha > \frac{2}{7}$ will result in the fracture volume increasing over time. This would occur due to an increase in the fracture length and/or half-width because of the injection of fluid at the fracture entry. Values where $0 < \alpha < \frac{2}{7}$ results in a decrease in volume over time. This could correspond to a growing fracture length with a narrowing half-width over time because of the extraction of fluid at the fracture entry.

When $\alpha = \frac{2}{7}$, exact analytical expressions can be obtained. The expressions for the fracture half-width, length and volume are derived in Section 4.3.1.1, given by (4.115), (4.116) and (4.117) respectively.

Figure 4.11 illustrates the fracture half-width in this scenario for varying t values and different values of the ratio $p = \frac{2K}{5l_0}$, as well as the fracture length. As expected for $\alpha = \frac{2}{7} < \frac{2}{3}$, the fracture half-width narrows over time. However, the fracture length increases with time. This happens in such a way that the fracture's volume remains perfectly constant throughout the fracture's evolution.

4.3.6.2 *Constant rate of fracture volume change*

The rate at which volume changes within a fracture is given by

$$\frac{dV}{dt} = \left(1 + \frac{1}{\alpha}\frac{1}{G(0)^2}\frac{2K}{5l_0}t\right)^{\frac{7}{4}\alpha - \frac{3}{2}} \cdot \left(\frac{7}{2} - \frac{1}{\alpha}\right)\left(\frac{2K}{5l_0}\right)\frac{1}{G(0)^3}\int_0^1 G(u)du. \tag{4.160}$$

From this, it can be seen that a fracture's volume will change at a constant rate if $\alpha = \frac{6}{7}$.

The problem statement in this scenario can be summarised as follows:

$$\frac{d}{du}\left[G(u)^{\frac{5}{2}}\left(-\frac{dG}{du}\right)^{\frac{1}{2}}\right] - \frac{d}{du}\left(uG(u)\right) + \frac{7}{6}G(u) = 0, \tag{4.161}$$

$$G(1) = 0, \tag{4.162}$$

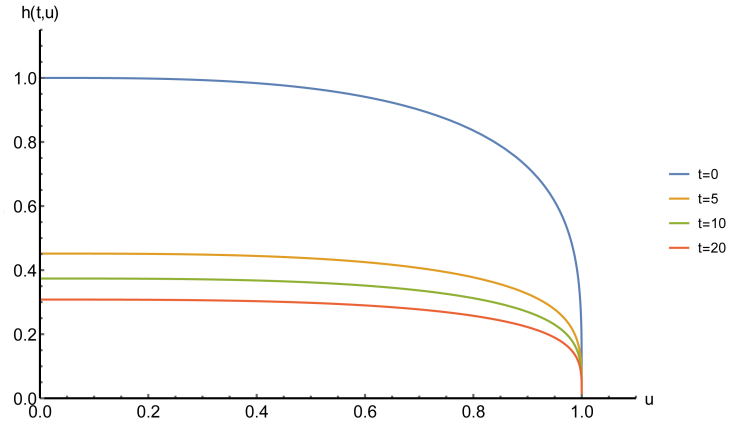
$$\frac{7}{6}\int_0^1 G(u)du = G(0)^{\frac{5}{2}}\left(-\frac{dG}{du}(0)\right)^{\frac{1}{2}}, \tag{4.163}$$

$$G(u)^{\frac{5}{2}}\left(-\frac{dG}{du}\right)^{\frac{1}{2}}\Big|_{u=1} = 0, \tag{4.164}$$

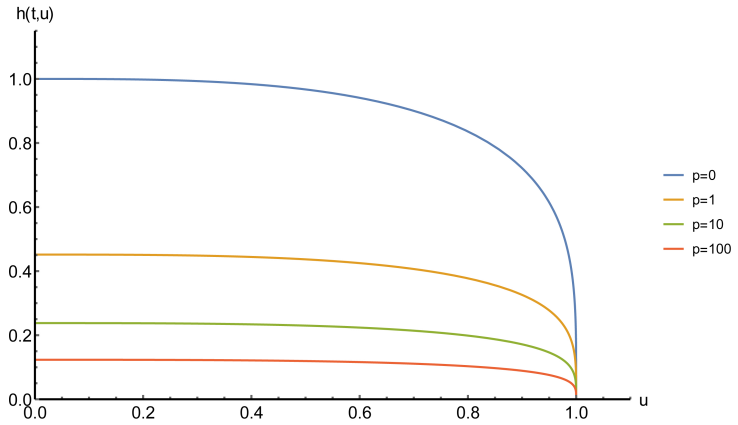
$$L(t) = \left(1 + \frac{7}{15}\frac{1}{G(0)^2}t\right)^{\frac{6}{7}}, \tag{4.165}$$

(4.166)

(a)



(b)



(c)

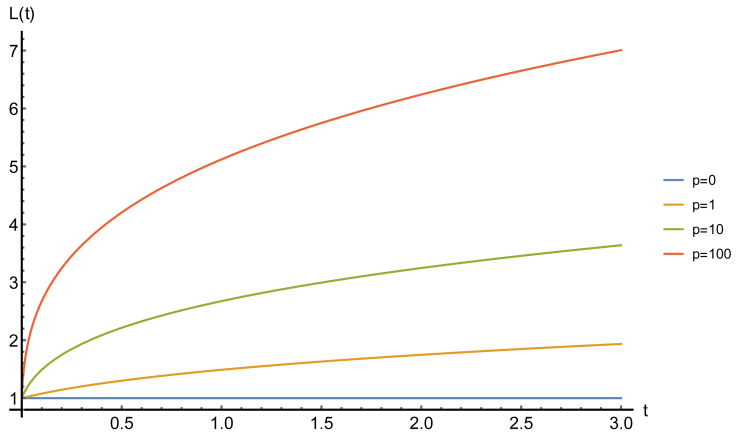


Figure 4.11: Graphs illustrating **(a)** the fracture half-width for different t at a fixed $p = \frac{2K}{5l_0} = 1$, **(b)** the fracture half-width for varying $p = \frac{2K}{5l_0}$ at $t = 1$ and **(c)** the fracture length for different $p = \frac{2K}{5l_0}$, where $\alpha = \frac{2}{7}$, corresponding to a constant fracture volume.

$$V(t) = \left(1 + \frac{7}{15}\frac{1}{G(0)^2}t\right) V_0, \tag{4.167}$$

$$V_0 = \frac{2}{G(0)}\int_0^1 G(u)du, \tag{4.168}$$

$$h(t,x) = \left(1 + \frac{7}{15}\frac{1}{G(0)^2}t\right)^{\frac{1}{7}} \frac{G(u)}{G(0)}. \tag{4.169}$$

Figure 4.12 illustrates the fracture half-width and fracture volume for a constant rate of change of volume, varying t values and the ratio $p = \frac{2K}{5l_0}$. As t or p increase, it can be noted that the fracture half-width as well as the length and volume increase.

4.3.6.3 *Constant fracture length change*

The rate that a fracture's length will increase over time is given by differentiating (4.104),

$$\frac{dL}{dt} = \frac{1}{G(0)^2}\left(\frac{2K}{5l_0}\right)\left(1 + \frac{1}{\alpha}\frac{1}{G(0)^2}\frac{2K}{5l_0}t\right)^{\alpha-1}. \tag{4.170}$$

Thus, the fracture length will change at a constant rate if $\alpha = 1$.

The problem is thus

$$\frac{d}{du}\left[G(u)^{\frac{5}{2}}\left(-\frac{dG}{du}\right)^{\frac{1}{2}} - uG(u)\right] + \frac{5}{4}G(u) = 0, \tag{4.171}$$

$$G(1) = 0, \tag{4.172}$$

$$\frac{5}{4}\int_0^1 G(u)du = G(0)^{\frac{5}{2}}\left(-\frac{dG}{du}(0)\right)^{\frac{1}{2}}, \tag{4.173}$$

$$G(u)^{\frac{5}{2}}\left(-\frac{dG}{du}\right)^{\frac{1}{2}}\Bigg|_{u=1} = 0, \tag{4.174}$$

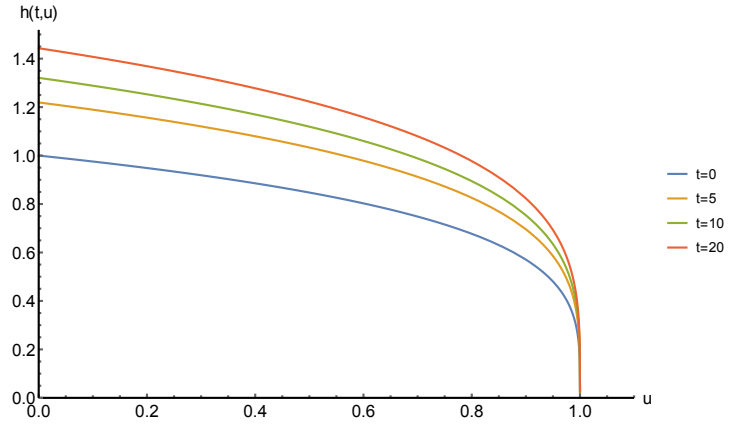
$$L(t) = \left(1 + \frac{2K}{5l_0}\frac{1}{G^2(0)}t\right), \tag{4.175}$$

$$V(t) = \left(1 + \frac{2K}{5l_0}\frac{1}{G^2(0)}t\right)^{\frac{5}{4}} V_0, \tag{4.176}$$

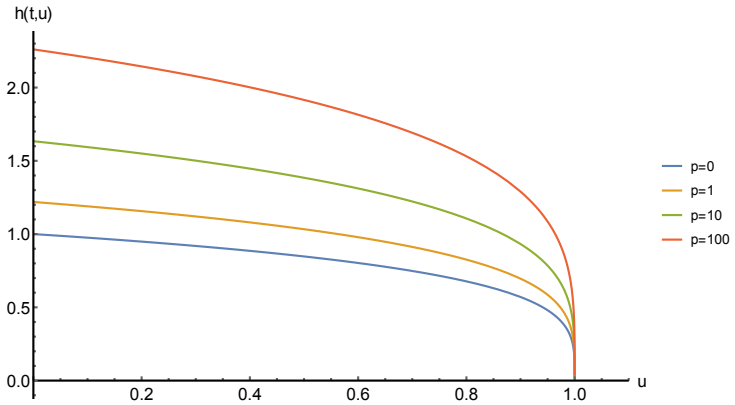
$$V_0 = \frac{2}{G(0)}\int_0^1 G(u)du, \tag{4.177}$$

$$h(t,x) = \left(1 + \frac{2K}{5l_0}\frac{1}{G^2(0)}t\right)^{\frac{1}{4}} \frac{G(u)}{G(0)}. \tag{4.178}$$

(a)



(b)



(c)

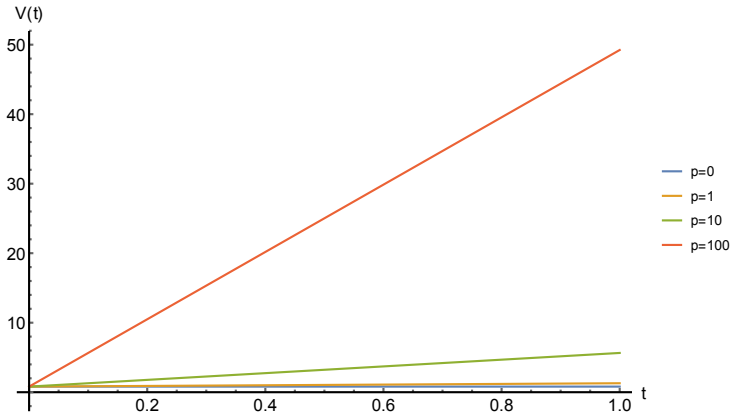


Figure 4.12: Graphs illustrating **(a)** the fracture half-width for different t at $p = \frac{2K}{5l_0} = 1$, **(b)** the fracture half-width for different $p = \frac{2K}{5l_0}$ at $t = 1$ and **(c)** the fracture volume for varying $p = \frac{2K}{5l_0}$, where $\alpha = 0.857143$, corresponding to a constant rate of change of volume.

Figure 4.13 illustrates the fracture half-width and fracture length, varying t values and the ratio $p = \frac{2K}{5l_0}$, for $\alpha = 1$. As expected, the fracture half-width increases with increase of t or p, as does the length. The length of the fracture clearly grows linearly, which is consistent with this value of α.

4.3.6.4 *Constant pressure at fracture entry*

As a result of the PKN approximation (3.63) used within this model, the pressure at the fracture entry is given by

$$\overline{p}(t,0) = \Lambda h(t,0) = \Lambda \left(1 + \frac{1}{\alpha}\frac{1}{G(0)^2}\frac{2K}{5l_0}t\right)^{\frac{3}{4}\alpha-\frac{1}{2}}. \tag{4.179}$$

Thus, the pressure at the fracture entry will remain constant for all time t if $\alpha = \frac{2}{3}$.

If $0 < \alpha < \frac{2}{3}$, this implies that pressure will decrease over time, whereas $\alpha > \frac{2}{3}$ results in increasing pressure over time.

For $\alpha = \frac{2}{3}$, the problem is summarised below:

$$\frac{d}{du}\left[G(u)^{\frac{5}{2}}\left(-\frac{dG}{du}\right)^{\frac{1}{2}}\right] - \frac{d}{du}\left(uG(u)\right) + G(u) = 0, \tag{4.180}$$

$$G(1) = 0, \tag{4.181}$$

$$\int_0^1 G(u)du = G(0)^{\frac{5}{2}}\left(-\frac{dG}{du}(0)\right)^{\frac{1}{2}}, \tag{4.182}$$

$$G(u)^{\frac{5}{2}}\left(-\frac{dG}{du}\right)^{\frac{1}{2}}\Bigg|_{u=1} = 0, \tag{4.183}$$

$$L(t) = \left(1 + \frac{3K}{5l_0}\frac{1}{G(0)^2}t\right)^{\frac{2}{3}}, \tag{4.184}$$

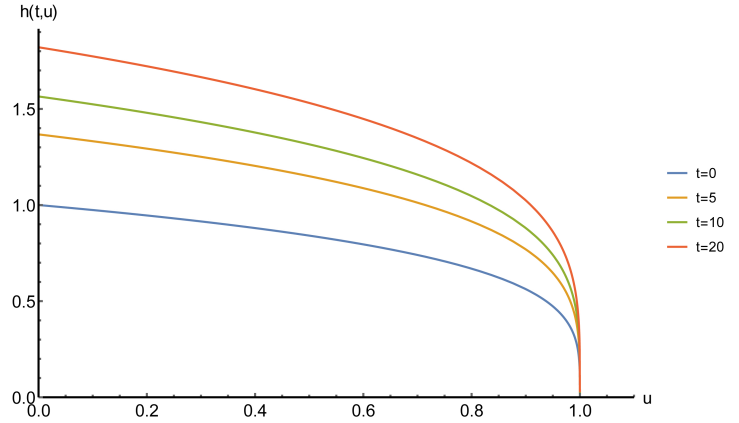
$$V(t) = \left(1 + \frac{3K}{5l_0}\frac{1}{G(0)^2}t\right)^{\frac{2}{3}} V_0, \tag{4.185}$$

$$V_0 = \frac{2}{G(0)}\int_0^1 G(u)du, \tag{4.186}$$

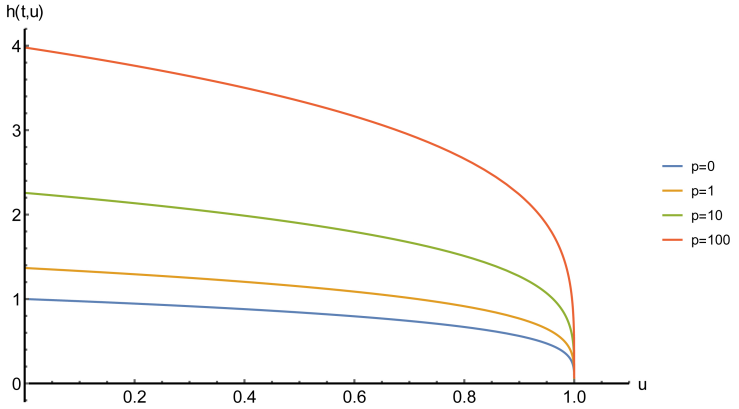
$$h(t,x) = \frac{G(u)}{G(0)}. \tag{4.187}$$

Figure 4.14 illustrates the fracture half-width, fracture length and fracture volume for various values of t and $p = \frac{2K}{5l_0}$, for constant pressure at the fracture entry. It can be noted that, as either t or p vary, the fracture half-width profile, when scaled by the length of the fracture $L(t)$, remains the

(a)



(b)



(c)

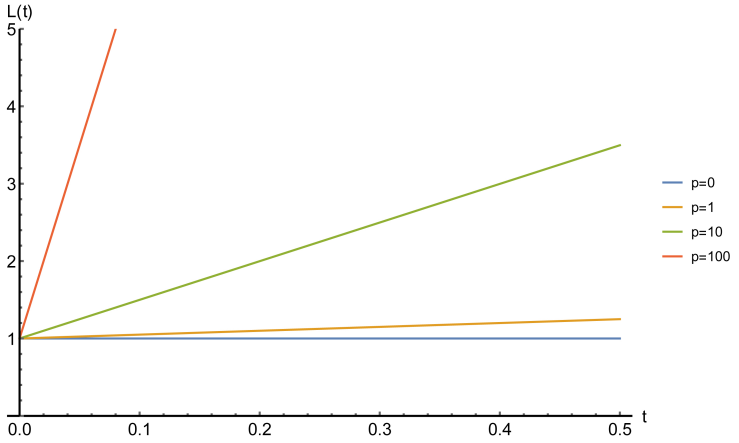


Figure 4.13: Graphs illustrating **(a)** the fracture half-width for different t for $p = \frac{2K}{5l_0} = 1$, **(b)** the fracture half-width for different values of $p = \frac{2K}{5l_0}$ at $t = 1$ and **(c)** the fracture length for varying $p = \frac{2K}{5l_0}$, where $\alpha = 1$, corresponding to a constant speed of propagation of the fracture.

same. However, the length is still growing with time. This implies that, as the fracture evolves, it retains the same profile when plotted against $u = \frac{x}{L(t)}$. This is consistent with $\alpha = \frac{2}{3}$ being the transitional value.

4.3.7 *Comparison of average fluid velocity and fracture length propagation speed*

Comparing the average fluid velocity across a fracture against the speed of propagation of the fracture can give additional insight.

From equation (3.61), the mean fluid velocity is given by

$$\bar{v}_x(t,x,z) = \frac{2K}{3l_0}(-h_x)^{\frac{1}{2}}\left[h^{\frac{3}{2}} - z^{\frac{3}{2}}\right], \quad 0 \leqslant z \leqslant h(t,x). \tag{4.188}$$

Since the fracture is thin, it makes sense in modelling to average this mean velocity across the upper half of the fracture.

The average x−component of the mean velocity over the upper half of the fracture, $\bar{v}_x^*$, is given by

$$\bar{v}_x^*(t,x) = \frac{1}{h}\int_0^h \bar{v}_x(t,x,z)\,dz, \tag{4.189}$$

yielding

$$\bar{v}_x^*(t,x) = \left(\frac{2K}{5l_0}\right)h^{\frac{3}{2}}(-h_x)^{\frac{1}{2}}. \tag{4.190}$$

Using the expressions for $h(t,u)$, (4.107), and $L(t)$, (4.104), this becomes

$$\bar{v}_x^*(t,x) = \left(\frac{2K}{5l_0}\right)L(t)^{1-\frac{1}{\alpha}}\frac{G(u)^{\frac{3}{2}}}{G^2(0)}\left(-\frac{dG}{du}\right)^{\frac{1}{2}}. \tag{4.191}$$

But, from (4.104),

$$\frac{dL}{dt} = \left(\frac{2K}{5l_0}\right)\frac{1}{G^2(0)}L(t)^{1-\frac{1}{\alpha}}. \tag{4.192}$$

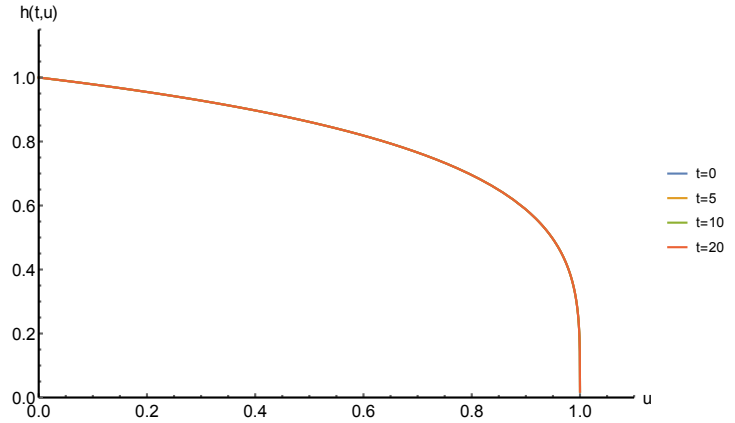
As a result, the ratio $\frac{\bar{v}_x^*}{L'(t)}$, which will be used for analysis, is given by

$$\frac{\bar{v}_x^*(t,x)}{L'(t)} = G(u)^{\frac{3}{2}}(-G'(u))^{\frac{1}{2}}. \tag{4.193}$$

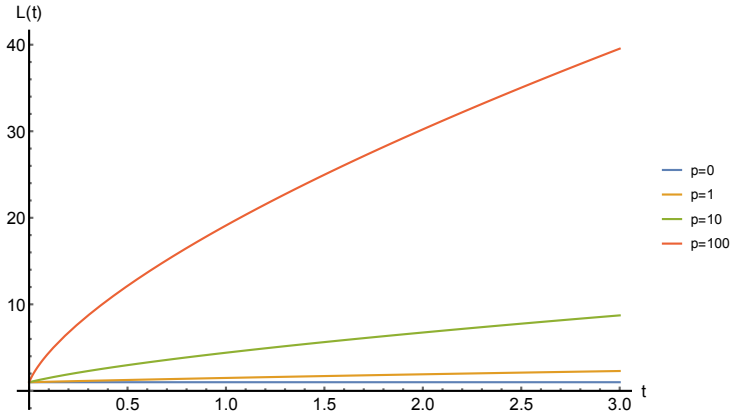
This expression depends solely on α.

Figure 4.15 illustrates the ratio $\frac{\bar{v}_x^*}{L'(t)}$ for different values of α. The values of $\alpha = \frac{2}{7}$ (constant volume) and $\alpha = 1$ (constant speed of propagation of

(a)



(b)



(c)

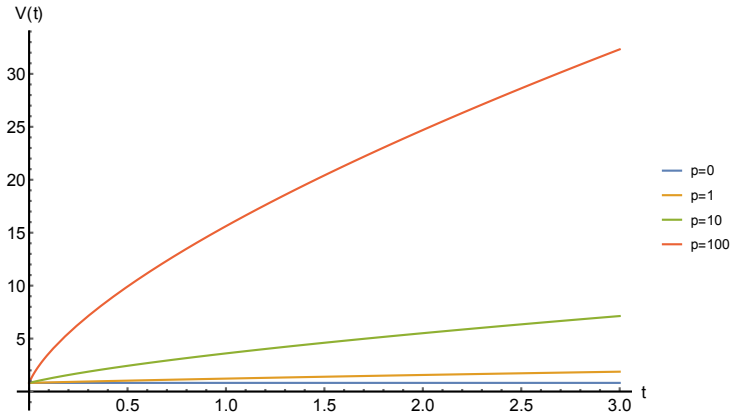


Figure 4.14: Graphs illustrating **(a)** the fracture half-width for different t at $p = \frac{2K}{5l_0} = 1$, **(b)** the fracture length for different $p = \frac{2K}{5l_0}$ and **(c)** the fracture volume for varying $p = \frac{2K}{5l_0}$, where $\alpha = \frac{2}{3}$, corresponding to a constant pressure at the fracture entry.

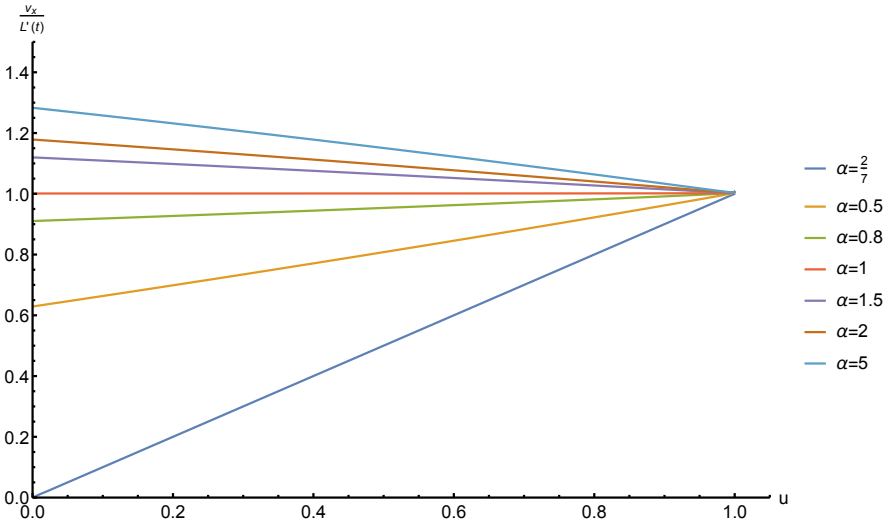


Figure 4.15: A graph illustrating the ratios $\frac{\overline{v}_x^*}{L'(t)}$ for $\alpha = \frac{2}{7}, 0.5, 0.8, 1, 1.5, 2$ and 5.

the fracture) have ratios which are perfectly straight lines. It can also be noted that this ratio results in plots for other α values that are approximately straight lines on the domain.

It can also be observed that, for $\alpha < 1$, the average mean fluid velocity across the fracture is slower than the speed of propagation of the fracture. However, as the fluid moves towards the fracture tip, this average velocity increases and equals the speed at which the tip propagates, which is as expected.

When $\alpha = 1$, the fracture length increases at a constant rate. The width average mean velocity of the fluid is constant along the length of the fracture and equals the speed of propagation of the fracture tip. It is for this reason that the ratio plot here is simply given by $\frac{\overline{v}_x^*}{L'(t)} = 1$, for all $0 \leqslant u \leqslant 1$.

When $\alpha > 1$ however, the average mean fluid velocity across the fracture is faster than the speed at which the fracture's length propagates. As the fluid moves towards the fracture tip, this average velocity decreases and tends to the speed at which the tip propagates.

4.3.7.1 *Approximate solutions derivable from the ratio* $\frac{\overline{v}_x^*}{L'(t)}$

As previously noted, the ratios corresponding to constant fracture volume ($\alpha = \frac{2}{7}$) and constant propagation speed of the fracture ($\alpha = 1$) are straight lines. All α values lying between these two result in ratios that are approximately straight lines. We can thus approximate these graphs for different α values as straight lines to derive an approximate expression for $\frac{\overline{v}_x^*}{L'(t)} = 1$ and thus also for $G(u)$.

Consider Figure 4.16. The line $\frac{\overline{v}_x^*}{L'(t)} = 1$ corresponds to $\alpha = 1$, and the line $\frac{\overline{v}_x^*}{L'(t)} = u$ corresponds to $\alpha = \frac{2}{7}$. We consider the approximate solution of

$\frac{\overline{v}_x^*}{L'(t)}$ for some $\frac{2}{7} < \alpha < 1$ as a straight line from $(0, q)$ to $(1, 1)$, where q remains to be determined. The exact analytic solution for $q = 1$ is known. We suppose $q \neq 1$, $0 < q < 1$.

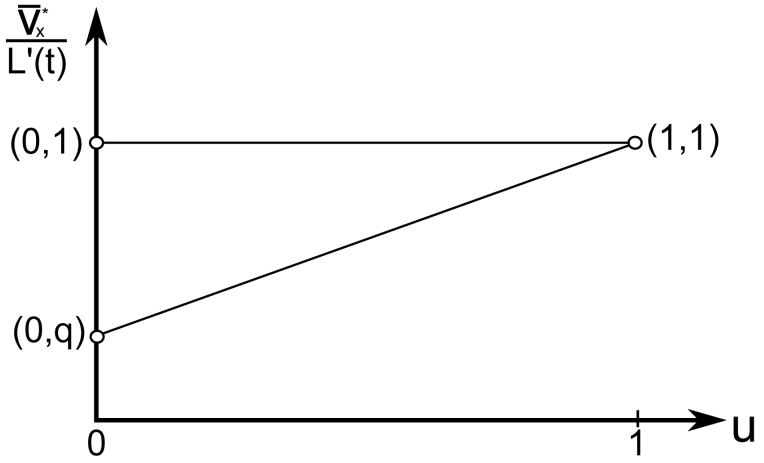


Figure 4.16: A figure illustrating the ratio graph for $\frac{\overline{v}_x^*}{L'(t)} = 1$ corresponding to $\alpha = 1$, and for $\frac{\overline{v}_x^*}{L'(t)}$ for some $\frac{2}{7} < \alpha < 1$.

This approximate expression is given by

$$\frac{\overline{v}_x^*}{L'(t)} = G(u)^{\frac{3}{2}}(-G'(u))^{\frac{1}{2}} = (1-q)u + q. \tag{4.194}$$

This is simply a first order, variable separable ODE for $G(u)$ which can be solved with the boundary condition $G(1) = 0$ to give

$$G(u) = \left(\frac{4}{3}\right)^{\frac{1}{4}} \frac{1}{(1-q)^{\frac{1}{4}}} \left[1 - ((1-q)u + q)^3\right]^{\frac{1}{4}}. \tag{4.195}$$

The value of q may now be determined using boundary condition (4.102). Substituting (4.195) into this boundary condition results in

$$q(1-q^3)^{\frac{1}{4}} = \left(\frac{7}{4} - \frac{1}{2\alpha}\right) \int_0^1 \left(1 - q^3 \left(\frac{(1-q)}{q}u + 1\right)^3\right)^{\frac{1}{4}} du. \tag{4.196}$$

This integral cannot be calculated directly. However, the bracket $\left(\frac{(1-q)}{q}u + 1\right)^3$ can be expanded and all terms of $\mathcal{O}(u^2)$ and higher can be neglected as they will be relatively small because $u \in [0,\ 1]$.

Neglecting these terms and integrating, results in

$$\left(\frac{7}{4} - \frac{1}{2\alpha}\right)\left(-\frac{(1+q-2q^2)^{\frac{5}{4}}}{(q^2+q+1)^{\frac{1}{4}}} + (q^2+q+1)\right) - \frac{15q^3}{4} = 0, \tag{4.197}$$

α	q	Maximum error between $\frac{\overline{v}_x^*}{L'(t)}$ and $(1-q)u+q$
0.3	0.0831342	0.0071933
0.4	0.472348	0.0414099
0.5	0.675717	0.0467463
0.6	0.797598	0.0416076
0.7	0.877342	0.032611
0.8	0.932516	0.0221714
0.9	0.971968	0.0111172

Table 4.4: A table showing the corresponding q value for each choice of α, where q is obtained by solving equation (4.197).

on condition that $0 < q < 1$, for convergence. This implies we may not use this approximate solution for $\alpha \geqslant 1$, as this will require $q \geqslant 1$.

Equation (4.197) can be solved numerically, once a value for α is specified. Table 4.4 shows the value of q for different values of α, and gives the maximum error between the approximate solution and actual ratio. Figure 4.17 illustrates this graphically.

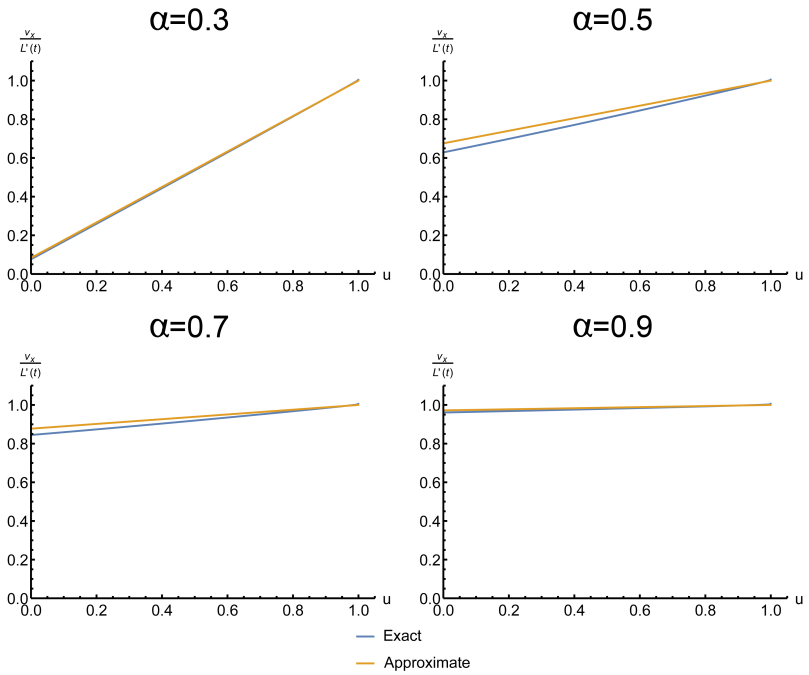


Figure 4.17: Graphs of $\frac{\overline{v}_x^*}{L'(t)}$ compared with their approximations $\alpha = 0.3$, $\alpha = 0.5$, $\alpha = 0.7$ and $\alpha = 0.9$.

It can be observed that for values of α near either of the straight line ratios (that is, $\alpha = \frac{2}{7}$ or $\alpha = 1$), the error is small. However, for values of α near the

middle of the interval $\left(\frac{2}{7}, 1\right)$, the error is comparatively large in magnitude and the approximate solution is less accurate.

Figures 4.18 and 4.19 illustrate the approximate $h(t,u)$ functions generated using this method against the solutions obtained numerically. It can be noted that the margin of error is generally quite small.

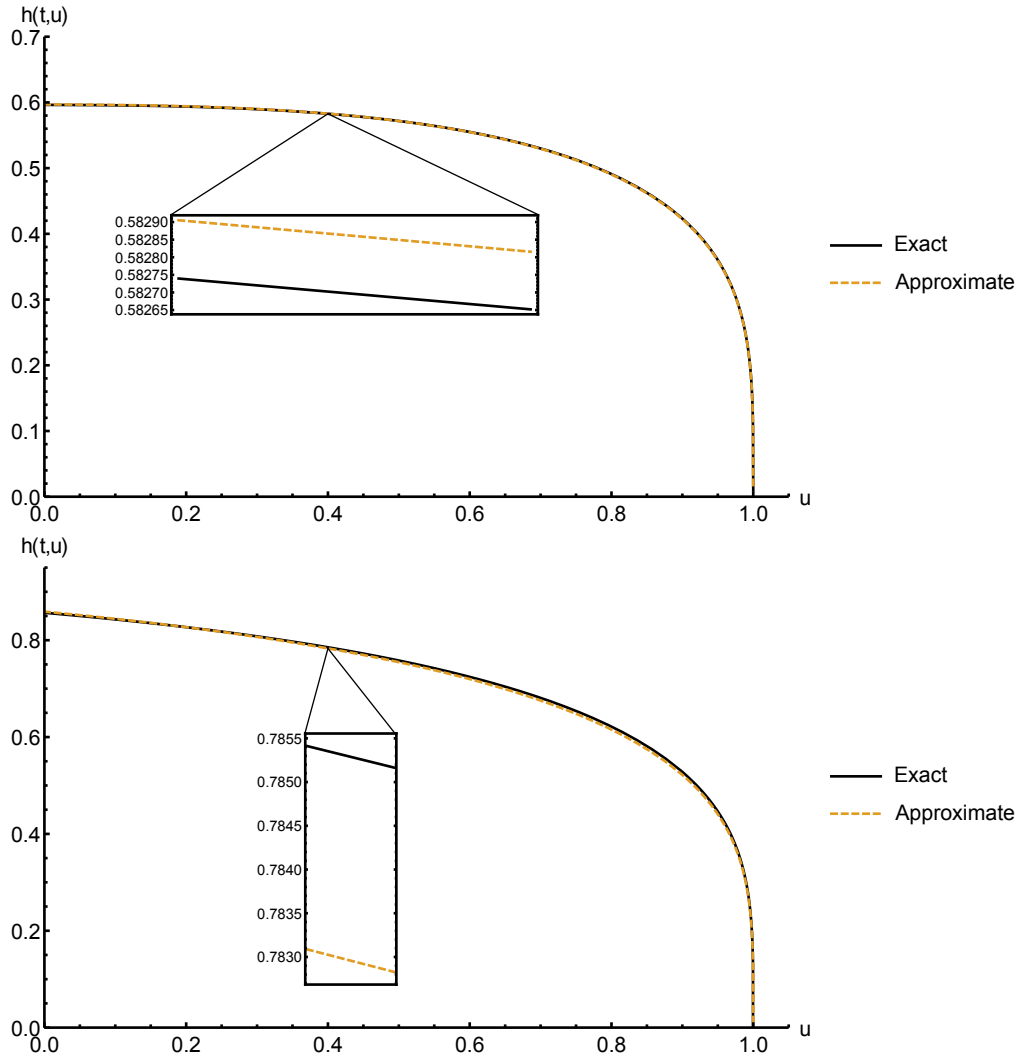


Figure 4.18: The numerical solution of $h(t,u)$ plotted against the approximate solution obtained for $\alpha = 0.3$ and $\alpha = 0.5$ respectively. Here, $t = 1$ and $p = 2$.

Similarly, approximate solutions for $\alpha > 1$ can be obtained for certain α, with reasonable accuracy. Figure 4.20 shows the scenario under consideration. Here, the α value is assumed to result in $p < 2$. Also, p is defined as $p = 1 + r$, for some $0 \leqslant r < 1$.

This has an approximate expression is given by

$$\frac{\overline{v}_x^*}{L'(t)} = G(u)^{\frac{3}{2}}(-G'(u))^{\frac{1}{2}} \approx -ru + (1 + r). \tag{4.198}$$

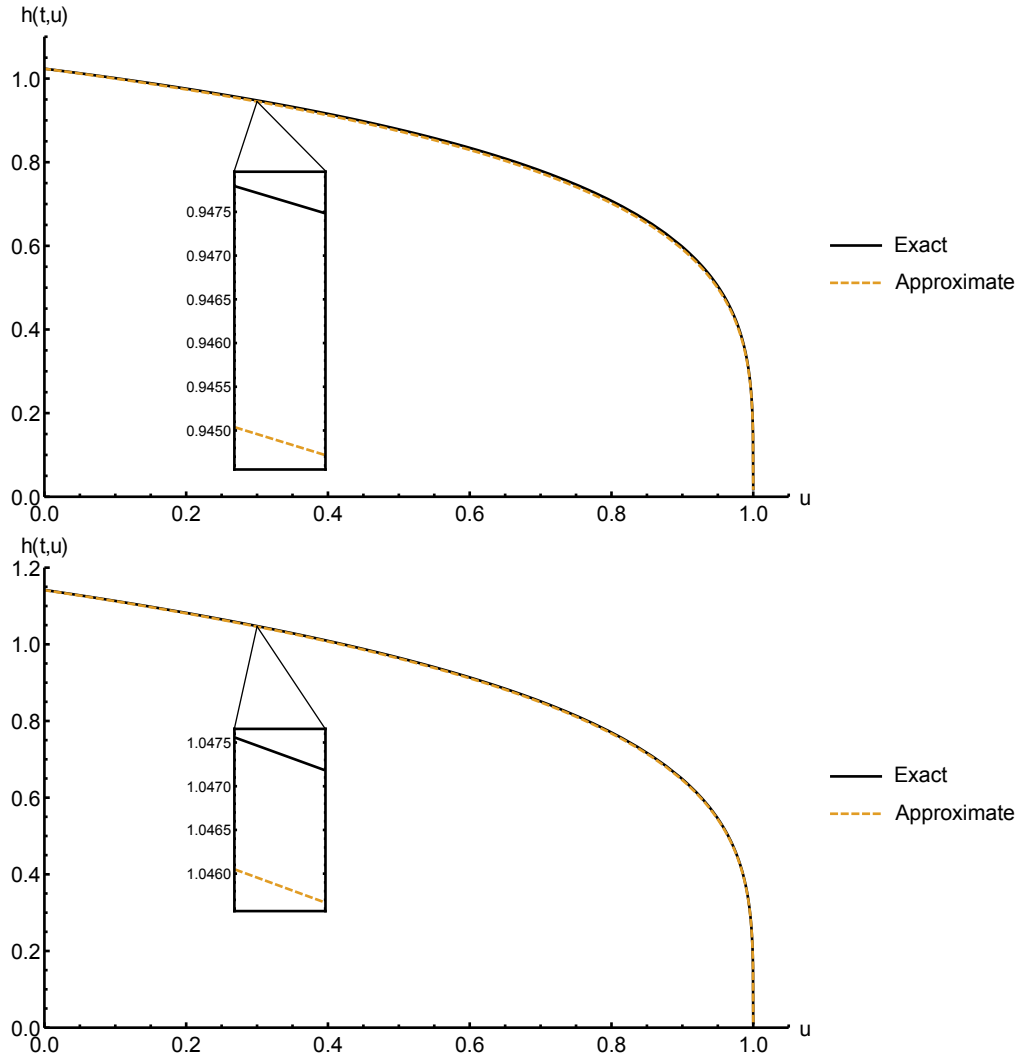


Figure 4.19: The numerical solution of $h(t,u)$ plotted against the approximate solution obtained for $\alpha = 0.7$ and $\alpha = 0.9$ respectively. Here, $t = 1$ and $p = 2$.

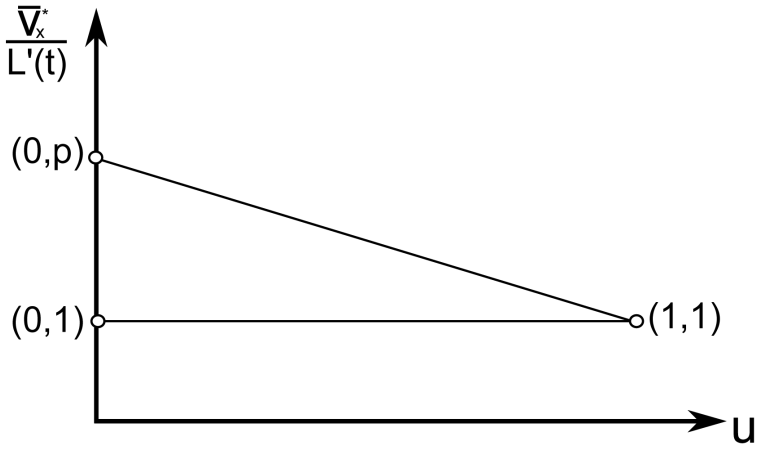


Figure 4.20: Illustration of the graph of the ratio $\frac{\bar{v}_x^*}{L'(t)} \geqslant 1$ plotted against u corresponding to $\alpha \geqslant 1$.

Solving this ODE for $G(u)$ results in the expression

$$G(u) = \left(\frac{4}{3}\right)^{\frac{1}{4}} \frac{1}{r^{\frac{1}{4}}} \left((1 + r(1-u))^3 - 1\right)^{\frac{1}{4}}. \tag{4.199}$$

Once again, using boundary condition (4.102),

$$\begin{aligned} &\left(\frac{4}{3}\right)^{\frac{1}{4}} \frac{(r+1)}{r^{\frac{1}{4}}} \left[(r+1)^3 - 1\right]^{\frac{1}{4}} \\ &= \left(\frac{7}{4} - \frac{1}{2\alpha}\right) \left(\frac{4}{3}\right)^{\frac{1}{4}} \frac{1}{r^{\frac{1}{4}}} \int_0^1 \left((1 + r(1-u))^3 - 1\right)^{\frac{1}{4}} du, \end{aligned} \tag{4.200}$$

allows the determination of r. No terms need to be neglected in order to analytically evaluate the integral, as

$$\begin{aligned} &\int_0^1 \left((1 + r(1-u))^3 - 1\right)^{\frac{1}{4}} du = \frac{4}{7r^{\frac{3}{4}}} 4 \Bigg((r+1)(r(r+3)+3)^{\frac{1}{4}} \\ &- \sqrt[4]{3}\,\text{AppellF}_1\left(\frac{1}{4}; \frac{3}{4}, \frac{3}{4}; \frac{5}{4}; -\frac{\sqrt[6]{-1}r}{\sqrt{3}}, \frac{(-1)^{5/6}r}{\sqrt{3}}\right)\Bigg), \end{aligned} \tag{4.201}$$

where AppellF_1 is Appell hypergeometric function.

The resulting equation from boundary condition (4.102) can be solved numerically for various values of α. Table 4.5 shows the value of q for different values of α, and gives the maximum error between the approximate solution and actual ratio.

Figure 4.21 illustrates the approximate result for the half-width $h(t,u)$ generated using this method against the solutions obtained numerically. Once again, it can be noted that the margin of error is reasonably small.

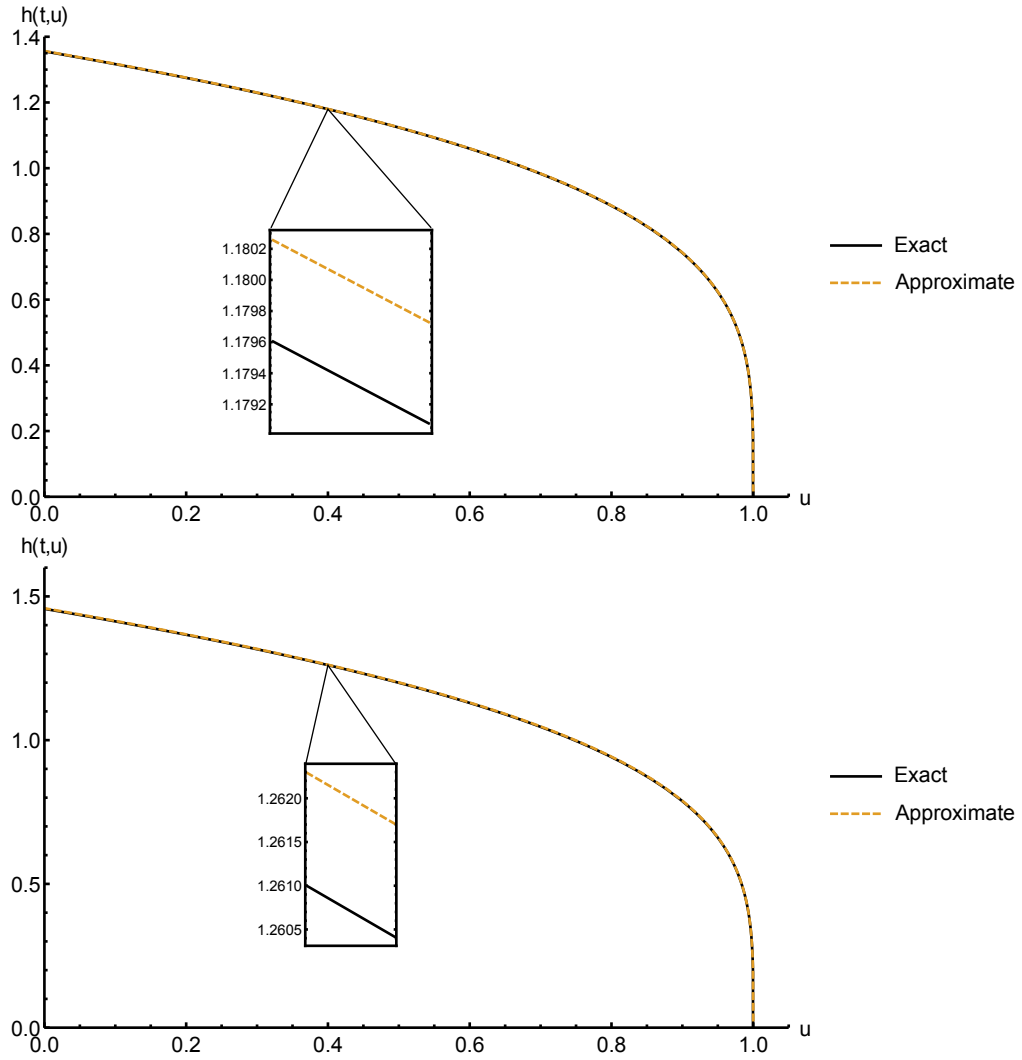


Figure 4.21: The numerical solution of $h(t,u)$ plotted against the approximate solution obtained for $\alpha = 1.5$ and $\alpha = 2$ respectively. Here, $t = 1$ and $p = 2$.

α	r
1	0
1.1	0.0326424
1.2	0.059718
1.3	0.0825415
1.4	0.102043
1.5	0.1189
1.6	0.133616
1.7	0.146575
1.8	0.158075
1.9	0.168349
2.	0.177583

Table 4.5: The value of r for each choice of α.

4.3.8 *Special symmetry solutions*

Considering special cases of the Lie point symmetry generator, (4.49), can yield additional solutions. One such solution is obtained by letting the constants c_1, c_3 and c_5 be equal to zero.

Letting $c_1 = c_3 = c_5 = 0$ results in the Lie point symmetry generator,

$$X = c_2 \frac{\partial}{\partial t} + c_4 \frac{\partial}{\partial x}. \tag{4.202}$$

From (A.52), the mixing length is constant, $l(x) = l_0$.

A function $h(t,x) = \psi(t,x)$ is a group invariant solution of the partial differential equation (3.65) provided condition (4.51) holds. This results in the partial differential equation,

$$c_2 \frac{\partial \psi}{\partial t} + c_4 \frac{\partial \psi}{\partial x} = 0. \tag{4.203}$$

The differential equations describing the characteristic curves of (4.203) are given by

$$\frac{dt}{c_2} = \frac{dx}{c_4} = \frac{d\psi}{0}. \tag{4.204}$$

Considering the first differential equation and solving results in the invariant,

$$I_1 = x - \frac{c_4}{c_2} t. \tag{4.205}$$

The second invariant is given by

$$I_2 = \psi(t,x). \tag{4.206}$$

A group invariant solution of (4.203) is of the form $I_2 = F(I_1)$, where F is an arbitrary function. Remembering that $h(t,x) = \psi(t,x)$, this solution is given by

$$h(t,x) = F(\gamma), \tag{4.207}$$

where

$$\gamma = x - \frac{c_4}{c_2}t. \tag{4.208}$$

Substituting the group invariant solution into PDE (3.65) reduces it to an ODE given by

$$\frac{d}{d\gamma}\left[\frac{2K}{5l_0}F(\gamma)^{\frac{5}{2}}\left(-\frac{dF}{d\gamma}\right)^{\frac{1}{2}} - \frac{c_4}{c_2}F(\gamma)\right] = 0. \tag{4.209}$$

Boundary condition (3.49) also reduces to

$$F\left(L(t) - \frac{c_4}{c_2}t\right) = 0. \tag{4.210}$$

Differentiating (4.210) with respect to t results in

$$\left(\frac{dL}{dt} - \frac{c_4}{c_2}\right)\frac{dF}{d\gamma} = 0. \tag{4.211}$$

Since $\frac{dF}{d\gamma} \neq 0$,

$$\frac{dL}{dt} = \frac{c_4}{c_2}, \tag{4.212}$$

and so

$$L(t) = C + \frac{c_4}{c_2}t, \tag{4.213}$$

where C is a constant to be determined. Since $L(0) = 1$, it follows that $C = 1$, and thus

$$L(t) = 1 + \frac{c_4}{c_2}t. \tag{4.214}$$

Substituting (4.214) into boundary condition (4.210) further reduces it to

$$F(1) = 0. \tag{4.215}$$

The second boundary condition at the fracture tip is that the volume flux vanishes;

$$h^{\frac{5}{2}}(t,x)\left(-\frac{\partial h}{\partial x}(t,x)\right)^{\frac{1}{2}}\Bigg|_{x=L(t)} = 0, \tag{4.216}$$

and therefore

$$F^{\frac{5}{2}}(\gamma)\left(-\frac{dF}{d\gamma}(\gamma)\right)^{\frac{1}{2}}\Bigg|_{\gamma=1}=0. \tag{4.217}$$

Now, ODE (4.209) can be integrated once in conjunction with (4.215) and (4.217) to obtain

$$\frac{2K}{5l_0}F(\gamma)^{\frac{5}{2}}\left(-\frac{dF}{d\gamma}\right)^{\frac{1}{2}}-\frac{c_4}{c_2}F(\gamma)=0. \tag{4.218}$$

This can be further integrated to obtain

$$F(\gamma)=\left(D-\left(\frac{c_4}{c_2}\right)^2\left(\frac{5l_0}{K}\right)^2\gamma\right)^{\frac{1}{4}}, \tag{4.219}$$

where D is a constant. Using boundary condition (4.215), it can be shown that

$$F(\gamma)=\left(\frac{c_4}{c_2}\right)^{\frac{1}{2}}\left(\frac{5l_0}{K}\right)^{\frac{1}{2}}(1-\gamma)^{\frac{1}{4}}. \tag{4.220}$$

Since

$$\gamma=x-\frac{c_4}{c_2}t=1+x-L(t), \tag{4.221}$$

(4.220) for $F(\gamma)$ becomes

$$F(\gamma)=\left(\frac{c_4}{c_2}\right)^{\frac{1}{2}}\left(\frac{5l_0}{K}\right)^{\frac{1}{2}}(L(t)-x)^{\frac{1}{4}}. \tag{4.222}$$

Defining the variable $u=\frac{x}{L(t)}$ allows the half-width to reduce to

$$h(t,u)=F(u)=\left(\frac{c_4}{c_2}\right)^{\frac{1}{2}}\left(\frac{5l_0}{K}\right)^{\frac{1}{2}}(1-u)^{\frac{1}{4}}. \tag{4.223}$$

Using boundary condition (3.51) that $h(0,0)=1$, it follows that

$$\frac{c_4}{c_2}=\frac{K}{5l_0}. \tag{4.224}$$

Thus,

$$h(t,u)=L(t)^{\frac{1}{4}}(1-u)^{\frac{1}{4}}, \tag{4.225}$$

$$L(t)=1+\frac{K}{5l_0}t, \tag{4.226}$$

and

$$V(t)=2\int_0^{L(t)}h(t,x)dx=\frac{8}{5}\left(1+\frac{K}{5l_0}t\right)^{\frac{5}{4}}. \tag{4.227}$$

These results agree with the results derived in Subsection 4.3.1.2.

4.4 Non-classical Symmetries

The non-classical symmetry analysis of equation (3.65) with $l(x) = l_0$ is completed in Appendix A.2. The mixing length was chosen to be constant to avoid the same problem with the balance law, (4.102), as obtained in Section 4.2. The non-classical symmetry generator of equation (3.65) is given by

$$X = \frac{\partial}{\partial t} + (a(t)x + b(t))\frac{\partial}{\partial x} + c(t)h\frac{\partial}{\partial h}, \tag{4.228}$$

where $a(t)$, $b(t)$ and $c(t)$ satisfy the equations

$$2a'(t) + (3a(t) - 4c(t))a(t) = 0, \tag{4.229}$$

$$2b'(t) + (3a(t) - 4c(t))b(t) = 0, \tag{4.230}$$

$$2c'(t) + (3a(t) - 4c(t))c(t) = 0. \tag{4.231}$$

Any solutions of the above equations give non-classical symmetries of equation (3.65). The most interesting, special case will be considered in this section.

4.4.1 *Case:* $a(t) = c(t) = 0$

Letting $a(t) = c(t) = 0$ results in $b'(t) = 0$, whose solution is a constant. As a result, the symmetry generator (4.228) becomes

$$X = \frac{\partial}{\partial t} + c_1\frac{\partial}{\partial x}. \tag{4.232}$$

Eliminating $\frac{\partial h}{\partial t}$ from equation (3.65) by using the invariant surface condition (A.57), which becomes

$$\frac{\partial h}{\partial t} = -c_1\frac{\partial h}{\partial x}, \tag{4.233}$$

results in the differential equation

$$\frac{2K}{5l_0}\frac{\partial}{\partial x}\left(h^{\frac{5}{2}}\left(-\frac{\partial h}{\partial x}\right)^{\frac{1}{2}}\right) = c_1\frac{\partial h}{\partial x}. \tag{4.234}$$

This can be integrated to give

$$\frac{2K}{5l_0}\left(h^{\frac{5}{2}}\left(-\frac{\partial h}{\partial x}\right)^{\frac{1}{2}}\right) - c_1 h + q(t) = 0, \tag{4.235}$$

where $q(t)$ is a function of time to be determined by the boundary conditions. Upon enforcing the condition $h(t, L(t)) = 0$ and the no flux condition at the fracture tip, $h^{\frac{5}{2}}\left(-\frac{\partial h}{\partial x}\right)^{\frac{1}{2}}\Big|_{x=L(t)} = 0$, we find $q(t) = 0$.

The resulting equation may be written as

$$\frac{\partial}{\partial x}(h^4) = -\left(\frac{5l_0 c_1}{K}\right)^2. \tag{4.236}$$

Solving this and implementing $h(t, L(t)) = 0$ again gives

$$h(t,x) = \pm\left(\frac{5l_0 c_1}{K}\right)^{\frac{1}{2}} L(t)^{\frac{1}{4}} \left(1 - \frac{x}{L(t)}\right)^{\frac{1}{4}}. \tag{4.237}$$

We take the positive root because we consider the upper half of the fracture.

We now implement the condition $h(0,0) = 1$ and $L(0) = 1$, giving

$$c_1 = \frac{K}{5l_0}. \tag{4.238}$$

Making the transformation

$$u = \frac{x}{L(t)}, \tag{4.239}$$

reduces (4.237) for $h(t,x)$ to

$$h(t,u) = L(t)^{\frac{1}{4}} (1-u)^{\frac{1}{4}}. \tag{4.240}$$

We may now substitute this expression for $h(t,x)$ back into the invariant surface condition (A.57) and obtain the fracture length. This gives the differential equation

$$L'(t) = c_1, \tag{4.241}$$

which when solved with the initial condition $L(0) = 1$ gives

$$L(t) = 1 + c_1 t, \tag{4.242}$$

where c_1 is given by (4.238).

We may also obtain the volume of the fracture from (4.67) using $h(t,x)$ and $L(t)$, giving

$$V(t) = \frac{8}{5}(1 + c_1 t)^{\frac{5}{4}}. \tag{4.243}$$

Finally, it can be shown that the balance law at the fracture entry (4.102) is satisfied by these results.

Thus, this case can be summarized into the following equations:

$$L(t) = 1 + \frac{K}{5l_0} t, \tag{4.244}$$

$$h(t,u) = L(t)^{\frac{1}{4}} (1-u)^{\frac{1}{4}}, \tag{4.245}$$

$$V(t) = \frac{8}{5}\left(1 + \frac{K}{5l_0} t\right)^{\frac{5}{4}}. \tag{4.246}$$

Figure 4.22 illustrates the fracture half-width, length and volume over a range of parameters. This solution is exactly the same as the second exact analytical solution derived in Section 4.3.1.2 and as the special symmetry solution derived in Section 4.3.8.

It can be noted that the solution of $h(t,u)$ (equation (4.245)) is very similar in form to asymptotic solutions obtained in many mathematical hydraulic fracturing studies [2, 15, 17], that take the form

$$h(t,u) = L(t)^n(1-u)^n, \tag{4.247}$$

for some n. The asymptotic solution derived in Section 4.3.2 is a special case for $n = \frac{1}{4}$.

The non-classical symmetry (4.232) is also a Lie point symmetry. It is a special case of the Lie point symmetry (4.49) with $c_1 = c_3 = c_5 = 0$ and it is the same as the Lie point symmetry (4.202) considered in Section 4.3.8.

The solution for $h(t,x)$ given in this section and Section 4.3.8 are systematic derivations. Previous derivations of results of this form [2, 15, 17] used the ad-hoc method described in Section 4.3.2.

4.4.2 *Other non-classical symmetry cases*

It can be noted that there are many possible solutions to equations (4.231)-(4.230), giving many additional non-classical symmetries. However, upon eliminating $\frac{\partial h}{\partial t}$ from the resulting invariant surface condition and the original PDE, the resulting equations are complex to solve, requiring much additional manipulation. These will not be considered within this body of work.

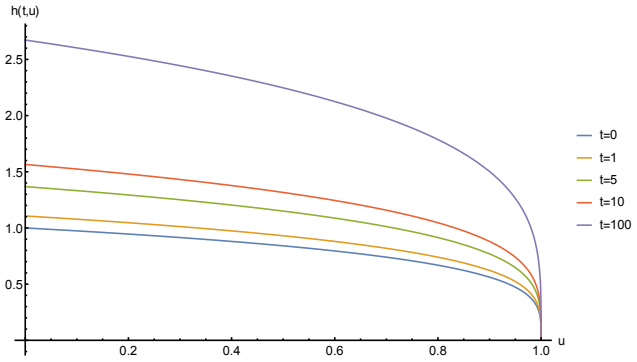
4.5 Analysis of results and conclusions

In this chapter, the conserved vectors of equation (3.65) were investigated. For the multiplier and conserved vectors considered, it was found that only the elementary conserved vector was admitted, yielding no extra information.

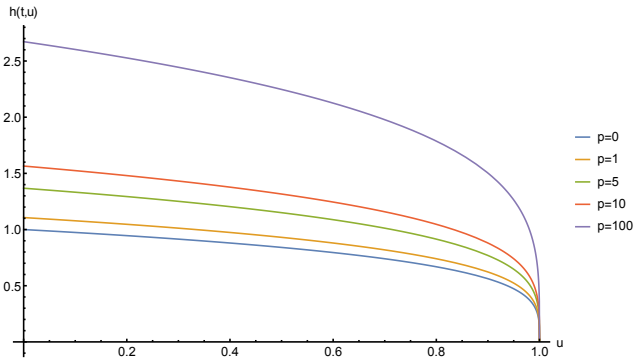
The Lie point symmetries of equation (3.65) were then obtained and a group invariant solution found. This solution was used to construct a set of expressions for the fracture half-width, length and volume, and the equations governing their dynamics.

Interestingly, it was found that the only viable mixing length usable in this model was a constant mixing length. This is justifiable physically because the fracture width is much less than the fracture length, thus not allowing for change in the transverse direction to occur.

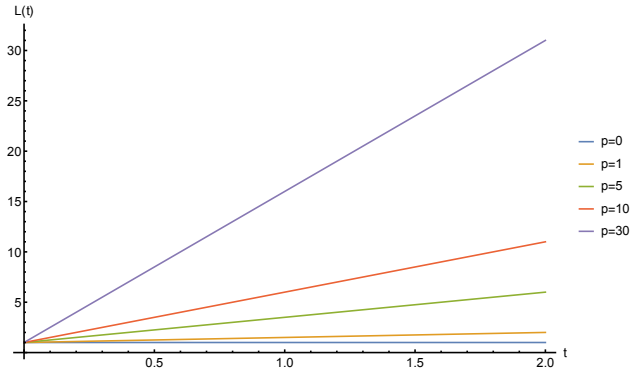
(a)



(b)



(c)



(d)

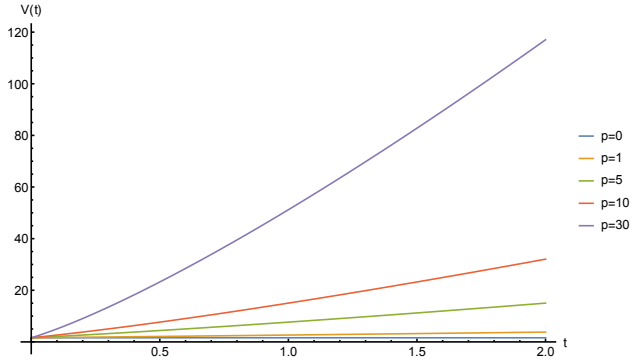


Figure 4.22: Graphs illustrating the non-classical symmetry solution for **(a)** the fracture profile for $p = \frac{2K}{5l_0} = 1$, **(b)** the fracture profile for $t = 1$, **(c)** the fracture length and **(d)** the fracture volume.

The fracture properties were then expressed in such a manner that they only depended on two parameters, for simpler analysis. These parameters were:

1. The working parameter α. This parameter relates back to the fluid pressure used at the fracture entrance and directly influences the fracture's half-width.

2. The ratio $p = \frac{2K}{5l_0}$. This ratio contains two important pieces of information. Firstly, it encapsulates the mixing length, thus allowing to partially capture the turbulence severity within the flow. It also captures the effective diffusion constant $K = E_0\Lambda$, where E_0 is the initial characteristic eddy viscosity, and Λ is a parameter relating the pressure and half-width. Here, Λ is given by (3.64) and it depends on the Young's modulus, Poisson ratio of the rock and the breadth of the fracture [14, 15]. Since K is partly determined by the rock in which the fracturing occurs, focus was placed on the effect of l_0 and how change of this parameter affected the half-width.

Numerical solutions were then computed, allowing the illustration of the fracture half-width, length and volume. From these graphs, a few interesting observations could be made.

Smaller values of α resulted in smaller fracture gradients at the fracture entry. This greatly determined the trajectory the fracture would form and thus influence the overall fracture profile.

The value $\alpha = \frac{2}{3}$ was also found to have very special significance. It not only corresponds to the values for which the pressure at the fracture entry remains constant, but it is also a reference value by which fracture behaviour can be determined. The fracture half-width evolves differently depending on whether α is greater or smaller than $\frac{2}{3}$.

This property is exhibited by the mathematical expression of the half-width (4.107), because it is the value of α that makes the time dependent component of the half-width vanish. For $\alpha < \frac{2}{3}$, the fracture half-width will narrow over time. However, for $\alpha > \frac{2}{3}$, the half-width will increase over time.

This feature is likely related back to how α affects the pressure at the fracture entrance. It is trivial to verify that for $\alpha > \frac{2}{3}$, the fluid entry pressure is increasing over time, whereas it decreases for $\alpha < \frac{2}{3}$. This relates directly to the half-width. For $\alpha < \frac{2}{3}$, this thus corresponds to pressures that are sufficient to initiate and propagate the fracture, but that are not strong enough to both extend the fracture and enlarge the half-width. Values of $\alpha > \frac{2}{3}$ likewise correspond to entrance pressures that are strong enough to not only extend the fracture but its half-width as well.

Similar effects are visible in changes of the parameter p. For $\alpha < \frac{2}{3}$, when the fluid flow is more turbulent (i.e. p is small), the fracture half-width is initially larger than if there were less turbulence. However, this half-width will still decrease rapidly with time. When $\alpha > \frac{2}{3}$ and the flow is more turbulent, the

fracture half-width increases over time, possibly due to the amount of energy turbulent flow loses. This result may be due to some relation between α and the amount of turbulence in the fluid flow, that influences how the energy in the flow is dissipated, thus influencing fracture behaviour.

The value $\alpha = \frac{2}{7}$ was also of importance. This corresponds to a constant fracture volume over time, while still resulting in fracture length growth. It can be noted that for $\alpha > \frac{2}{7}$ the fracture's volume will experience growth. As a result, generally $\alpha \geqslant \frac{2}{7}$ for practical purposes, because smaller α values will correspond to a decreasing fracture volume, meaning that fluid is being extracted instead of pumped in.

The ratio of the width averaged mean fluid velocity in the x-direction to the speed of growth of the fracture length,

$$\frac{\overline{v}_x^*}{L'(t)} = G(u)^{\frac{3}{2}}(-G'(u))^{\frac{1}{2}}, \tag{4.248}$$

was also calculated. This ratio gives an indication of how the average fluid velocity compares to the velocity of the tip of the fracture, which is the velocity of propagation of the fracture. It was found that $\alpha < 1$ resulted in fluid with a width average mean velocity slower than the propagation velocity of the fracture, while $\alpha > 1$ resulted in the opposite effect.

Another interesting result that emerged was that these velocity ratios were approximately linear in nature, irrespective of the value of $\alpha \in \left[\frac{2}{7}, 5\right]$ examined. Because of this ratio's relation to the function $G(u)$, an approximate solution for $G(u)$ could be constructed, for some α. These approximate solutions behaved incredibly well when compared with to the numerical solutions, with minimal error.

The non-classical symmetries of equation (3.65) were also investigated. While these were complicated and involved to calculate in general, one simple case could be solved relatively easily using analytical methods. This non-classical symmetry is a special case of the Lie point symmetry of the partial differential equation. It yielded the result (4.245) which mimics the form of asymptotic solutions obtained in this field of research. However, it was obtained systematically rather than through the ad-hoc asymptotic method, which is an important result.

Comparing this work with previous turbulent fracturing work carried out in [2] also gives some interesting insight. In [2], the turbulence was introduced through a Blasius wall shear stress at the fracture boundaries. The closest correspondence from [2] to this body of work is given when rough walled turbulence is studied, resulting in the fracture half-width equation

$$\frac{\partial h}{\partial t} + D\frac{\partial}{\partial x}\left(h^{\frac{3}{2}}\left(-\frac{\partial h}{\partial x}\right)^{\frac{1}{2}}\right) = 0. \tag{4.249}$$

Here, D depends some of the fracture's characteristic quantities and the fluid properties, as does $\frac{2K}{5l_0}$, which depends on the mixing length, the character-

istic effective viscosity E_0, and the rock's material properties. The parameter D allows for analysis to be considered on a wide range of turbulent flows. The qualitative features of the two models for the evolution of a hydraulic fracture with turbulent flow are the same [2]. A quantitative comparison can only be done for specific fractures once the physical properties of the fluid and rock mass have been given.

5

TRANSITIONAL TURBULENCE MODEL ANALYSIS

In this chapter, equation (3.74) will be examined. A similar analysis and discussion as in chapter 4 will be performed.

5.1 Conservation laws

Consider equation (3.74), written as

$$F(t, x, h, h_t, h_x, h_{xx}) = 0, \tag{5.1}$$

where

$$\begin{aligned} &F(t, x, h, h_t, h_x, h_{xx}) \\ &= h_t - K\left(\frac{2}{5}\frac{l'(x)}{l^2(x)}h^{\frac{5}{2}}(-h_x)^{\frac{1}{2}} + \frac{1}{l(x)}h^{\frac{3}{2}}(-h_x)^{\frac{3}{2}} + \frac{1}{5}\frac{1}{l(x)}h^{\frac{5}{2}}(-h_x)^{-\frac{1}{2}}h_{xx}\right) \\ &\quad + \frac{\nu}{2}\left(\frac{l'(x)}{l(x)^3}h^2 + \frac{1}{l(x)^2}h(-h_x)\right). \end{aligned} \tag{5.2}$$

Consider a multiplier of the form $\Lambda = \Lambda(t, x, h)$. We will look for a conserved vector with components of the form

$$T^i = T^i(t, x, h, h_t, h_x), \qquad i = 1,\ 2. \tag{5.3}$$

Using equation (4.5), the following equation is obtained:

$$\begin{aligned} &\frac{\partial T^1}{\partial t} + h_t\frac{\partial T^1}{\partial h} + h_{tt}\frac{\partial T^1}{\partial h_t} + h_{tx}\frac{\partial T^1}{\partial h_x} + \frac{\partial T^2}{\partial x} + h_x\frac{\partial T^2}{\partial h} + h_{tx}\frac{\partial T^2}{\partial h_t} + h_{xx}\frac{\partial T^2}{\partial h_x} \\ &-\Lambda(t, x, h)\left[h_t - K\left(\frac{2l'(x)}{5l(x)^2}h^{\frac{5}{2}}(-h_x)^{\frac{1}{2}} + \frac{1}{l(x)}h^{\frac{3}{2}}(-h_x)^{\frac{3}{2}}\right.\right. \\ &\left.\left. + \frac{1}{5l(x)}h^{\frac{5}{2}}(-h_x)^{-\frac{1}{2}}h_{xx}\right)\right] - \Lambda(t, x, h)\frac{\nu}{2}\left[\frac{l'(x)}{l(x)^3}h^2 + \frac{1}{l(x)^2}h(-h_x)\right] = 0, \end{aligned} \tag{5.4}$$

which is satisfied for all functions $h(t, x)$.

By a similar procedure as outlined in Section 4.1, it can be proved that $\Lambda = c_1$, and the components of the conserved vector are thus given by

$$T^1(t, x, h, h_x) = -C(t, x, h)h_x + B(t, x, h), \tag{5.5}$$

$$T^2(t, x, h, h_t, h_x) = \frac{2K}{5l(x)}c_1h^{\frac{5}{2}}(-h_x)^{\frac{1}{2}} + C(t, x, h)h_t + D(t, x, h), \tag{5.6}$$

where

$$\frac{\partial D}{\partial h} - \frac{\partial C}{\partial t} + \frac{\nu}{2}\frac{c_1}{l(x)^2}h = 0 \tag{5.7}$$

$$c_1 = \frac{\partial B}{\partial h} + \frac{\partial C}{\partial x}, \tag{5.8}$$

$$\frac{\partial B}{\partial t} + \frac{\partial D}{\partial x} - c_1\frac{\nu}{2}\frac{l'(x)}{l(x)^3}h^2 = 0. \tag{5.9}$$

From these equations, we can solve for $B(t,x,h)$ and $D(t,x,h)$ to obtain

$$B(t,x,h) = c_1 h + E(t,x) - \frac{\partial}{\partial x}F(t,x,h), \tag{5.10}$$

$$D(t,x,h) = -\frac{h^2\nu}{4l(x)^2}c_1 + \frac{\partial}{\partial t}F(t,x,h) + G(t,x), \tag{5.11}$$

where

$$F(t,x,h) = \int^h C(t,x,\bar{h})d\bar{h}. \tag{5.12}$$

Substituting (5.10) and (5.11) into the remaining determining equation (5.9) gives the condition

$$\frac{\partial E}{\partial t} + \frac{\partial G}{\partial x} = 0. \tag{5.13}$$

Equations (5.5) and (5.6) take the form

$$T^1(t,x,h,h_x) = c_1 h + T^1_*(t,x,h,h_x), \tag{5.14}$$

$$T^2(t,x,h,h_t,h_x) = c_1\left(\frac{2K}{5l(x)}h^{\frac{5}{2}}(-h_x)^{\frac{1}{2}} - \frac{\nu}{4l(x)^2}h^2\right) + T^2_*(t,x,h,h_t), \tag{5.15}$$

where

$$T^1_*(t,x,h,h_x) = -C(t,x,h)h_x + E(t,x) - \frac{\partial F(t,x,h)}{\partial x}, \tag{5.16}$$

$$T^2_*(t,x,h,h_t) = C(t,x,h)h_t + \frac{\partial F(t,x,h)}{\partial t} + G(t,x), \tag{5.17}$$

with $E(t,x)$ and $G(t,x)$ satisfying (5.13). But, as in Section 4.1,

$$D_1 T^1_* + D_2 T^2_* \equiv 0, \tag{5.18}$$

using (5.13), but without using the PDE (5.2). Thus, $\underline{\mathbf{T}} = (T^1_*,\ T^2_*)$ is a trivial conserved vector and we can set

$$T^1_* = 0, \qquad T^2_* = 0. \tag{5.19}$$

Equations (5.14) and (5.15) reduce to

$$T^1(h) = c_1 h, \tag{5.20}$$

$$T^2(x, h, h_x) = c_1 \left(\frac{2K}{5l(x)} h^{\frac{5}{2}} (-h_x)^{\frac{1}{2}} - \frac{\nu}{4l(x)^2} h^2 \right). \tag{5.21}$$

When $h(t, x)$ is a solution of the PDE (5.2) then (4.5) reduces to

$$D_1 T^1 + D_2 T^2 \Big|_{(5.2)} = 0, \tag{5.22}$$

and $\underline{\mathbf{T}} = (T^1, T^2)$ is a conserved vector for the PDE (5.2). Thus, (5.20) and (5.21), where h satisfies the PDE (5.2), are the components of the conserved vector for PDE (5.2). From (3.74), we see that these are the components of the elementary conserved vector.

5.2 Symmetries and group invariant solution

The most general Lie point symmetry generator of equation (3.74) is derived in Appendix B.1. The symmetry generator is given by

$$X = (c_1 t + c_2) \frac{\partial}{\partial t} + (c_3 x + c_4) \frac{\partial}{\partial x} + \frac{1}{3}(2c_3 - c_1) h \frac{\partial}{\partial h}, \tag{5.23}$$

where the mixing length takes on the form

$$l(x) = l_0 \, (c_3 x + c_4)^{\frac{1}{3} \frac{c_1}{c_3} - \frac{1}{6}}. \tag{5.24}$$

Using the general mixing length (5.24) when obtaining the group invariant solution results in a similar problem when obtaining the balance law as experienced in Chapter 4, equation (4.71). Thus, once again, a constant mixing length, given by

$$\alpha = \frac{c_3}{c_1} = 2, \tag{5.25}$$

will be examined.

An important difference between the group invariant solution for $\nu = 0$ and $\nu \neq 0$ is that, for $\nu \neq 0$, the parameter α is determined and takes on the value $\alpha = 2$. When $\nu = 0$, this parameter is undetermined by the group invariant solution and can thus be chosen to impose the working condition at the fracture entry to the solution. For $\nu \neq 0$, there is only a single working condition corresponding to $\alpha = 2$.

When $\alpha = 2$, the Lie point symmetry generator is given by

$$X = (c_1 t + c_2) \frac{\partial}{\partial t} + (2c_1 x + c_4) \frac{\partial}{\partial x} + c_1 h \frac{\partial}{\partial h}, \tag{5.26}$$

where the mixing length is a constant, $l(x) = l_0$.

By using the same method as outlined in Chapter 4, a group invariant solution of equation (3.74) can be calculated to be

$$h(t,x) = (c_1 t + c_2)F(\gamma), \tag{5.27}$$

where

$$\gamma = \frac{2c_1 x + c_4}{(c_1 t + c_2)^2}, \tag{5.28}$$

and

$$\frac{4K}{5l_0}(2c_1)^{\frac{1}{2}}\frac{d}{d\gamma}\left[F(\gamma)^{\frac{5}{2}}\left(-\frac{dF}{d\gamma}\right)^{\frac{1}{2}}\right] - \frac{\nu}{2l_0^2}\frac{d}{d\gamma}\left[F(\gamma)^2\right]$$

$$-2\frac{d}{d\gamma}(\gamma F(\gamma)) + 3F(\gamma) = 0. \tag{5.29}$$

Once again, we choose $\gamma(t,0) = 0$; thus, c_4 is set to zero. This does not affect (5.29).

By the same method as used in Chapter 4, the following results are also obtained:

$$F\left(2c_1 \cdot c_2^{-2}\right) = 0, \tag{5.30}$$

$$\frac{4K}{5l_0}(2c_1)^{\frac{1}{2}}F(0)^{\frac{5}{2}}\left(-\frac{dF}{d\gamma}(0)\right)^{\frac{1}{2}} - \frac{\nu}{2l_0^2}F(0)^2 = 3\int_0^{2c_1\cdot c_2^{-2}} F(\gamma)d\gamma, \tag{5.31}$$

$$L(t) = \left(1 + \frac{c_1}{c_2}t\right)^2, \tag{5.32}$$

$$V(t) = V_0\left(1 + \frac{c_1}{c_2}t\right)^3, \tag{5.33}$$

$$V_0 = \frac{c_2^3}{c_1}\int_0^{2c_1\cdot c_2^{-2}} F(\gamma)d\gamma. \tag{5.34}$$

We may now define the transformation

$$\gamma = 2c_1 \cdot c_2^{-2}u, \qquad u = \frac{x}{L(t)}, \tag{5.35}$$

and

$$F(\gamma) = \left(\frac{5l_0}{2K}\right)^{\frac{1}{2}} c_1^{\frac{1}{2}} c_2^{-\frac{3}{2}} G(u). \tag{5.36}$$

In doing so, the problem can be summarized into the following equations:

$$\frac{d}{du}\left[G(u)^{\frac{5}{2}}\left(-\frac{dG}{du}\right)^{\frac{1}{2}}\right]-\frac{\nu}{4l_0^2}\left(\frac{5L_0}{2k}\right)^{\frac{1}{2}}\left(\frac{c_2}{c_1}\right)^{\frac{1}{2}}\frac{d}{du}\left[G(u)^2\right]$$

$$-2\frac{d}{du}\left(uG(u)\right)+3G(u)=0, \tag{5.37}$$

$$G(1)=0, \tag{5.38}$$

$$G(0)^{\frac{5}{2}}\left(-\frac{dG}{du}(0)\right)^{\frac{1}{2}}-\frac{\nu}{4l_0^2}\left(\frac{5l_0}{2K}\right)^{\frac{1}{2}}\left(\frac{c_2}{c_1}\right)^{\frac{1}{2}}G(0)^2=3\int_0^1 G(u)du, \tag{5.39}$$

$$G(u)^{\frac{5}{2}}\left(-\frac{dG}{du}\right)^{\frac{1}{2}}\Big|_{u=1}=0, \tag{5.40}$$

$$L(t)=\left(1+\frac{c_1}{c_2}t\right)^2, \tag{5.41}$$

$$V(t)=\left(1+\frac{c_1}{c_2}t\right)^3 V_0, \tag{5.42}$$

$$V_0=2\left(\frac{5l_0}{2K}\right)^{\frac{1}{2}}\left(\frac{c_1}{c_2}\right)^{\frac{1}{2}}\int_0^1 G(u)du, \tag{5.43}$$

$$h(t,x)=\left(\frac{5l_0}{2K}\right)^{\frac{1}{2}}\left(\frac{c_1}{c_2}\right)^{\frac{1}{2}}\left(1+\frac{c_1}{c_2}t\right)G(u), \tag{5.44}$$

$$u=\frac{x}{L(t)}. \tag{5.45}$$

Finally, imposing the condition $h(0,0)=1$ on the system results in the relationship

$$\frac{c_1}{c_2}=\left(\frac{2K}{5l_0}\right)\frac{1}{G(0)^2}. \tag{5.46}$$

Thus, the system of equations can be summarised as:

$$\frac{d}{du}\left[G(u)^{\frac{5}{2}}\left(-\frac{dG}{du}\right)^{\frac{1}{2}}\right]-\frac{\nu}{4l_0^2}\left(\frac{5l_0}{2K}\right)G(0)\frac{d}{du}\left[G(u)^2\right]$$

$$-2\frac{d}{du}\left(uG(u)\right)+3G(u)=0, \tag{5.47}$$

$$G(1)=0, \tag{5.48}$$

$$G(0)^{\frac{5}{2}}\left(-\frac{dG}{du}(0)\right)^{\frac{1}{2}}-\frac{\nu}{4l_0^2}\left(\frac{5l_0}{2K}\right)G(0)^3=3\int_0^1 G(u)du, \tag{5.49}$$

$$G(u)^{\frac{5}{2}} \left(-\frac{dG}{du}\right)^{\frac{1}{2}} \Big|_{u=1} = 0, \tag{5.50}$$

$$L(t) = \left(1 + \frac{1}{G(0)^2} \left(\frac{2K}{5l_0}\right) t\right)^2, \tag{5.51}$$

$$V(t) = \left(1 + \frac{1}{G(0)^2} \left(\frac{2K}{5l_0}\right) t\right)^3 V_0, \tag{5.52}$$

$$V_0 = \frac{2}{G(0)} \int_0^1 G(u) du, \tag{5.53}$$

$$h(t, x) = \left(1 + \frac{1}{G(0)^2} \left(\frac{2K}{5l_0}\right) t\right) \frac{G(u)}{G(0)}, \tag{5.54}$$

$$u = \frac{x}{L(t)}. \tag{5.55}$$

5.3 Solutions

5.3.1 *Asymptotic solutions*

An approximation of the behaviour of $G(u)$ as $u \to 1$ can be once again obtained from the asymptotic solution of the ODE (5.47) as $u \to 1$. Employing the same method as outlined in subsection 4.3.2, an asymptotic solution of the form

$$G(u) \sim C(1-u)^n, \quad u \to 1, \tag{5.56}$$

can be looked for, which upon balancing the dominant terms in equation (5.47) results in $n = \frac{1}{4}$. Assuming that $C \neq 0$, this yields the equation

$$(1-u)^{-\frac{3}{4}} - \frac{C^2}{4}(1-u)^{-\frac{3}{4}} + \frac{5\nu}{8l_0K} G(0) C (1-u)^{-\frac{1}{2}} + C(1-u)^{\frac{1}{4}} = 0. \tag{5.57}$$

Multiplying by $(1-u)^{\frac{3}{4}}$ and letting $u \to 1$ yields

$$1 - \frac{C^2}{4} = 0, \tag{5.58}$$

and so $C = \pm 2$. We select the positive branch because we are considering the upper half of the fracture.

Thus, the asymptotic solution is given by

$$G(u) \sim 2(1-u)^{\frac{1}{4}}, \quad u \to 1. \tag{5.59}$$

Equation (5.59) satisfies the boundary condition $G(1) = 0$. The asymptotic solution as $u \to 1$ is not expected to satisfy the second boundary condition (5.49) which is imposed at $u = 0$.

It can be noted that next largest term in (5.57) is the term depending on ν which is $\mathcal{O}((1-u)^{-\frac{1}{2}})$ as $u \to 1$. It is much larger than the remaining term which is $\mathcal{O}((1-u)^{\frac{1}{4}})$ as $u \to 1$. As a result, the asymptotic solution for $\nu \neq 0$ is of a lesser accuracy than the asymptotic solution (4.132) for $\nu = 0$, although both asymptotic solutions have the same form.

5.3.2 *Numerical solutions*

It can readily be shown that there are no scaling symmetries for the ordinary differential equation (5.47). The shooting method may still be utilised to solve this equation, however, there is the added complication of not knowing the value of $G(0)$ explicitly. Since this value is featured in the ODE explicitly, this presents an additional issue to overcome.

Instead, this problem was solved as follows: a grid was made, consisting of linearly-spaced values for $G(0) \in [a_1,\ a_2]$ and $G'(0) = [b_1,\ b_2]$. The ODE was then solved for each permutation of the values within this grid, while enforcing the boundary condition $G(1) = 0$ (5.48). Upon completion of these calculations, the values $(G(0),\ G'(0)) = (a^*,\ b^*)$ which most closely satisfied the integral boundary condition (5.49) were selected. If this condition was still not satisfied to a specified tolerance, the process was repeated again for $G(0) \in [a^* - \epsilon,\ a^* + \epsilon]$, $G'(0) \in [b^* - \epsilon,\ b^* + \epsilon]$ for some small ϵ.

It can be noted that there are two parameters involved in solving for the fracture half-width, given by

$$p = \frac{2K}{5l_0}, \tag{5.60}$$

and

$$q = \frac{1}{p}\frac{\nu}{4l_0^2} = \frac{5\nu}{8Kl_0}. \tag{5.61}$$

The parameter q must remain relatively small in magnitude in order for the system to have a solution. This is consistent with the physical meaning of the parameter. Although ν is large enough to not be neglected, it is still small in relative terms when compared to the kinematic eddy viscosity.

Figures 5.1-5.3 illustrate the fracture half-width, length and volume respectively for different values of the parameter q. It can be noted from Figure 5.1 that as q approaches zero, the general half-width profile increases. Likewise, the fracture length and volume grow faster as q tends to zero. Figure 5.4 also illustrates that, as time increases, the fracture half-width rapidly increases.

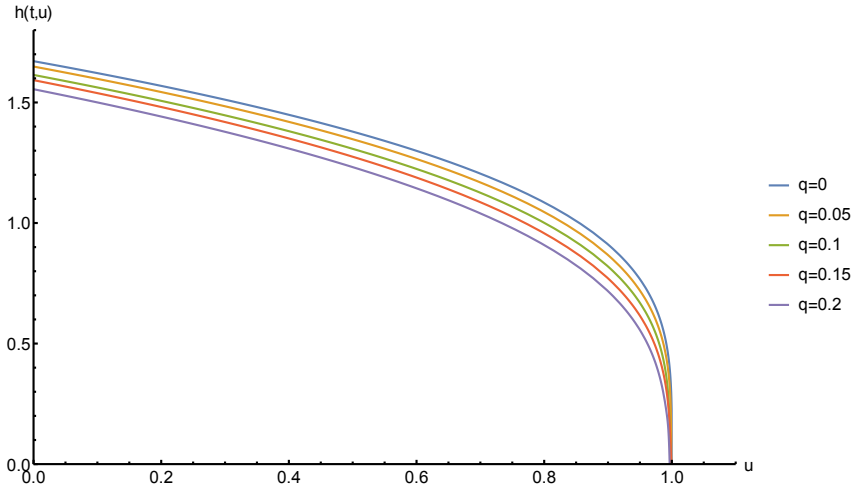


Figure 5.1: The fracture half-width, $h(t,u)$ plotted against u at $t = 3$ for $p = 1$ and $q = 0,\ 0.01,\ 0.05,\ 0.1,\ 0.15$ and 0.2.

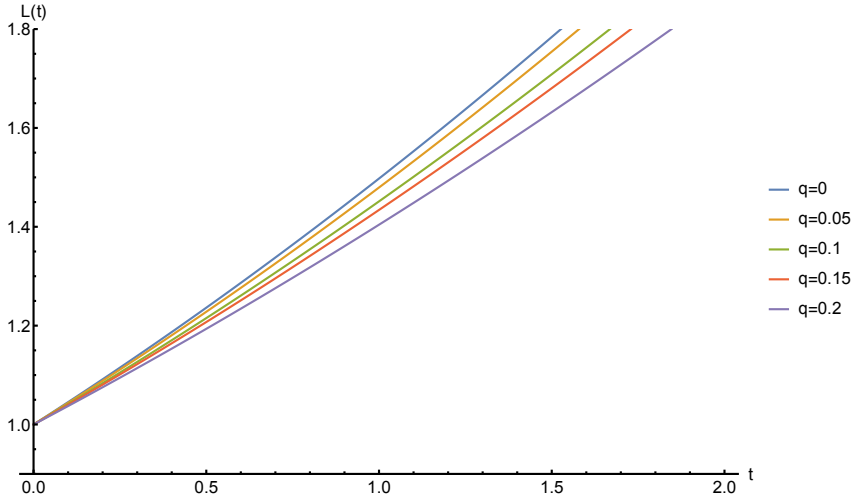


Figure 5.2: The fracture length, $L(t)$ plotted against time t for $p = 1$ and $q = 0,\ 0.05,\ 0.1,\ 0.15$ and 0.2.

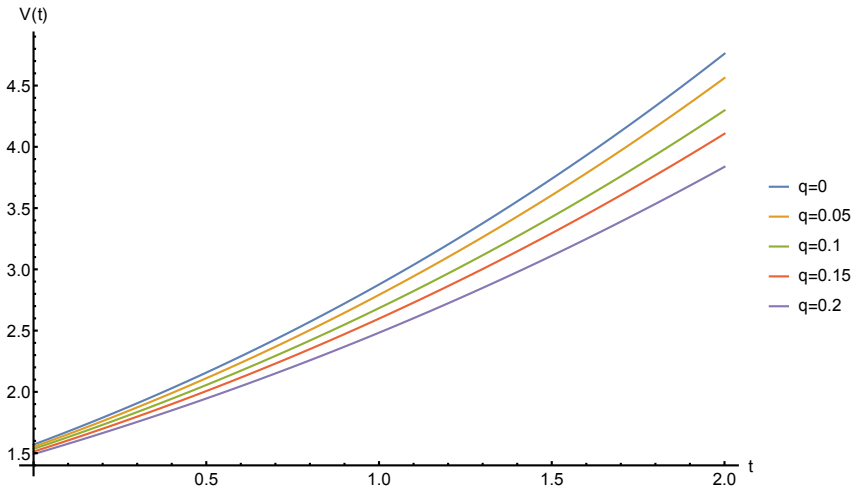


Figure 5.3: The fracture volume, $V(t)$ plotted against time t for $p = 1$ and $q = 0,\ 0.05,\ 0.1,\ 0.15$ and 0.2.

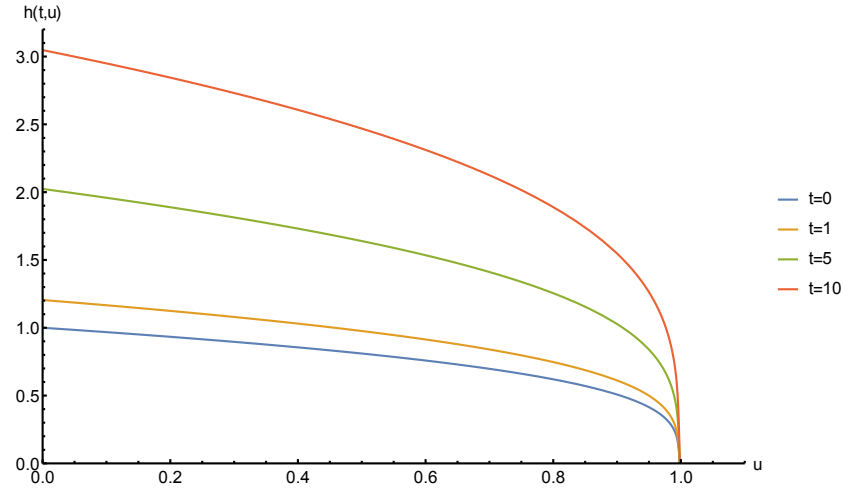


Figure 5.4: The fracture half-width $h(t, u)$ plotted against u for $p = 1$, $q = 0.1$ and $t = 0,\ 1,\ 5$ and 10.

There is no analytical solution against which to compare these numerical solutions. However, when $q = 0$, the equations simply reduce to those studied in Chapter 4 for $\alpha = 2$. Thus, the graph for $q = 0$ may used to determine accuracy of the numerical solution. Figure 5.5 firstly compares the numerical solution for the half-width, (4.107), from Chapter 4 for $\alpha = 2$ against the $\mathcal{O}(\nu)$ solution (5.54) with $q = 0$, and secondly compares the solution (4.107) for $\alpha = 2$ with (5.54) for increasing values of q. It can be observed from Figure 5.5 that the accuracy of the numerical solution is good.

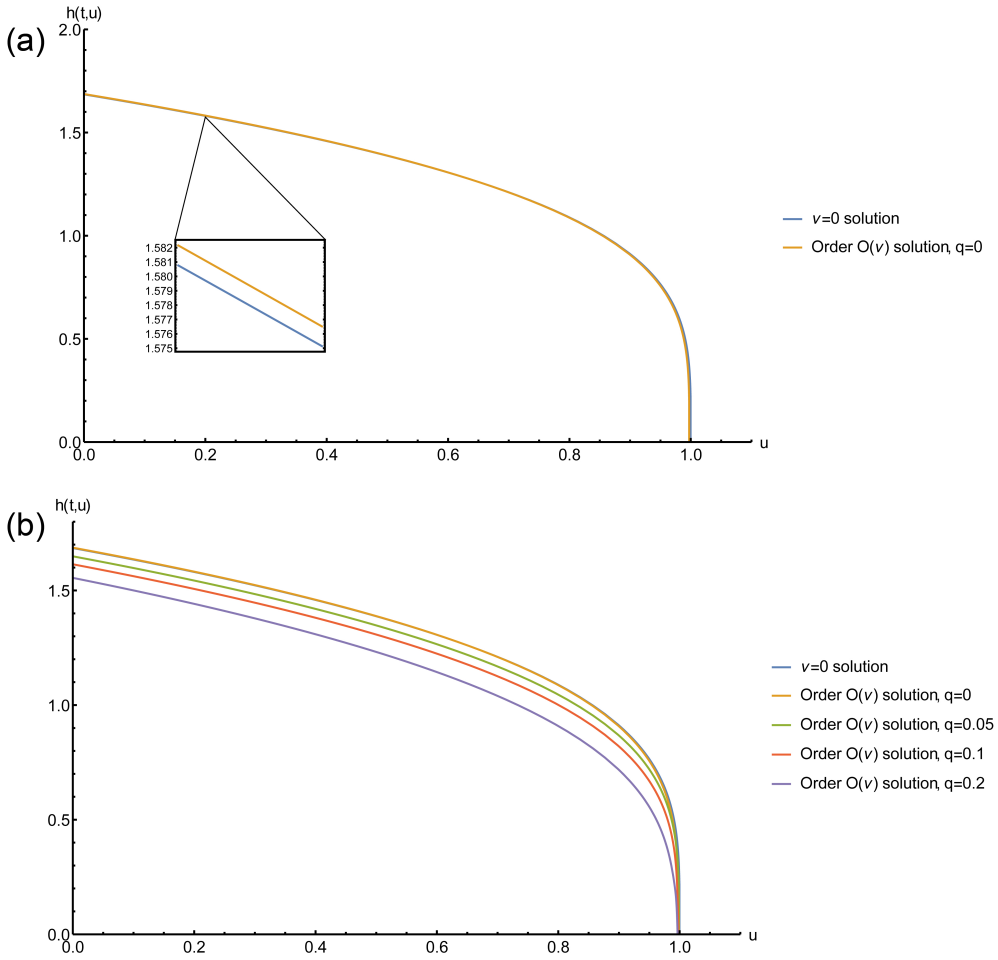


Figure 5.5: Comparison of the solution for the half-width (4.107) for $\nu = 0$ and $\alpha = 2$ with the solution (5.54) for $\nu \neq 0$ at $t = 3$, $p = 1$ and (a) $q = 0$ and (b) $q = 0$, 0.05, 0.1 and 0.2.

5.4 Non-classical Symmetries

The derivation of the non-classical symmetries of equation (3.74) with constant mixing length $l(x) = l_0$ is detailed in Appendix B.2. It results in the generator

$$X = \frac{\partial}{\partial t} + (2c(t) + b(t))\frac{\partial}{\partial x} + c(t)h\frac{\partial}{\partial h}, \tag{5.62}$$

where the functions $b(t)$, $c(t)$ satisfy

$$b'(t) + b(t)c(t) = 0, \tag{5.63}$$

$$c'(t) + c(t)^2 = 0. \tag{5.64}$$

It can be noted that this result is a special case of the non-classical symmetry calculated for equation (3.65), where $a(t) = 2c(t)$. This is an interesting result. Introducing the $\mathcal{O}(\nu)$ term into the equation imposes an additional condition within the calculation, allowing for this further reduction to be made.

5.4.1 *Case:* $c(t) = 0$

Setting $c(t) = 0$ reduces the system of equations to $b'(t) = 0$, which has the solution $b(t) = c_1$. Thus, the symmetry generator becomes

$$X = \frac{\partial}{\partial t} + c_1 \frac{\partial}{\partial x}. \tag{5.65}$$

It can be noted that conditional symmetry (5.65) is a special case of the Lie point symmetry (5.26) with $c_1 = 0$.

The invariant surface condition (A.57) becomes

$$\frac{\partial h}{\partial t} = -c_1 \frac{\partial h}{\partial x}. \tag{5.66}$$

Eliminating $\frac{\partial h}{\partial t}$ between the PDE (3.74) and the invariant surface condition (5.66) gives

$$\frac{2K}{5l_0} \frac{\partial}{\partial x} \left(h^{\frac{5}{2}} (-h_x)^{\frac{1}{2}} \right) - \frac{\nu}{4l_0^2} \frac{\partial}{\partial x} \left(h^2 \right) = c_1 h_x. \tag{5.67}$$

This may be integrated once with the boundary condition $h(t, L(t)) = 0$ and the no fluid flux condition at the fracture tip which for $\nu \neq 0$ still is $h^{\frac{5}{2}} \left(-\frac{\partial h}{\partial x}\right)^{\frac{1}{2}} \Big|_{x=L(t)} = 0$. Doing so, we obtain:

$$\frac{2K}{5l_0} h^{\frac{5}{2}} \left(-\frac{\partial h}{\partial x} \right)^{\frac{1}{2}} - \frac{\nu}{4l_0^2} h^2 = c_1 h. \tag{5.68}$$

Solving for $\frac{\partial h}{\partial x}$ gives

$$\frac{\partial h}{\partial x} = -\left(\frac{5\nu}{8Kl_0} \right)^2 \frac{1}{h^3} \left[\frac{4l_0^2}{\nu} c_1 + h \right]^2. \tag{5.69}$$

This can be solved, resulting in

$$\frac{h^2}{2} - \frac{8l_0^2}{\nu} c_1 h - \frac{8l_0^4}{\nu^2} c_1^2 \left(\frac{12c_1 l_0^2 + 5h\nu}{4c_1 l_0^2 + h\nu} \right) + \frac{48l_0^4}{\nu^2} c_1^2 \ln \left(\frac{4c_1 l_0^2}{\nu} + h \right) = -\left(\frac{5\nu}{8Kl_0} \right)^2 x + q(t). \tag{5.70}$$

Using the condition $h(t, L(t)) = 0$, the function $q(t)$ can be obtained. However, upon using $h(0, 0) = 1$, it can be seen that the resulting expression cannot be solved for c_1. However, the function $h(t, x)$ cannot be solved for explicitly, and only an implicit expression can be obtained.

We could expand (5.70) in powers of ν and investigate a solution correct to first order in ν. In the derivation of the PDE (3.74), terms of order ν^2 were neglected and therefore a solution correct to order ν is the best that can be derived with this model. However, we will not consider the perturbation expansion here.

Other symmetry cases that can be attempted result in similar difficulties, and will not be considered here.

5.5 Analysis of results and conclusions

This chapter studied a fracture half-width equation whereby the viscosity was not small enough to be neglected. The research carried out in this chapter was similar to that of Chapter 4; however, new and interesting results were found.

The conserved vectors for equation (3.74) were investigated, yielding only the elementary conserved vector. The Lie point symmetries of (3.74) were also calculated, and a group invariant solution was constructed. From this, expressions for the fracture half-width, length, volume were found. As before, the result that the mixing length must remain constant was obtained.

One of the most important results emerging from this work was that, by enforcing that the equation was correct to $\mathcal{O}(\nu)$, the working condition α was automatically determined and given a fixed value of 2. This strongly contrasts with the work in Chapter 4 where α was left undetermined. In other words, by incorporating this additional $\mathcal{O}(\nu)$ term in the PDE, the exact behaviour of the fracture was determinable. This possibly gives insight into how a fracture will more likely behave in practice. Interestingly, this value for α is significantly larger than was anticipated prior to these calculations. When $\alpha = 2$, the length grows like $\mathcal{O}(t^2)$ and the volume like $\mathcal{O}(t^3)$. The velocity of propagation of the fracture undergoes acceleration.

The remaining parameters that were left within the system of equations were:

1. The ratio $p = \frac{2K}{5l_0}$, which also appeared in Chapter 4.
2. The ratio $q = \frac{1}{p}\frac{\nu}{4l_0^2} = \frac{5\nu}{8Kl_0}$. This parameter incorporates p as well as the viscosity ν. This parameter needs to be kept small within the calculation both for physical reasons and mathematical reasons. Physically, even though ν is large enough not to be neglected, it is small when compared with the eddy viscosity. Mathematically, as q is multiplies

the term $\frac{d}{du}G(u)^2$ in ODE (5.47), it can quickly introduce instability when solving the equation numerically.

Numerical solutions were obtained for the fracture half-width, length and volume from equation (3.74). To study the effect the viscosity introduced into the problem, the parameter p was set to 1 and only q was varied, to model differing viscosities and the effect this had on fracture growth. It could be noted that, as $q \to 0$, the fracture half-width increased in width. The fracture half-width also grew steadily over time. Similarly, as q increases, the fracture length and volume grow at a slower rate over time. This solution also behaves similarly to the Chapter 4 solution as $q \to 0$.

Attempts to obtain a non-classical symmetry solution for equation (3.74) were also made. However, only implicit solutions for the fracture half-width were obtained.

CONCLUSIONS

6

CONCLUSIONS

The aim of this research was to study turbulent hydraulic fracturing, as there is a very limited amount of work done on the topic, despite the phenomenon being known to occur. This problem was studied by modelling turbulent fluid flow, using Prandtl's mixing length model for the eddy viscosity, and examining the effect that this flow had on the fracture's evolution. This problem was considered for two different cases: one where the ratio of the kinematic viscosity to the effective viscosity was sufficiently small enough to neglect, and the other being where the ratio was not neglected, with a model formulated to be correct to $\mathcal{O}(\nu)$.

Extensive analysis was carried out on both models. The conserved vectors for each were calculated, but only the elementary conserved vector was found in each case. The Lie point symmetries of both equations were then calculated, as a means of solution. Group invariant solutions were obtained and, as a result, expressions for the fracture half-width, length and volume could be defined in terms of these solutions.

A result that emerged from the balance law for both models was that a constant mixing length was required in order for the models to remain physically consistent. As the fracture is quite narrow, this leaves little room for variation across the fracture, making it a usable result.

Interestingly, in the model where the viscosity was neglected, a working condition α appeared that was not determinable by the boundary conditions or in the derivation of the Lie point symmetry. This value could thus be selected to model a range of physically important working conditions. The value $\alpha = \frac{2}{3}$ was of particular importance. Depending on whether α was smaller or greater than this critical value, the fracture behaviour would change significantly. If $\alpha > \frac{2}{3}$, the fracture half-width would expand with time; however, if it was smaller than this value, the half-width would decrease with time. By simple calculation, it was shown that this parameter value is linked to when pressure at the fracture entry is either increasing or decreasing, thus showing why this interesting fracturing behaviour occurred.

For the model where viscosity was not neglected, there was no equivalent working condition like α present. It can be noted however that the set of equations that resulted from this case were exceptionally similar to the prior model for $\alpha = 2$. Thus, incorporating the $\mathcal{O}(\nu)$ term into this model allowed for an extra parameter to be determined. This model may thus be more indicative of how turbulent hydraulic fracturing may occur because ignoring

the viscosity altogether may be over-simplification. The viscosity will always have an effect no matter how small it may be. It can however be noted that the $\mathcal{O}(\nu)$ solution tends towards the solution for $\nu = 0$ with $\alpha = 2$ for very small kinematic viscosities, as expected. Thus, when dealing with smaller kinematic viscosities, the solution for $\nu = 0$ can be utilised with reasonable accuracy. This is particularly interesting as setting $\alpha = 2$ results in fracture lengths and volumes that increase at an accelerated rate.

A number of approximate solutions were also constructed in this work for both models. They performed quite accurately against the numerical solutions calculated and they are a much simpler means of obtaining fracture estimates than the numerical methods utilised.

The non-classical symmetries were also calculated in this analysis to search for additional solutions. For the model neglecting kinematic viscosity, this proved to be fruitful as a solution of significance was found. The solution obtained had a form that was exceptionally similar to special solutions found in other hydraulic fracturing work. However, unlike these solutions, it was derived in a systematic manner. A non-classical symmetry solution was attempted for the $\mathcal{O}(\nu)$ model, however the resulting expression for the fracture half-width was implicit in form and less useful. Although the non-classical symmetries found in this work were a special case of the Lie point symmetries of the PDEs, they indicated that the special case was significant and should not be overlooked.

Overall, this work gave insight into how turbulent flow may affect hydraulic fracturing in comparison to the laminar flow research existing in the literature. It also illuminated the fact that the existing research may have underestimated the value of the working condition, since by incorporating the kinematic viscosity into the model, the fracture evolution rates are significantly larger. Areas for possible further research could include examining different models for the eddy viscosity and determining the influence and variation introduced by the models.

APPENDIX

APPENDIX A

a.1 Lie point symmetries of the governing PDE (3.65)

This Appendix will detail the calculation of the Lie point symmetry generator for equation (3.65).

The PDE (3.65) can be expanded and re-written in the form

$$F(t,x,h,h_t,h_x,h_{xx}) = h_t - K\left[\frac{2}{5}\frac{l'(x)}{l(x)^2}h^{\frac{5}{2}}(-h_x)^{\frac{1}{2}} + \frac{1}{l(x)}h^{\frac{3}{2}}(-h_x)^{\frac{3}{2}} + \frac{1}{5}\frac{1}{l(x)}h^{\frac{5}{2}}(-h_x)^{-\frac{1}{2}}h_{xx}\right] = 0. \tag{A.1}$$

Thus,

$$h_t = K\left[\frac{2}{5}\frac{l'(x)}{l(x)^2}h^{\frac{5}{2}}(-h_x)^{\frac{1}{2}} + \frac{1}{l(x)}h^{\frac{3}{2}}(-h_x)^{\frac{3}{2}} + \frac{1}{5}\frac{1}{l(x)}h^{\frac{5}{2}}(-h_x)^{-\frac{1}{2}}h_{xx}\right]. \tag{A.2}$$

We are searching for a Lie point symmetry generator [7]

$$X = \xi^1(t,x,h)\frac{\partial}{\partial t} + \xi^2(t,x,h)\frac{\partial}{\partial x} + \eta(t,x,h)\frac{\partial}{\partial h}, \tag{A.3}$$

of equation (3.65). In order to obtain this, we prolong the symmetry generator (A.3) to second order as we have a second-order PDE (3.65),

$$\begin{aligned} X^{[2]} = {} & \xi^1(t,x,h)\frac{\partial}{\partial t} + \xi^2(t,x,h)\frac{\partial}{\partial x} + \eta(t,x,h)\frac{\partial}{\partial h} \\ & + \zeta_t(t,x,h)\frac{\partial}{\partial h_t} + \zeta_x(t,x,h)\frac{\partial}{\partial h_x} + \zeta_{tt}(t,x,h)\frac{\partial}{\partial h_{tt}} \\ & + \zeta_{tx}(t,x,h)\frac{\partial}{\partial h_{tx}} + \zeta_{xx}(t,x,h)\frac{\partial}{\partial h_{xx}}, \end{aligned} \tag{A.4}$$

where [7]

$$\zeta_t = \eta_t + (\eta_h - \xi^1_t)h_t - \xi^2_t h_x - \xi^1_h h_t^2 - \xi^2_h h_t h_x, \tag{A.5}$$

$$\zeta_x = \eta_x + (\eta_h - \xi^2_x)h_x - \xi^1_x h_t - \xi^2_h h_x^2 - \xi^1_h h_t h_x, \tag{A.6}$$

$$\begin{aligned}\zeta_{tt} =& \eta_{tt} + (2\eta_{th} - \xi^1_{tt})h_t - \xi^2_{tt}h_x + (\eta_h - 2\xi^1_t)h_{tt} - 2\xi^2_t h_{tx} \\ &+ (\eta_{hh} - 2\xi^1_{th})h_t^2 - 2\xi^2_{th}h_t h_x - \xi^1_{hh}h_t^3 - \xi^2_{hh}h_t^2 h_x \\ &- 3\xi^1_h h_t h_{tt} - \xi^2_h h_x h_{tt} - 2\xi^2_h h_t h_{tx},\end{aligned} \tag{A.7}$$

$$\begin{aligned}\zeta_{tx} =& \eta_{tx} + (\eta_{th} - \xi^2_{tx})h_x + (\eta_{xh} - \xi^1_{tx})h_t - \xi^2_t h_{xx} - \xi^1_x h_{tt} \\ &+ (\eta_h - \xi^1_t - \xi^2_x)h_{tx} - \xi^2_{th}h_x^2 + (\eta_{hh} - \xi^1_{th} - \xi^2_{xh})h_t h_x \\ &- \xi^1_{xh}h_t^2 - \xi^2_{hh}h_t h_x^2 - \xi^1_{hh}h_t^2 h_x - 2\xi^2_h h_x h_{tx} - 2\xi^1_h h_t h_{tx} \\ &- \xi^1_h h_x h_{tt} - \xi^2_h h_t h_{xx},\end{aligned} \tag{A.8}$$

$$\begin{aligned}\zeta_{xx} =& \eta_{xx} + (2\eta_{xh} - \xi^2_{xx})h_x - \xi^1_{xx}h_t + (\eta_h - 2\xi^2_x)h_{xx} - 2\xi^1_x h_{tx} \\ &+ (\eta_{hh} - 2\xi^2_{xh})h_x^2 - 2\xi^1_{xh}h_t h_x - \xi^2_{hh}h_x^3 - \xi^1_{hh}h_x^2 h_t \\ &- 3\xi^2_h h_x h_{xx} - \xi^1_h h_t h_{xx} - 2\xi^1_h h_x h_{tx}.\end{aligned} \tag{A.9}$$

The Lie point symmetry (A.3) satisfies

$$X^{[2]}(F)\big|_{F=0} = 0. \tag{A.10}$$

Applying (A.4) and (A.1) to (A.10) and treating t, x, $h(t,x)$ and all the derivatives of $h(t,x)$ as independent variables results in

$$\begin{aligned}&-\frac{2}{5}K\xi^2\left(\frac{l''(x)}{l(x)^2} - 2\frac{l'(x)^2}{l(x)^3}\right)h^{\frac{5}{2}}(-h_x)^{\frac{1}{2}} + K\xi^2\frac{l'(x)}{l(x)^2}h^{\frac{3}{2}}(-h_x)^{\frac{3}{2}} \\ &+\frac{1}{5}K\xi^2\frac{l'(x)}{l(x)^2}h^{\frac{5}{2}}(-h_x)^{-\frac{1}{2}}h_{xx} - K\eta\frac{l'(x)}{l(x)^2}h^{\frac{3}{2}}(-h_x)^{\frac{1}{2}} \\ &-\frac{3}{2}K\eta\frac{1}{l(x)}h^{\frac{1}{2}}(-h_x)^{\frac{3}{2}} - \frac{1}{2}K\eta\frac{1}{l(x)}h^{\frac{3}{2}}(-h_x)^{-\frac{1}{2}}h_{xx} + \zeta_t \\ &+\frac{1}{5}K\zeta_x\frac{l'(x)}{l(x)^2}h^{\frac{5}{2}}(-h_x)^{-\frac{1}{2}} + \frac{3}{2}K\zeta_x\frac{1}{l(x)}h^{\frac{3}{2}}(-h_x)^{\frac{1}{2}} \\ &-\frac{1}{10}K\zeta_x\frac{1}{l(x)}h^{\frac{5}{2}}(-h_x)^{-\frac{3}{2}}h_{xx} - \frac{1}{5}K\zeta_{xx}\frac{1}{l(x)}h^{\frac{5}{2}}(-h_x)^{-\frac{1}{2}}\Big|_{(A.2)} = 0.\end{aligned} \tag{A.11}$$

The values of ζ_t, ζ_x and ζ_{xx}, where equation (A.2) is used to eliminate h_t, is substituted into equation (A.11). Upon expanding the equation, we obtain

$$
\begin{aligned}
&-\frac{2K^2}{25}\frac{l'(x)^2}{l(x)^4}h^5(-h_x)\xi^1_h-\frac{2K^2}{25}\frac{l'(x)^2}{l(x)^4}h^5\xi^1_x-\frac{K^2}{50}\frac{1}{l(x)^2}h^5(-h_x)^{-1}h^2_{xx}\xi^1_h\\
&+\frac{K^2}{25}\frac{1}{l(x)^2}h^5(-h_x)h_{xx}\xi^1_{hh}+\frac{K^2}{50}\frac{1}{l(x)^2}h^5(-h_x)^{-2}h^2_{xx}\xi^1_x-\frac{2K^2}{25}\frac{1}{l(x)^2}h^5h_{xx}\xi^1_{xh}\\
&+\frac{K^2}{25}\frac{1}{l(x)^2}h^5(-h_x)^{-1}h_{xx}\xi^1_{xx}-\frac{2K^2}{25}\frac{l'(x)}{l(x)^3}h^5h_{xx}\xi^1_h+\frac{2K^2}{25}\frac{l'(x)}{l(x)^3}h^5(-h_x)^2\xi^1_{hh}\\
&-\frac{4K^2}{25}\frac{l'(x)}{l(x)^3}h^5(-h_x)\xi^1_{xh}+\frac{2K^2}{25}\frac{l'(x)}{l(x)^3}h^5\xi^1_{xx}+\frac{K^2}{5}\frac{1}{l(x)^2}h^4(-h_x)^3\xi^1_{hh}\\
&-\frac{K^2}{5}\frac{1}{l(x)^2}h^4h_{xx}\xi^1_x-\frac{2K^2}{5}\frac{1}{l(x)^2}h^4(-h_x)^2\xi^1_{xh}+\frac{K^2}{5}\frac{1}{l(x)^2}h^4(-h_x)\xi^1_{xx}\\
&-\frac{4K^2}{5}\frac{l'(x)}{l(x)^3}h^4(-h_x)\xi^1_x+\frac{K^2}{2}\frac{1}{l(x)^2}h^3(-h_x)^3\xi^1_h-\frac{3K^2}{2}\frac{1}{l(x)^2}h^3(-h_x)^2\xi^1_x\\
&+\frac{4K}{5}\frac{l'(x)^2}{l(x)^3}h^{\frac{5}{2}}(-h_x)^{\frac{1}{2}}\xi^2+\frac{K}{10}\frac{1}{l(x)}h^{\frac{5}{2}}(-h_x)^{-\frac{1}{2}}h_{xx}\eta_h-\frac{K}{5}\frac{1}{l(x)}h^{\frac{5}{2}}(-h_x)^{\frac{3}{2}}\eta_{hh}\\
&-\frac{K}{10}\frac{1}{l(x)}h^{\frac{5}{2}}(-h_x)^{-\frac{3}{2}}h_{xx}\eta_x+\frac{2K}{5}\frac{1}{l(x)}h^{\frac{5}{2}}(-h_x)^{\frac{1}{2}}\eta_{xh}-\frac{K}{5}\frac{1}{l(x)}h^{\frac{5}{2}}(-h_x)^{-\frac{1}{2}}\eta_{xx}\\
&-\frac{2K}{5}\frac{1}{l(x)}h^{\frac{5}{2}}(-h_x)^{\frac{1}{2}}h_{tx}\xi^1_h-\frac{K}{5}\frac{1}{l(x)}h^{\frac{5}{2}}(-h_x)^{-\frac{1}{2}}h_{xx}\xi^1_t+\frac{2K}{5}\frac{1}{l(x)}h^{\frac{5}{2}}(-h_x)^{-\frac{1}{2}}h_{tx}\xi^1_x\\
&-\frac{3K}{10}\frac{1}{l(x)}h^{\frac{5}{2}}(-h_x)^{\frac{1}{2}}h_{xx}\xi^2_h-\frac{K}{5}\frac{1}{l(x)}h^{\frac{5}{2}}(-h_x)^{\frac{5}{2}}\xi^2_{hh}+\frac{3K}{10}\frac{1}{l(x)}h^{\frac{5}{2}}(-h_x)^{-\frac{1}{2}}h_{xx}\xi^2_x\\
&+\frac{2K}{5}\frac{1}{l(x)}h^{\frac{5}{2}}(-h_x)^{\frac{3}{2}}\xi^2_{xh}-\frac{K}{5}\frac{1}{l(x)}h^{\frac{5}{2}}(-h_x)^{\frac{1}{2}}\xi^2_{xx}+\frac{K}{5}\frac{l'(x)}{l(x)^2}h^{\frac{5}{2}}(-h_x)^{-\frac{1}{2}}h_{xx}\xi^2\\
&+\frac{K}{5}\frac{l'(x)}{l(x)^2}h^{\frac{5}{2}}(-h_x)^{\frac{1}{2}}\eta_h+\frac{K}{5}\frac{l'(x)}{l(x)^2}h^{\frac{5}{2}}(-h_x)^{-\frac{1}{2}}\eta_x-\frac{2K}{5}\frac{l'(x)}{l(x)^2}h^{\frac{5}{2}}(-h_x)^{\frac{1}{2}}\xi^1_t\\
&+\frac{K}{5}\frac{l'(x)}{l(x)^2}h^{\frac{5}{2}}(-h_x)^{\frac{3}{2}}\xi^2_h+\frac{K}{5}\frac{l'(x)}{l(x)^2}h^{\frac{5}{2}}(-h_x)^{\frac{1}{2}}\xi^2_x-\frac{2K}{5}\frac{l''(x)}{l(x)^2}h^{\frac{5}{2}}(-h_x)^{\frac{1}{2}}\xi^2\\
&-\frac{K}{2}\frac{1}{l(x)}h^{\frac{3}{2}}(-h_x)^{-\frac{1}{2}}h_{xx}\eta-\frac{K}{2}\frac{1}{l(x)}h^{\frac{3}{2}}(-h_x)^{\frac{3}{2}}\eta_h+\frac{3K}{2}\frac{1}{l(x)}h^{\frac{3}{2}}(-h_x)^{\frac{1}{2}}\eta_x\\
&-K\frac{1}{l(x)}h^{\frac{3}{2}}(-h_x)^{\frac{3}{2}}\xi^1_t-\frac{K}{2}\frac{1}{l(x)}h^{\frac{3}{2}}(-h_x)^{\frac{5}{2}}\xi^2_h+\frac{3K}{2}\frac{1}{l(x)}h^{\frac{3}{2}}(-h_x)^{\frac{3}{2}}\xi^2_x\\
&+K\frac{l'(x)}{l(x)^2}h^{\frac{3}{2}}(-h_x)^{\frac{3}{2}}\xi^2-K\frac{l'(x)}{l(x)^2}h^{\frac{3}{2}}(-h_x)^{\frac{1}{2}}\eta-\frac{3K}{2}\frac{1}{l(x)}h^{\frac{1}{2}}(-h_x)^{\frac{3}{2}}\eta\\
&+\eta_t+(-h_x)\xi^2_t=0. \qquad \text{(A.12)}
\end{aligned}
$$

As ξ^1, ξ^2 and η are all independent of the derivatives of $h(t,x)$, the coefficients of the partial derivatives of $h(t,x)$ must all separately vanish. As a result of this, the equation can be separated by the partial derivatives of $h(t,x)$, resulting in the following set of determining equations:

$$(-h_x)^{-\frac{1}{2}}h_{tx}: \quad \frac{2K}{5}\frac{1}{l(x)}h^{\frac{5}{2}}\xi^1_x = 0, \tag{A.13}$$

$$(-h_x)^{\frac{1}{2}}h_{tx}: \quad \frac{2K}{5}\frac{1}{l(x)}h^{\frac{5}{2}}\xi^1_h = 0, \tag{A.14}$$

$$(-h_x)^{-1}h^2_{xx}: \quad \frac{K^2}{50}\frac{1}{l(x)^2}h^5\xi^1_h = 0, \tag{A.15}$$

$$(-h_x)^{-2}h^2_{xx}: \quad \frac{K^2}{50}\frac{1}{l(x)^2}h^5\xi^1_x = 0, \tag{A.16}$$

$$(-h_x)^{-\frac{1}{2}}h_{xx}: \quad \frac{h^{\frac{3}{2}}}{10}\frac{K}{l(x)}\left(2\frac{hl'(x)}{l(x)}\xi^2 - 2h\xi^1_t - 5\eta + h\eta_h + 3h\xi^2_x\right) = 0, \tag{A.17}$$

$$(-h_x)^{-\frac{3}{2}}h_{xx}: \quad \frac{K}{10l(x)}h^{\frac{5}{2}}\eta_x = 0, \tag{A.18}$$

$$(-h_x)h_{xx}: \quad \frac{K^2}{25l(x)^2}h^5\xi^1_{hh} = 0, \tag{A.19}$$

$$(-h_x)^{-1}h_{xx}: \quad \frac{K^2}{25l(x)^2}h^5\xi^1_{xx} = 0, \tag{A.20}$$

$$(-h_x)^{\frac{1}{2}}h_{xx}: \quad \frac{3K}{10l(x)}h^{\frac{5}{2}}\xi^2_h = 0, \tag{A.21}$$

$$h_{xx}: \quad \frac{K^2h^4}{25l(x)^2}\left(-\frac{2hl'(x)}{l(x)}\xi^1_h - 2h\xi^1_{xh} - 5\xi^1_x\right) = 0, \tag{A.22}$$

$$(-h_x)^{\frac{3}{2}}: \quad \frac{K\sqrt{h}}{10l(x)}\left(-2h^2\eta_{hh} + 10\frac{hl'(x)}{l(x)}\xi^2 + 2\frac{h^2l'(x)}{l(x)}\xi^2_h - 10h\xi^1_t - 5h\eta_h + 15h\xi^2_x + 4h^2\xi^2_{xh} - 15\eta\right) = 0, \tag{A.23}$$

$$(-h_x)^{\frac{1}{2}}: \quad \frac{Kh^{\frac{3}{2}}}{l(x)}\left(-\frac{2hl''(x)}{5l(x)}\xi^2 - \frac{2hl'(x)}{5l(x)}\xi^1_t - \frac{l'(x)}{l(x)}\eta + \frac{hl'(x)}{5l(x)}\eta_h + \frac{4hl'(x)^2}{5l(x)^2}\xi^2 + \frac{hl'(x)}{5l(x)}\xi^2_x + \frac{3}{2}\eta_x + \frac{2h}{5}\eta_{xh} - \frac{h}{5}\xi^2_{xx}\right) = 0, \tag{A.24}$$

$$(-h_x)^{-\frac{1}{2}}: \quad \frac{Kh^{\frac{5}{2}}}{l(x)}\left(\frac{l'(x)}{5l(x)}\eta_x - \frac{1}{5}\eta_{xx}\right) = 0, \tag{A.25}$$

$$(-h_x)^{\frac{5}{2}}: \quad \frac{Kh^{\frac{3}{2}}}{l(x)}\left(-\frac{h}{5}\xi^2_{hh}-\frac{\xi^2_h}{2}\right)=0, \tag{A.26}$$

$$(-h_x)^{3}: \quad \frac{K^2h^3}{l(x)^2}\left(\frac{h\xi^1_{hh}}{5}+\frac{\xi^1_h}{2}\right)=0, \tag{A.27}$$

$$(-h_x)^{2}: \quad \frac{K^2h^3}{l(x)^2}\left(\frac{2h^2l'(x)}{25l(x)}\xi^1_{hh}-\frac{2h}{5}\xi^1_{xh}-\frac{3}{2}\xi^1_x\right)=0, \tag{A.28}$$

$$(-h_x): \quad \frac{K^2l'(x)}{l(x)^2}h^4\left(-\frac{2hl'(x)}{25l(x)^2}\xi^1_h-\frac{4h}{25l(x)}\xi^1_{xh}-\frac{4}{5l(x)}\xi^1_x +\frac{1}{5}\xi^1_{xx}+\frac{l(x)^2}{K^2h^4l'(x)}\xi^2_t\right)=0, \tag{A.29}$$

$$1: \quad -\frac{2h^5k^2l'(x)^2}{25l(x)^4}\xi^1_x+\frac{2h^5k^2l'(x)}{25l(x)^3}\xi^1_{xx}+\eta_t=0. \tag{A.30}$$

From equations (A.13) and (A.14), it can be noted that since $K \neq 0$, ξ^1 is independent of both x and h. Similarly, from equations (A.21) and (A.18) we see that ξ^2 and η are independent of h and x respectively. Thus,

$$\xi^1=\xi^1(t), \quad \xi^2=\xi^2(t,x), \quad \eta=\eta(t,h). \tag{A.31}$$

As a result of (A.31), the determining equations reduce to

$$(-h_x)^{-\frac{1}{2}}h_{xx}: \quad 2\frac{hl'(x)}{l(x)}\xi^2-2h\xi^1_t-5\eta+h\eta_h+3h\xi^2_x=0, \tag{A.32}$$

$$(-h_x)^{\frac{3}{2}}: \quad -2h^2\eta_{hh}+10\frac{hl'(x)}{l(x)}\xi^2-10h\xi^1_t-5h\eta_h +15h\xi^2_x-15\eta=0, \tag{A.33}$$

$$(-h_x)^{\frac{1}{2}}: \quad -\frac{2hl''(x)}{5l(x)}\xi^2-\frac{2hl'(x)}{5l(x)}\xi^1_t-\frac{l'(x)}{l(x)}\eta+\frac{hl'(x)}{5l(x)}\eta_h +\frac{4hl'(x)^2}{5l(x)^2}\xi^2+\frac{hl'(x)}{5l(x)}\xi^2_x-\frac{h}{5}\xi^2_{xx}=0, \tag{A.34}$$

$$(-h_x): \quad \xi^2_t=0, \tag{A.35}$$

$$1: \quad \eta_t=0. \tag{A.36}$$

From equations (A.35) and (A.36), the result

$$\xi^1=\xi^1(t), \quad \xi^2=\xi^2(x), \quad \eta=\eta(h), \tag{A.37}$$

is obtained.

Also, upon differentiating (A.32) with respect to t, we obtain

$$\xi^1_{tt}=0. \tag{A.38}$$

Integrating (A.38) twice gives the form

$$\xi^1 = c_1 t + c_2, \tag{A.39}$$

where c_1 and c_2 are arbitrary constants.

Using ξ^1, the determining equations reduce to

$$\eta_h - \frac{5}{h}\eta + \left(2\frac{l'(x)}{l(x)}\xi^2 - 2c_1 + 3\xi_x^2\right) = 0, \tag{A.40}$$

$$-15\eta - 2h^2\eta_{hh} + h\left(10\frac{l'(x)}{l(x)}\xi^2 - 10c_1 - 5\eta_h + 15\xi_x^2\right) = 0, \tag{A.41}$$

$$-5\eta + h\left(-\frac{2l''(x)}{l'(x)}\xi^2 - 2c_1 + \eta_h + \frac{4l'(x)}{l(x)}\xi^2 + \xi_x^2 - \frac{l(x)}{l'(x)}\xi_{xx}^2\right) = 0. \tag{A.42}$$

Equation (A.40) is now a first-order ODE for $\eta = \eta(h)$ that can be solved exactly, resulting in

$$\eta = h\left(-\frac{1}{2}c_1 + \frac{3}{4}\xi_x^2 + \frac{1}{2}\frac{l'(x)}{l(x)}\xi^2\right) + c_3^* h^5, \tag{A.43}$$

where $c_5 = -\frac{1}{2}c_1 + \frac{3}{4}\xi_x^2 + \frac{1}{2}\frac{l'(x)}{l(x)}\xi^2$. Here, c_5 is constant because $\eta = \eta(h)$, and c_3^* is an arbitrary constant.

Substituting η into equation (A.41) results in $c_3^* = 0$, because the different powers of h must vanish separately. Thus,

$$\xi^1 = c_1 t + c_2, \quad \xi^2 = \xi^2(x), \quad \eta = c_5 h, \tag{A.44}$$

where

$$c_5 = -\frac{1}{2}c_1 + \frac{3}{4}\xi_x^2 + \frac{1}{2}\frac{l'(x)}{l(x)}\xi^2. \tag{A.45}$$

Finally, upon substituting η into equation (A.42), the ODE

$$\xi_{xx}^2 + 2\frac{l'(x)}{l(x)}\xi_x^2 + 2\xi^2\left(\frac{l''(x)}{l(x)} - \frac{l'(x)^2}{l(x)^2}\right) = 0, \tag{A.46}$$

is admitted. Writing

$$2\frac{l'(x)}{l(x)}\xi_x^2 + 2\xi^2\left(\frac{l''(x)}{l(x)} - \frac{l'(x)^2}{l(x)^2}\right) = 2\frac{d}{dx}\left(\frac{l'(x)}{l(x)}\xi^2\right), \tag{A.47}$$

allows ODE (A.46) to be expressed as

$$\frac{d}{dx}\left(\xi_x^2 + 2\frac{l'(x)}{l(x)}\xi^2\right) = 0. \tag{A.48}$$

Condition (A.45) can be multiplied by 4 and differentiated once with respect to x to obtain the expression

$$\frac{d}{dx}\left(3\xi_x^2 + 2\frac{l'(x)}{l(x)}\xi^2\right) = 0. \tag{A.49}$$

Subtracting (A.48) from (A.49) results in

$$\xi^2_{xx} = 0, \tag{A.50}$$

which can be integrated twice with respect to x to give

$$\xi^2 = c_3 x + c_4. \tag{A.51}$$

This expression can then be substituted back into (A.45), resulting in the ODE

$$\frac{l'(x)}{l(x)} = \left(2c_5 + c_1 - \frac{3}{2}c_3\right)\frac{1}{c_3 x + c_4}, \tag{A.52}$$

which, when integrated, gives the mixing length

$$l(x) = l_0\,(c_3 x + c_4)^{2\frac{c_5}{c_3} + \frac{c_1}{c_3} - \frac{3}{2}}, \tag{A.53}$$

where l_0 is a constant.

Substitution into (A.49) shows that these expressions for ξ^2 and $l(x)$ identically satisfy the equation.

Thus, the final forms for the infinitesimals in the Lie point symmetry generator (A.3) for equation (3.65) are

$$\xi^1 = c_1 t + c_2, \quad \xi^2 = c_3 x + c_4, \quad \eta = c_5 h, \tag{A.54}$$

where (A.45) holds and the mixing length is given by (A.53).

a.2 Non-classical symmetries of the governing PDE (3.65)

This Appendix provides the calculation of the non-classical symmetries for equation (3.65) with a constant mixing length, given by

$$h_t - \frac{K}{l_0}\left(h^{\frac{3}{2}}(-h_x)^{\frac{3}{2}} + \frac{1}{5}h^{\frac{5}{2}}(-h_x)^{-\frac{1}{2}}h_{xx}\right) = 0. \tag{A.55}$$

We will make use of the invariant surface condition

$$\xi^1 h_t + \xi^2 h_x = \eta, \tag{A.56}$$

as the condition that must remain invariant simultaneously with equation (A.55) under the symmetry generator. We can assume that $\xi^1 \neq 0$ and thus the invariant surface condition reduces to

$$h_t = \eta_* + \xi^2_*(-h_x). \tag{A.57}$$

Suppressing the stars for notational convenience, we see this is effectively like taking $\xi^1 = 1$ and solving for the remaining two infinitesimals, ξ^2 and η.

As we already have an expression for h_t, we can use equation (A.55) to solve for h_{xx},

$$h_{xx} = \frac{5l_0}{K} h^{-\frac{5}{2}}(-h_x)^{\frac{1}{2}}(\eta + \xi^2(-h_x)) - 5h^{-1}(-h_x)^2. \tag{A.58}$$

Using equation (A.57) and taking the total derivative with respect to x results in

$$h_{tx} = \eta_x - (-h_x)\eta_h + (-h_x)\xi^2_x - (-h_x)^2\xi^2_h - \xi^2 h_{xx}. \tag{A.59}$$

As a result of equations (A.58) and (A.59), all second order derivatives required for obtaining the non-classical symmetry can be replaced by expressions that are in terms of the first order derivatives only.

We now search for a symmetry generator of the form

$$X = \frac{\partial}{\partial t} + \xi^2(t,x,h)\frac{\partial}{\partial x} + \eta(t,x,h)\frac{\partial}{\partial h}, \tag{A.60}$$

where

$$X^{[2]}((A.55))|_{((A.55=0),(A.57))} = 0, \tag{A.61}$$

holds.

We prolong the symmetry generator to second order,

$$\begin{aligned} X^{[2]} = {} & \frac{\partial}{\partial t} + \xi^2(t,x,h)\frac{\partial}{\partial x} + \eta(t,x,h)\frac{\partial}{\partial h} + \zeta_t(t,x,h)\frac{\partial}{\partial h_t} \\ & + \zeta_x(t,x,h)\frac{\partial}{\partial h_x} + \zeta_{tt}(t,x,h)\frac{\partial}{\partial h_{tt}} + \zeta_{tx}(t,x,h)\frac{\partial}{\partial h_{tx}} + \zeta_{xx}(t,x,h)\frac{\partial}{\partial h_{xx}}, \end{aligned} \tag{A.62}$$

since PDE (A.55) is of second order, where [7]

$$\zeta_t = \eta_t + \eta_h h_t - \xi_t^2 h_x - \xi_h^2 h_t h_x, \tag{A.63}$$

$$\zeta_x = \eta_x + (\eta_h - \xi_x^2) h_x - \xi_h^2 h_x^2, \tag{A.64}$$

$$\begin{aligned}\zeta_{tt} =& \eta_{tt} + 2\eta_{th} h_t - \xi_{tt}^2 h_x + \eta_h h_{tt} - 2\xi_t^2 h_{tx} \\ &+ \eta_{hh} h_t^2 - 2\xi_{th}^2 h_t h_x - \xi_{hh}^2 h_t^2 h_x \\ &- \xi_h^2 h_x h_{tt} - 2\xi_h^2 h_t h_{tx},\end{aligned} \tag{A.65}$$

$$\begin{aligned}\zeta_{tx} =& \eta_{tx} + (\eta_{th} - \xi_{tx}^2) h_x + \eta_{xh} h_t - \xi_t^2 h_{xx} \\ &+ (\eta_h - \xi_x^2) h_{tx} - \xi_{th}^2 h_x^2 + (\eta_{hh} - \xi_{xh}^2) h_t h_x \\ &- \xi_{hh}^2 h_t h_x^2 - 2\xi_h^2 h_x h_{tx} - \xi_h^2 h_t h_{xx},\end{aligned} \tag{A.66}$$

$$\begin{aligned}\zeta_{xx} =& \eta_{xx} + (2\eta_{xh} - \xi_{xx}^2) h_x + (\eta_h - 2\xi_x^2) h_{xx} \\ &+ (\eta_{hh} - 2\xi_{xh}^2) h_x^2 - \xi_{hh}^2 h_x^3 - 3\xi_h^2 h_x h_{xx}.\end{aligned} \tag{A.67}$$

Equation (A.61) becomes

$$\begin{aligned}&-\frac{K}{l_0}\eta\left(\frac{3}{2}h^{\frac{1}{2}}(-h_x)^{\frac{3}{2}} + \frac{1}{2}h^{\frac{3}{2}}(-h_x)^{-\frac{1}{2}}h_{xx}\right) + \zeta_t \\ &-\frac{K}{l_0}\zeta_x\left(-\frac{3}{2}h^{\frac{3}{2}}(-h_x)^{\frac{1}{2}} + \frac{1}{10}h^{\frac{5}{2}}(-h_x)^{-\frac{3}{2}}h_{xx}\right) \\ &-\frac{K}{l_0}\zeta_{xx}\left(\frac{1}{5}h^{\frac{5}{2}}(-h_x)^{-\frac{1}{2}}\right)\Bigg|_{((A.55),(A.57))} = 0.\end{aligned} \tag{A.68}$$

Replacing h_{xx} with equation (A.58) and collecting like powers of the derivatives of h in equation (A.68) results in

$$\begin{aligned}&\left(-\frac{5}{2}h^{-1}\eta^2 + \frac{1}{2}\eta\eta_h + \eta_t - \frac{1}{2}\xi^2\eta_x + \frac{3}{2}\eta\xi_x^2\right) \\ &-(-h_x)^{-1}\left(\frac{1}{2}\eta\eta_x\right) + (-h_x)^{-\frac{1}{2}}\left(-\frac{K}{5l_0}h^{\frac{5}{2}}\eta_{xx}\right) \\ &+(-h_x)^{\frac{1}{2}}\left(2\frac{K}{l_0}h^{\frac{3}{2}}\eta_x + \frac{2K}{5l_0}h^{\frac{5}{2}}\eta_{xh} - \frac{K}{5l_0}h^{\frac{5}{2}}\xi_{xx}^2\right)\end{aligned}$$

$$-(-h_x)\left(\frac{5}{2}h^{-1}\eta\xi^2-\frac{1}{2}\xi^2\eta_h+\frac{3}{2}\eta\xi^2_h-\xi^2_t-\frac{3}{2}\xi\xi^2_x\right)$$

$$-(-h_x)^{\frac{3}{2}}\left(-\frac{K}{l_0}\sqrt{h}\eta+\frac{K}{l_0}h^{\frac{3}{2}}\eta_h+\frac{K}{5l_0}h^{\frac{5}{2}}\eta_{hh}-\frac{2K}{5l_0}h^{\frac{5}{2}}\xi^2_{xh}\right)$$

$$(-h_x)^2\left(-\frac{3}{2}\xi^2\xi^2_h\right)-(-h_x)^{\frac{5}{2}}\left(\frac{K}{l_0}h^{\frac{3}{2}}\xi^2_h-\frac{K}{5l_0}h^{\frac{5}{2}}\xi^2_{hh}\right)=0. \tag{A.69}$$

As ξ^2 and η are independent of the derivatives of $h(t,x)$, we may separate by the derivatives, resulting in the following set of determining equations:

$$(-h_x)^{\frac{5}{2}}: \quad \frac{K}{l_0}h^{\frac{3}{2}}\left(\xi^2_h-\frac{1}{5}h\xi^2_{hh}\right)=0, \tag{A.70}$$

$$(-h_x)^2: \quad \frac{3}{2}\xi^2\xi^2_h=0, \tag{A.71}$$

$$(-h_x)^{\frac{3}{2}}: \quad \frac{K}{l_0}\sqrt{h}\left(-\eta+h\eta_h+\frac{1}{5}h^2\eta_{hh}-\frac{2}{5}h^2\xi^2_{xh}\right)=0, \tag{A.72}$$

$$(-h_x): \quad \frac{5}{2}h^{-1}\eta\xi^2-\frac{1}{2}\xi^2\eta_h+\frac{3}{2}\eta\xi^2_h-\xi^2_t-\frac{3}{2}\xi\xi^2_x=0, \tag{A.73}$$

$$(-h_x)^{\frac{1}{2}}: \quad \frac{K}{l_0}h^{\frac{3}{2}}\left(2\eta_x+\frac{2}{5}h\eta_{xh}-\frac{1}{5}h\xi^2_{xx}\right)=0, \tag{A.74}$$

$$(-h_x)^{-1}: \quad \frac{1}{2}\eta\eta_x=0, \tag{A.75}$$

$$(-h_x)^{-\frac{1}{2}}: \quad \frac{K}{5l_0}h^{\frac{5}{2}}\eta_{xx}=0, \tag{A.76}$$

$$1: \quad -\frac{5}{2}h^{-1}\eta^2+\frac{1}{2}\eta\eta_h+\eta_t-\frac{1}{2}\xi^2\eta_x+\frac{3}{2}\eta\xi^2_x=0. \tag{A.77}$$

From equations (A.71) and (A.75), we see $\xi^2_h=0$ and $\eta_x=0$ respectively. Thus,

$$\xi^1=1, \quad \xi^2=\xi^2(t,x), \quad \eta=\eta(t,h). \tag{A.78}$$

As a result, the determining equations reduce:

$$(-h_x)^{\frac{3}{2}}: \quad -\eta+h\eta_h+\frac{1}{5}h^2\eta_{hh}, \tag{A.79}$$

$$(-h_x): \quad 5h^{-1}\eta\xi^2-\eta_h\xi^2-2\xi^2_t-3\xi\xi^2_x=0, \tag{A.80}$$

$$(-h_x)^{\frac{1}{2}}: \quad \xi^2_{xx}=0, \tag{A.81}$$

$$1: \quad -5h^{-1}\eta^2+\eta\eta_h+2\eta_t+3\eta\xi^2_x=0. \tag{A.82}$$

From equation (A.81), we can integrate twice with respect to x to obtain

$$\xi^2=a(t)x+b(t), \tag{A.83}$$

where $a(t)$ and $b(t)$ are functions of time whose form is still to be determined.

Similarly, by solving the PDE (A.79), we obtain

$$\eta = c(t)h + d(t)h^{-5}, \tag{A.84}$$

where $c(t)$ and $d(t)$ are time functions to be determined.

Substituting the expressions for ξ^2 and η into equation (A.80) yields $d(t) = 0$. Thus,

$$\xi^1 = 1, \quad \xi^2 = a(t)x + b(t), \quad \eta = c(t)h, \tag{A.85}$$

where equations (A.80) and (A.82) reduce to

$$4c(t)^2 - 2c'(t) - 3a(t)c(t) = 0, \tag{A.86}$$

$$4a(t)c(t) - 2a'(t) - 3a(t)^2 = 0, \tag{A.87}$$

$$4b(t)c(t) - 2b'(t) - 3a(t)b(t) = 0. \tag{A.88}$$

This is a set of non-linear equations which cannot be solved generally, as predicted by [9]. Special cases will need to be taken in order to obtain solutions. Any solution of the non-linear set of equations will result in a symmetry generator that simultaneously leaves the PDE and the invariant surface condition invariant.

B

APPENDIX B

b.1 Lie point symmetries of the governing order ν equation

This Appendix details the calculation of the Lie point symmetry generator for equation (3.74), which can be written as

$$\begin{aligned} F(t,x,h,h_5,h_x,h_{xx}) = h_t &- K\left[\frac{2}{5}\frac{l'(x)}{l(x)^2}h^{\frac{5}{2}}(-h_x)^{\frac{1}{2}} + \frac{1}{l(x)}h^{\frac{3}{2}}(-h_x)^{\frac{3}{2}}\right] \\ &- K\left[\frac{1}{5}\frac{1}{l(x)}h^{\frac{5}{2}}(-h_x)^{-\frac{1}{2}}h_{xx}\right] \\ &+ \frac{\nu}{2}\left[\frac{l'(x)}{l(x)^3}h^2 + \frac{1}{l(x)^2}h(-h_x)\right] = 0. \end{aligned} \tag{B.1}$$

Thus,

$$\begin{aligned} h_t = &K\left[\frac{2}{5}\frac{l'(x)}{l(x)^2}h^{\frac{5}{2}}(-h_x)^{\frac{1}{2}} + \frac{1}{l(x)}h^{\frac{3}{2}}(-h_x)^{\frac{3}{2}}\right] \\ &+ K\left[\frac{1}{5}\frac{1}{l(x)}h^{\frac{5}{2}}(-h_x)^{-\frac{1}{2}}h_{xx}\right] \\ &- \frac{\nu}{2}\left[\frac{l'(x)}{l(x)^3}h^2 + \frac{1}{l(x)^2}h(-h_x)\right]. \end{aligned} \tag{B.2}$$

We prolong the general symmetry generator to second order, as given by (A.4), and make use of the expressions (A.5-A.9).

The Lie point symmetry (A.3) satisfies (A.10) where F is given by (B.1).

Treating t, x, $h(t,x)$ and all the derivatives of $h(t,x)$ as independent variables, (A.10) becomes

$$\begin{aligned} &-K\xi^2\left[\frac{2}{5}\left(\frac{l''(x)}{l(x)^2} - 2\frac{l'(x)^2}{l(x)^3}\right)h^{\frac{5}{2}}(-h_x)^{\frac{1}{2}} - \frac{l'(x)}{l(x)^2}h^{\frac{3}{2}}(-h_x)^{\frac{3}{2}}\right] \\ &-K\xi^2\left[-\frac{1}{5}\frac{l'(x)}{l(x)^2}h^{\frac{5}{2}}(-h_x)^{-\frac{1}{2}}h_{xx}\right] + \frac{\nu}{2}\xi^2\left[-3\frac{l'(x)^2}{l(x)^4}h^2\right] \\ &+\frac{\nu}{2}\xi^2\left[\frac{l''(x)}{l(x)^3}h^2 - 2\frac{l'(x)}{l(x)^3}h(-h_x)\right] - K\eta\left[\frac{l'(x)}{l(x)^2}h^{\frac{3}{2}}(-h_x)^{\frac{1}{2}}\right] \end{aligned}$$

$$
\begin{aligned}
&- K\eta\left[\frac{3}{2}\frac{1}{l(x)}h^{\frac{1}{2}}(-h_x)^{\frac{3}{2}}+\frac{1}{2}\frac{1}{l(x)}h^{\frac{3}{2}}(-h_x)^{-\frac{1}{2}}h_{xx}\right]\\
&+\frac{\nu}{2}\eta\left[2\frac{l'(x)}{l(x)^3}h+\frac{1}{l(x)^2}(-h_x)\right]+\zeta_t\\
&- K\zeta_x\left[-\frac{1}{5}\frac{l'(x)}{l(x)^2}h^{\frac{5}{2}}(-h_x)^{-\frac{1}{2}}\right]-K\zeta_x\left[-\frac{3}{2}\frac{1}{l(x)}h^{\frac{3}{2}}(-h_x)^{\frac{1}{2}}\right]\\
&- K\zeta_x\left[\frac{1}{10}\frac{1}{l(x)}h^{\frac{5}{2}}(-h_x)^{-\frac{3}{2}}h_{xx}\right]+\frac{\nu}{2}\zeta_x\left[-\frac{1}{l(x)^2}h\right]\\
&\qquad\qquad- K\zeta_{xx}\left[\frac{1}{5}\frac{1}{l(x)}h^{\frac{5}{2}}(-h_x)^{-\frac{1}{2}}\right]\Bigg|_{(B.2)}=0. \quad \text{(B.3)}
\end{aligned}
$$

Upon expanding equation (B.3), we obtain

$$
\begin{aligned}
&-(-h_x)^{\frac{3}{2}}\left(\frac{K\eta_h h^{\frac{3}{2}}}{2l(x)}+\frac{K\xi^1_t h^{\frac{3}{2}}}{l(x)}-\frac{3K\xi^2_x h^{\frac{3}{2}}}{2l(x)}-\frac{K\xi^2 l'(x)h^{\frac{3}{2}}}{l(x)^2}+\frac{K\eta_{hh}h^{\frac{5}{2}}}{5l(x)}-\frac{2K\xi^2_{xh}h^{\frac{5}{2}}}{5l(x)}\right.\\
&-\frac{K\xi^2_h l'(x)h^{\frac{5}{2}}}{5l(x)^2}-\frac{5K\nu\xi^1_x h^{\frac{5}{2}}}{4l(x)^3}-\frac{K\nu\xi^1_{xh}h^{\frac{7}{2}}}{5l(x)^3}-\frac{7K\nu\xi^1_h l'(x)h^{\frac{7}{2}}}{20l(x)^4}+\frac{K\nu\xi^1_{hh}l'(x)h^{\frac{9}{2}}}{10l(x)^4}\\
&\left.+\frac{3K\eta\sqrt{h}}{2l(x)}\right)+(-h_x)^{\frac{5}{2}}\left(-\frac{K\xi^2_h h^{\frac{3}{2}}}{2l(x)}-\frac{K\xi^2_{hh}h^{\frac{5}{2}}}{5l(x)}-\frac{K\nu\xi^1_h h^{\frac{5}{2}}}{4l(x)^3}-\frac{K\nu\xi^1_{hh}h^{\frac{7}{2}}}{10l(x)^3}\right)\\
&+\sqrt{-h_x}\left(\frac{3K\eta_x h^{\frac{3}{2}}}{2l(x)}-\frac{K\eta l'(x)h^{\frac{3}{2}}}{l(x)^2}+\frac{4K\xi^2 l'(x)^2h^{\frac{5}{2}}}{5l(x)^3}+\frac{2K\eta_{xh}h^{\frac{5}{2}}}{5l(x)}+\frac{K\eta_h l'(x)h^{\frac{5}{2}}}{5l(x)^2}\right.\\
&+\frac{K\xi^2_x l'(x)h^{\frac{5}{2}}}{5l(x)^2}-\frac{K\xi^2_{xx}h^{\frac{5}{2}}}{5l(x)}-\frac{2K\xi^1_t l'(x)h^{\frac{5}{2}}}{5l(x)^2}-\frac{2K\xi^2 l''(x)h^{\frac{5}{2}}}{5l(x)^2}+\frac{21K\nu\xi^1_x l'(x)h^{\frac{7}{2}}}{20l(x)^4}\\
&\left.-\frac{K\nu\xi^1_{xx}h^{\frac{7}{2}}}{10l(x)^3}+\frac{3K\nu\xi^1_h l'(x)^2h^{\frac{9}{2}}}{10l(x)^5}+\frac{K\nu\xi^1_{xh}l'(x)h^{\frac{9}{2}}}{5l(x)^4}\right)-\frac{2h^{\frac{5}{2}}K\xi^1_h h_{tx}\sqrt{-h_x}}{5l(x)}\\
&+h_{xx}\sqrt{-h_x}\left(\frac{h^{\frac{7}{2}}K\nu\xi^1_h}{20l(x)^3}-\frac{3h^{\frac{5}{2}}K\xi^2_h}{10l(x)}\right)-(-h_x)^3\left(-\frac{K^2\xi^1_{hh}h^4}{5l(x)^2}-\frac{K^2\xi^1_h h^3}{2l(x)^2}\right)\\
&+(-h_x)^2\left(\frac{2K^2\xi^1_{hh}l'(x)h^5}{25l(x)^3}-\frac{2K^2\xi^1_{xh}h^4}{5l(x)^2}-\frac{3K^2\xi^1_x h^3}{2l(x)^2}\right)+\left(\frac{2K^2\xi^1_{xx}l'(x)h^5}{25l(x)^3}\right.\\
&-\frac{2K^2\xi^1_x l'(x)^2h^5}{25l(x)^4}-\frac{\nu^2\xi^1_h l'(x)^2h^4}{4l(x)^6}-\frac{\nu^2\xi^1_x l'(x)h^3}{4l(x)^5}+\frac{\nu\xi^1_t l'(x)h^2}{2l(x)^3}+\frac{\nu\xi^2 l''(x)h^2}{2l(x)^3}\\
&\left.-\frac{\nu\eta_h l'(x)h^2}{2l(x)^3}-\frac{3\nu\xi^2 l'(x)^2h^2}{2l(x)^4}+\frac{\nu\eta l'(x)h}{l(x)^3}-\frac{\nu\eta_x h}{2l(x)^2}+\eta_t\right)
\end{aligned}
$$

$$-\frac{h_{xx}}{\sqrt{-h_x}}\left(\frac{K\eta h^{\frac{3}{2}}}{2l(x)}+\frac{K\xi^1_t h^{\frac{5}{2}}}{5l(x)}-\frac{K\eta_h h^{\frac{5}{2}}}{10l(x)}-\frac{3K\xi^2_x h^{\frac{5}{2}}}{10l(x)}-\frac{K\xi^2 l'(x)h^{\frac{5}{2}}}{5l(x)^2}-\frac{K\nu\xi^1_x h^{\frac{7}{2}}}{20l(x)^3}\right.$$

$$\left.-\frac{3K\nu\xi^1_h l'(x)h^{\frac{9}{2}}}{20l(x)^4}\right)-\frac{1}{\sqrt{-h_x}}\left(\frac{K\eta_{xx}h^{\frac{5}{2}}}{5l(x)}-\frac{K\eta_x l'(x)h^{\frac{5}{2}}}{5l(x)^2}+\frac{K\nu\xi^1_{xx}l'(x)h^{\frac{9}{2}}}{10l(x)^4}\right.$$

$$\left.-\frac{K\nu\xi^1_x l'(x)^2h^{\frac{9}{2}}}{10l(x)^5}\right)+\frac{2h^{\frac{5}{2}}K\xi^1_x h_{tx}}{5l(x)\sqrt{-h_x}}+\frac{h^5K^2\xi^1_x h^2_{xx}}{50l(x)^2\,(-h_x)^2}-\frac{h^5K^2\xi^1_h h^2_{xx}}{50l(x)^2\,(-h_x)}+\frac{h^5K^2\xi^1_{xx}h_{xx}}{25l(x)^2(-h_x)}$$

$$+\frac{h_{xx}}{(-h_x)^{\frac{3}{2}}}\left(-\frac{K\eta_x h^{\frac{5}{2}}}{10l(x)}-\frac{K\nu\xi^1_x l'(x)h^{\frac{9}{2}}}{20l(x)^4}\right)+\left(\frac{2K^2\xi^1_h l'(x)^2h^5}{25l(x)^4}+\frac{4K^2\xi^1_{xh}l'(x)h^5}{25l(x)^3}\right.$$

$$+\frac{4K^2\xi^1_x l'(x)h^4}{5l(x)^3}-\frac{K^2\xi^1_{xx}h^4}{5l(x)^2}+\frac{\nu^2\xi^1_h l'(x)h^3}{4l(x)^5}+\frac{\nu^2\xi^1_x h^2}{4l(x)^4}+\frac{\nu\xi^2_h l'(x)h^2}{2l(x)^3}+\frac{\nu\xi^2_x h}{2l(x)^2}$$

$$\left.+\frac{\nu\xi^2 l'(x)h}{l(x)^3}-\frac{\nu\xi^1_t h}{2l(x)^2}-\xi^2_t-\frac{\nu\eta}{2l(x)^2}\right)h_x+\left(-\frac{2K^2\xi^1_{xh}h^5}{25l(x)^2}-\frac{2K^2\xi^1_h l'(x)h^5}{25l(x)^3}\right.$$

$$\left.-\frac{K^2\xi^1_x h^4}{5l(x)^2}\right)h_{xx}-\frac{h^5K^2\xi^1_{hh}(-h_x)h_{xx}}{25l(x)^2}=0. \quad \text{(B.4)}$$

Now, ξ^1, ξ^2 and η are all independent of the derivatives of $h(t,x)$, thus equation (B.4) can be separated by the derivatives of $h(t,x)$, resulting in the following set of determining equations:

$$(-h_x)^{-\frac{1}{2}}h_{tx}: \quad \frac{2K}{5}\frac{1}{l(x)}h^{\frac{5}{2}}\xi^1_x=0, \quad \text{(B.5)}$$

$$(-h_x)^{\frac{1}{2}}h_{tx}: \quad \frac{2K}{5}\frac{1}{l(x)}h^{\frac{5}{2}}\xi^1_h=0, \quad \text{(B.6)}$$

$$(-h_x)^3: \quad \frac{K^2}{l(x)^2}h^3\left(\frac{1}{5}h\xi^1_{hh}+\frac{1}{2}\xi^1_h\right)=0, \quad \text{(B.7)}$$

$$(-h_x)^{-1}h^2_{xx}: \quad \frac{K^2}{50}\frac{1}{l(x)^2}h^5\xi^1_h=0, \quad \text{(B.8)}$$

$$(-h_x)^{-2}h^2_{xx}: \quad \frac{K^2}{50}\frac{1}{l(x)^2}h^5\xi^1_x=0, \quad \text{(B.9)}$$

$$(-h_x)^{\frac{5}{2}}: \quad \frac{K\nu}{l(x)^3}h^{\frac{5}{2}}\left(-\frac{1}{10}h\xi^1_{hh}-\frac{1}{4}\xi^1_h\right)$$

$$+\frac{K}{l(x)}h^{\frac{3}{2}}\frac{1}{10}\left(-\frac{h}{5}\xi^2_{hh}-\frac{1}{2}\xi^2_h\right)=0, \quad \text{(B.10)}$$

$$(-h_x)^2: \quad \frac{K^2}{l(x)^2}h^3\left(\frac{2l'(x)}{25l(x)}h^2\xi^1_{hh}-\frac{2}{5}h\xi^1_{xh}-\frac{3}{2}\xi^1_x\right)=0, \tag{B.11}$$

$$\begin{aligned}(-h_x)^{-\frac{1}{2}} \quad & -\frac{K\nu l'(x)}{10l(x)^4}h^{\frac{9}{2}}\left(-\frac{l'(x)}{l(x)}\xi^1_x+\xi^1_{xx}\right)\\ & -\frac{K}{5l(x)}h^{\frac{5}{2}}\left(-\frac{l'(x)}{l(x)}\eta_x+\eta_{xx}\right)=0,\end{aligned} \tag{B.12}$$

$$(-h_x)^{\frac{1}{2}}h_{xx}: \quad \frac{K}{l(x)}h^{\frac{5}{2}}\left(\frac{h\nu}{20l(x)^2}\xi^1_h-\frac{3}{10}\xi^2_h\right)=0, \tag{B.13}$$

$$(-h_x)h_{xx}: \quad \frac{K^2}{25}\frac{1}{l(x)^2}h^5\xi^1_{hh}=0, \tag{B.14}$$

$$h_{xx}: \quad \frac{K^2}{l(x)^2}h^4\left(-\frac{2hl'(x)}{25l(x)}\xi^1_h-\frac{2h}{25}\xi^1_{xh}-\frac{1}{5}\xi^1_x\right)=0, \tag{B.15}$$

$$\begin{aligned}h_{xx}(-h_x)^{-\frac{1}{2}}: \quad & \frac{K}{l(x)}h^{\frac{3}{2}}\left(-\frac{3h^3\nu l'(x)}{20l(x)^3}\xi^1_h-\frac{hl'(x)}{5l(x)}\xi^2+\frac{h\xi^1_t}{5}\right.\\ & \left.-\frac{h^2\nu}{20l(x)^2}\xi^1_x-\frac{h}{10}\eta_h+\frac{\eta}{2}-\frac{3h}{10}\xi^2_x\right)=0,\end{aligned} \tag{B.16}$$

$$h_{xx}(-h_x)^{-1}: \quad \frac{h^5K^2}{25l(x)^2}\xi^1_{xx}=0, \tag{B.17}$$

$$h_{xx}(-h_x)^{-\frac{3}{2}}: \quad \frac{K}{10l(x)}h^{\frac{5}{2}}\left(-\frac{h^2\nu l'(x)}{2l(x)^2}\xi^1_x-\eta_x\right)=0, \tag{B.18}$$

$$\begin{aligned}(-h_x): \quad & -\frac{K^2}{5l(x)^2}h^4\left(\frac{2l'(x)^2}{5l(x)^2}h\xi^1_h+\frac{4l'(x)}{5l(x)}h\xi^1_{xh}+\frac{4l'(x)}{l(x)}\xi^1_x-\xi^1_{xx}\right)\\ & -\frac{\nu}{l(x)^2}h\left(\frac{\nu l'(x)}{4l(x)^3}h^2\xi^1_h+\nu\frac{l'(x)}{2l(x)}h\xi^2_h+\frac{\nu}{4l(x)^2}h\xi^1_x\right.\\ & \left.+\frac{l'(x)}{l(x)}\xi^2-\frac{1}{2}\xi^1_t-\eta_h+\frac{1}{2}\xi^2_x-\frac{1}{2h}\eta\right)+\xi^2_t=0,\end{aligned} \tag{B.19}$$

$$\begin{aligned}(-h_x)^{\frac{3}{2}} \quad & \frac{K}{l(x)}h^{\frac{1}{2}}\left(\frac{\nu l'(x)}{10l(x)^3}h^4\xi^1_{hh}+\frac{1}{5}h^2\eta_{hh}+\frac{7\nu l'(x)}{20l(x)^3}h^3\xi^1_h\right.\\ & -\frac{l'(x)}{5l(x)}h^2\xi^2_h-\frac{l'(x)}{l(x)}h\xi^2+h\xi^1_t-\frac{5\nu}{4l(x)^2}h^2\xi^1_x\\ & \left.-\frac{\nu}{5l(x)^2}h^3\xi^1_{xh}+\frac{1}{2}h\eta_h-\frac{3}{2}h\xi^2_x-\frac{2}{5}h^2\xi^2_{xh}+\frac{3}{2}\eta\right)=0,\end{aligned} \tag{B.20}$$

$$
\begin{aligned}
(-h_x)^{\frac{1}{2}} \quad & \frac{K}{l(x)} h^{\frac{3}{2}} \left(-\frac{2l''(x)}{5l(x)} h\xi^2 - \frac{2l'(x)}{5l(x)} h\xi^1_t + \frac{3\nu l'(x)^2}{10l(x)^4} h^3 \xi^1_h \right. \\
& + \frac{21\nu l'(x)}{20l(x)^3} h^2 \xi^1_x + \frac{\nu l'(x)}{5l(x)^3} h^3 \xi^1_{xh} + \frac{l'(x)}{5l(x)} h\eta_h \\
& + \frac{4l'(x)^2}{5l(x)^2} h\xi^2 + \frac{l'(x)}{5l(x)} h\xi^2_x - \frac{\nu}{10l(x)^2} h^2 \xi^1_{xx} \\
& \left. + \frac{2}{5} h\eta_{xh} - \frac{1}{5} h\xi^2_{xx} - \frac{l'(x)}{l(x)} \eta + \frac{3}{2} \eta_x \right) = 0, \qquad \text{(B.21)} \\
1: \quad & \frac{2K^2 l'(x)}{25l(x)^3} h^5 \left(-\frac{l'(x)}{l(x)} \xi^1_x + \xi^1_{xx} \right) - \frac{\nu^2 l'(x)}{l(x)^5} h^3 \left(\frac{l'(x)}{4l(x)} h\xi^1_h \right. \\
& \left. + \frac{1}{4} \xi^1_x \right) + \frac{\nu}{l(x)^2} h \left(\frac{l''(x)}{2l(x)} h\xi^2 + \frac{l'(x)}{2l(x)} h\xi^1_t - \frac{l'(x)}{2l(x)} h\eta_h \right. \\
& \left. - \frac{3l'(x)^2}{2l(x)^2} h\xi^2 + \frac{l'(x)}{l(x)} \eta - \frac{1}{2} \eta_x \right) + \eta_t = 0. \qquad \text{(B.22)}
\end{aligned}
$$

We restrict $K \neq 0$. From equations (B.5) and (B.6), ξ^1 is independent of both x and h. Thus,

$$\xi^1 = \xi^1(t), \quad \xi^2 = \xi^2(t, x, h), \quad \eta = \eta(t, x, h). \qquad \text{(B.23)}$$

The determining equations thus reduce:

$$
\begin{aligned}
(-h_x)^{\frac{5}{2}} \quad & \frac{1}{5} h\xi^2_{hh} + \frac{1}{2} \xi^2_h = 0, \qquad \text{(B.24)} \\
(-h_x)^{-\frac{1}{2}}: \quad & \frac{l'(x)}{l(x)} \eta_x - \eta_{xx} = 0, \qquad \text{(B.25)} \\
(-h_x)^{\frac{1}{2}} h_{xx}: \quad & \frac{3h^{\frac{5}{2}} K}{10l(x)} \xi^2_h = 0, \qquad \text{(B.26)} \\
h_{xx}(-h_x)^{-\frac{1}{2}}: \quad & -2\frac{l'(x)}{l(x)} h\xi^2 + 2h\xi^1_t - h\eta_h + 5\eta - 3h\xi^2_x = 0, \qquad \text{(B.27)} \\
h_{xx}(-h_x)^{-\frac{3}{2}}: \quad & \frac{h^{\frac{5}{2}} K}{10l(x)} \eta_x = 0, \qquad \text{(B.28)} \\
(-h_x): \quad & \nu \frac{l'(x)}{2l(x)} h\xi^2_h + \frac{l'(x)}{l(x)} \xi^2 - \frac{1}{2} \xi^1_t - \eta_h + \frac{1}{2} \xi^2_x - \frac{\eta}{2h} \\
& - \frac{l(x)^2}{\nu h} \xi^2_t = 0, \qquad \text{(B.29)}
\end{aligned}
$$

$$(-h_x)^{\frac{3}{2}} \quad \frac{h^2}{5}\eta_{hh} - \frac{h^2 l'(x)}{5l(x)}\xi^2_h - \frac{hl'(x)}{l(x)}\xi^2 + h\xi^1_t + \frac{h}{2}\eta_h$$
$$- \frac{3h}{2}\xi^2_x - \frac{2h^2}{5}\xi^2_{xh} + \frac{3}{2}\eta = 0, \tag{B.30}$$
$$(-h_x)^{\frac{1}{2}}: \quad - \frac{2l''(x)}{5l(x)}h\xi^2 - \frac{2l'(x)}{5l(x)}h\xi^1_t + \frac{l'(x)}{5l(x)}h\eta_h$$
$$+ \frac{4l'(x)^2}{5l(x)^2}h\xi^2 + \frac{l'(x)}{5l(x)}h\xi^2_x + \frac{2}{5}h\eta_{xh}$$
$$- \frac{1}{5}h\xi^2_{xx} - \frac{l'(x)}{l(x)}\eta + \frac{3}{2}\eta_x = 0, \tag{B.31}$$
$$1: \quad \frac{hl''(x)}{2l(x)}\xi^2 + \frac{hl'(x)}{2l(x)}\xi^1_t + \frac{l(x)^2}{\nu h}\eta_t - \frac{hl'(x)}{2l(x)}\eta_h$$
$$- \frac{3hl'(x)^2}{2l(x)^2}\xi^2 + \frac{l'(x)}{l(x)}\eta - \frac{1}{2}\eta_x = 0. \tag{B.32}$$

From equations (B.26) and (B.28) we see that ξ^2 and η are independent of h and x respectively. Thus,

$$\xi^1 = \xi^1(t), \quad \xi^2 = \xi^2(t,x), \quad \eta = \eta(t,h). \tag{B.33}$$

The determining equations can thus be further simplified:

$$(-h_x)^{-\frac{1}{2}}h_{xx}: \quad 5\eta + h\left(-\frac{2l'(x)}{l(x)}\xi^2 + 2\xi^1_t - \eta_h - 3\xi^2_x\right) = 0, \tag{B.34}$$
$$(-h_x): \quad \eta + 2\frac{l(x)^2}{\nu}\xi^2_t + h\left(2\eta_h - \frac{2l'(x)}{l(x)}\xi^2 - \xi^1_t - \xi^2_x\right) = 0, \tag{B.35}$$
$$(-h_x)^{\frac{3}{2}}: \quad 15\eta + 2h^2\eta_{hh} + h\left(-10\frac{\xi^2 l'(x)}{l(x)} + 10\xi^1_t\right)$$
$$+ h\left(5\eta_h - 15\xi^2_x\right) = 0, \tag{B.36}$$

$$(-h_x)^{\frac{1}{2}}: \quad -5l'(x)\eta + h\left(-2l''(x)\xi^2 - 2l'(x)\xi^1_t + l'(x)\eta_h\right. \tag{B.37}$$
$$\left. + \frac{4(l'(x))^2}{l(x)}\xi^2\right) + h\left(l'(x)\xi^2_x - l(x)\xi^2_{xx}\right) = 0, \tag{B.38}$$
$$1: \quad 2\frac{l'(x)}{l(x)^3}\eta + \eta_t\frac{2}{\nu h} + \frac{h}{l(x)^3}\left(\xi^2 l''(x) - l'(x)\xi^1_t\right.$$
$$\left. + l'(x)\eta_h - \frac{3\xi^2(l'(x))^2}{l(x)}\right) = 0. \tag{B.39}$$

Equation (B.34) is a first order partial differential equation for η that can be solved exactly, giving

$$\eta = h\left(-\frac{1}{2}\xi_t^1 + \frac{3}{4}\xi_x^2 + \frac{1}{2}\frac{l'(x)}{l(x)}\xi^2\right) + q(t)h^5, \tag{B.40}$$

where $q(t)$ is a function of time to be determined.

Upon substitution of η into equation (B.36), it is found that $q(t) = 0$. Thus,

$$\xi^1 = \xi^1(t), \quad \xi^2 = \xi^2(t,x), \quad \eta(t,h) = c_5(t)h, \tag{B.41}$$

where

$$c_5(t) = -\frac{1}{2}\xi_t^1 + \frac{3}{4}\xi_x^2 + \frac{1}{2}\xi^2\frac{l'(x)}{l(x)}. \tag{B.42}$$

Substituting η into (B.35) and separating by h results in $\xi_t^2 = 0$. Simplifying the remaining determining equations gives

$$10\xi_t^1 - 5\xi_x^2 + 2\frac{l'(x)}{l(x)}\xi^2 = 0, \tag{B.43}$$

$$\xi_{xx}^2 + 2\frac{l'(x)}{l(x)}\xi_x^2 + 2\xi^2\left(\frac{l''(x)}{l(x)} - \frac{l'(x)^2}{l(x)^2}\right) = 0, \tag{B.44}$$

$$hl'(x)\left(2\xi_t^1 - \frac{10l'(x)}{l(x)}\xi^2 + \frac{4l''(x)}{l'(x)}\xi^2 + 3\xi_x^2\right) - \xi_{tt}^1\frac{4l(x)^3}{\nu h} = 0. \tag{B.45}$$

Separating equation (B.45) by h allows for ξ^1 to be obtained. It also shows that $\eta = \eta(h)$. Thus,

$$\xi^1 = c_1 t + c_2, \quad \xi^2 = \xi^2(x), \quad \eta(h) = c_5 h, \tag{B.46}$$

where

$$10c_1 - 5\xi_x^2 + 2\frac{l'(x)}{l(x)}\xi^2 = 0, \tag{B.47}$$

$$\frac{d}{dx}\left(\xi_x^2 + 2\frac{l'(x)}{l(x)}\xi^2\right) = 0, \tag{B.48}$$

$$2c_1 + 3\xi_x^2 - 10\frac{l'(x)}{l(x)}\xi^2 + 4\frac{l''(x)}{l'(x)}\xi^2 = 0. \tag{B.49}$$

and

$$c_5 = -\frac{1}{2}c_1 + \frac{3}{4}\xi_x^2 + \frac{1}{2}\frac{l'(x)}{l(x)}\xi^2. \tag{B.50}$$

By differentiating equation (B.47) with respect to x, it can be written in the form

$$\frac{d}{dx}\left(-5\xi_x^2 + 2\frac{l'(x)}{l(x)}\xi^2\right) = 0. \tag{B.51}$$

This can be added to equation (B.48) giving

$$\xi^2_{xx} = 0. \tag{B.52}$$

Integrating (B.51) twice with respect to x gives $\xi^2 = c_3 x + c_4$. This reduces the remaining set of equations to

$$\begin{aligned} &\xi^1 = c_1 t + c_2, \quad \xi^2 = c_3 x + c_4, \\ &\eta(h) = h\left(-\frac{1}{2}c_1 + \frac{3}{4}c_3 + \frac{1}{2}(c_3 x + c_4)\frac{l'(x)}{l(x)}\right), \end{aligned} \tag{B.53}$$

where

$$2c_1 + 3c_3 - 10(c_3 x + c_4)\frac{l'(x)}{l(x)} + 4\frac{l''(x)}{l'(x)}(c_3 x + c_4) = 0, \tag{B.54}$$

$$(c_3 x + c_4)\left(\frac{l'(x)^2}{l(x)} - l''(x)\right) - l'(x)c_3 = 0, \tag{B.55}$$

$$10c_1 - 5c_3 + 2(c_3 x + c_4)\frac{l'(x)}{l(x)} = 0, \tag{B.56}$$

and (B.50) holds.

A general expression for the mixing length can be obtained by solving the ordinary differential equation (B.50), giving

$$l(x) = l_0\,(c_3 x + c_4)^{2\frac{c_5}{c_3} + \frac{c_1}{c_3} - \frac{3}{2}}. \tag{B.57}$$

Substituting this expression into the remaining equations results in the final condition,

$$c_5 = \frac{1}{3}\,(2c_3 - c_1)\,. \tag{B.58}$$

Thus, the final expressions for the infinitesimals are given by

$$\xi^1(t) = c_1 t + c_2, \quad \xi^2(x) = c_3 x + c_4, \quad \eta(h) = \frac{h}{3}\,(2c_3 - c_1)\,, \tag{B.59}$$

where

$$l(x) = l_0\,(c_3 x + c_4)^{\frac{1}{3}\frac{c_1}{c_3} - \frac{1}{6}}. \tag{B.60}$$

B.2 Non-classical symmetries of the governing order ν equation (3.74)

The calculation of the non-classical symmetries for the equation (3.74) with a constant mixing length,

$$h_t - \frac{K}{l_0}\left[h^{\frac{3}{2}}(-h_x)^{\frac{3}{2}} + \frac{1}{5}h^{\frac{5}{2}}(-h_x)^{-\frac{1}{2}}h_{xx}\right] + \frac{\nu}{2l_0^2}\,[h(-h_x)] = 0, \tag{B.61}$$

will be shown in this Appendix.

Once again, we assume that $\xi^1 \neq 0$ and that the invariant surface condition is given by (A.57). The expression for h_{tx} is still given by (A.59).

We may now use equation (B.61) and (A.57) to solve for h_{xx},

$$h_{xx} = \frac{5\nu(-h_x)^{\frac{3}{2}}}{2h^{\frac{3}{2}}Kl_0} + \frac{5\eta l_0(-h_x)^{\frac{1}{2}}}{h^{\frac{5}{2}}K} + \frac{5l_0\xi^2(-h_x)^{\frac{3}{2}}}{h^{\frac{5}{2}}K} - \frac{5(-h_x)^2}{h}. \tag{B.62}$$

We now search for a symmetry generator of the form

$$X = \frac{\partial}{\partial t} + \xi^2\frac{\partial}{\partial x} + \eta\frac{\partial}{\partial h}, \tag{B.63}$$

where

$$X^{[2]}((B.61))_{|_{((B.61),(A.57))}} = 0, \tag{B.64}$$

holds.

We prolong the symmetry generator to second order, as given by (A.62), and use the expressions (A.63)-(A.67).

Equation (B.64) becomes

$$\begin{aligned}
&-\frac{K}{l_0}\eta\left(\frac{3}{2}h^{\frac{1}{2}}(-h_x)^{\frac{3}{2}} + \frac{1}{2}h^{\frac{3}{2}}(-h_x)^{-\frac{1}{2}}h_{xx}\right) + \frac{\nu}{2l_0^2}(-h_x)\eta + \zeta_t \\
&-\frac{K}{l_0}\zeta_x\left(-\frac{3}{2}h^{\frac{3}{2}}(-h_x)^{\frac{1}{2}} + \frac{1}{10}h^{\frac{5}{2}}(-h_x)^{-\frac{3}{2}}h_{xx}\right) - \frac{\nu}{2l_0^2}h\zeta_x \\
&-\frac{K}{l_0}\zeta_{xx}\left(\frac{1}{5}h^{\frac{5}{2}}(-h_x)^{\frac{1}{2}}\right)_{|_{((B.61),(A.57))}} = 0.
\end{aligned} \tag{B.65}$$

Replacing h_{xx} with equation (B.62) and collecting like powers of the partial derivatives of h in equation (B.65) results in

$$\begin{aligned}
&\left(-\frac{5\eta^2}{2h} + \frac{\eta\eta_h}{2} - \frac{3h\nu\eta_x}{4l_0^2} + \eta_t - \frac{\xi^2\eta_x}{2} + \frac{3\eta\xi_x^2}{2}\right) \\
&+ (-h_x)^{\frac{1}{2}}\left(\frac{2h^{\frac{3}{2}}K\eta_x}{l_0} + \frac{2h^{\frac{5}{2}}K\eta_{xh}}{5l_0} - \frac{h^{\frac{5}{2}}K\xi_{xx}^2}{5l_0}\right) \\
&- (-h_x)^{-1}\left(\frac{\eta\eta_x}{2}\right) - (-h_x)^{-\frac{1}{2}}\left(\frac{h^{\frac{5}{2}}K\eta_{xx}}{5l_0}\right) \\
&- (-h_x)\left(\frac{5\eta\xi^2}{2h} + \frac{3\eta\nu}{4l_0^2} - \frac{\xi^2\eta_h}{2} - \frac{h\nu\eta_h}{4l_0^2} + \frac{3\eta\xi_h^2}{2} - \frac{h\nu\xi_x^2}{4l_0^2} - \xi_t^2 - \frac{3\xi^2\xi_x^2}{2}\right) \\
&- (-h_x)^{\frac{3}{2}}\left(-\frac{\eta\sqrt{h}K}{l_0} + \frac{h^{\frac{5}{2}}K\eta_{hh}}{5l_0} + \frac{h^{\frac{3}{2}}K\eta_h}{l_0} - \frac{2h^{\frac{5}{2}}K\xi_{xh}^2}{5l_0}\right)
\end{aligned}$$

$$+(-h_x)^2\left(-\frac{3h\nu\xi^2_h}{4l_0^2}-\frac{3\xi^2\xi^2_h}{2}\right)$$

$$-(-h_x)^{\frac{5}{2}}\left(\frac{h^{\frac{3}{2}}K\xi^2_h}{l_0}-\frac{h^{\frac{5}{2}}K\xi^2_{hh}}{5l_0}\right)=0. \tag{B.66}$$

Since ξ^2 and η are independent of the partial derivatives of $h(t,x)$, we may separate by the derivatives, resulting in the following set of determining equations:

$$(-h_x)^{\frac{5}{2}}: \quad \xi^2_h-\frac{h}{5}\xi^2_{hh}=0, \tag{B.67}$$

$$(-h_x)^2: \quad \frac{3}{2}\xi^2_h\left(\frac{h\nu}{2l_0^2}+\xi^2\right)=0, \tag{B.68}$$

$$(-h_x)^{\frac{3}{2}}: \quad \frac{K}{l_0}\sqrt{h}\left(-\eta+\frac{h^2}{5}\eta_{hh}+h\eta_h-\frac{2h^2}{5}\xi^2_{xh}\right)=0, \tag{B.69}$$

$$(-h_x): \quad \left(\frac{5\eta\xi^2}{2h}-\frac{\xi^2\eta_h}{2}+\frac{3\eta\xi^2_h}{2}-\xi^2_t-\frac{3\xi^2\xi^2_x}{2}\right)$$
$$+\frac{\nu}{4l_0^2}\left(3\eta-h\eta_h-h\xi^2_x\right)=0, \tag{B.70}$$

$$(-h_x)^{\frac{1}{2}}: \quad \frac{K}{5l_0}h^{\frac{3}{2}}\left(10\eta_x+2h\eta_{xh}-h\xi^2_{xx}\right)=0, \tag{B.71}$$

$$(-h_x)^{-1}: \quad \frac{\eta\eta_x}{2}=0, \tag{B.72}$$

$$(-h_x)^{-\frac{1}{2}}: \quad \frac{h^{\frac{5}{2}}K\eta_{xx}}{5l_0}=0, \tag{B.73}$$

$$1: \quad -\frac{5\eta^2}{2h}+\frac{\eta\eta_h}{2}-\frac{3h\nu\eta_x}{4l_0^2}+\eta_t-\frac{\xi^2\eta_x}{2}+\frac{3\eta\xi^2_x}{2}=0. \tag{B.74}$$

From equation (B.72), we see that η is independent of x. Thus,

$$\xi^1=1, \quad \xi^2=\xi^2(t,x,h), \quad \eta=\eta(t,h). \tag{B.75}$$

As a result, the determining equations reduce:

$$(-h_x)^{\frac{5}{2}}: \quad 5\xi^2_h-h\xi^2_{hh}=0, \tag{B.76}$$

$$(-h_x)^2: \quad \xi^2_h\left(\frac{h\nu}{2l_0^2}+\xi^2\right)=0, \tag{B.77}$$

$$(-h_x)^{\frac{3}{2}}: \quad -5\eta+h^2\eta_{hh}+5h\eta_h-2h^2\xi^2_{xh}=0, \tag{B.78}$$

$$(-h_x): \quad \left(\frac{5\eta\xi^2}{2h} - \frac{\xi^2\eta_h}{2} + \frac{3\eta\xi_h^2}{2} - \xi_t^2 - \frac{3\xi^2\xi_x^2}{2}\right) + \frac{\nu}{4l_0^2}\left(3\eta - h\eta_h - h\xi_x^2\right) = 0, \tag{B.79}$$

$$(-h_x)^{\frac{1}{2}}: \quad \xi_{xx}^2 = 0, \tag{B.80}$$

$$1: \quad -5\eta^2 + h\left(\eta\eta_h + 2\eta_t + 3\eta\xi_x^2\right) = 0. \tag{B.81}$$

From equation (B.77), we select $\xi_h^2 = 0$ for generality. If the case where $\xi^2 = -\frac{h\nu}{2l_0^2}$ was considered, it would eventually lead to imposing the condition that $\nu = 0$, which simply reduces the problem to that considered in Appendix A.2. Thus, taking $\xi_h^2 = 0$, we can integrate (B.80) twice with respect to x to obtain

$$\xi^2 = a(t)x + b(t), \tag{B.82}$$

where $a(t)$ and $b(t)$ are functions of time whose form is still to be determined. Thus,

$$\xi^1 = 1, \quad \xi^2 = a(t)x + b(t), \quad \eta = \eta(t,h), \tag{B.83}$$

where,

$$-5\eta + h^2\eta_{hh} + 5h\eta_h = 0, \tag{B.84}$$

$$(a(t)x + b(t))\left(\frac{5\eta}{2h} - \frac{\eta_h}{2} - \frac{3a(t)}{2}\right) - (a'(t)x + b'(t)) + \frac{\nu}{4l_0^2}(3\eta - h\eta_h - ha(t)) = 0, \tag{B.85}$$

$$-5\eta^2 + h(\eta\eta_h + 2\eta_t + 3\eta a(t)) = 0. \tag{B.86}$$

By solving the PDE (B.84), we obtain

$$\eta = c(t)h + d(t)h^{-5}, \tag{B.87}$$

where $c(t)$ and $d(t)$ are functions of time to be determined. Substituting this expression for η into the system of equations shows that $d(t) = 0$. Thus,

$$\xi^1 = 1, \quad \xi^2 = a(t)x + b(t), \quad \eta = c(t)h, \tag{B.88}$$

where

$$x\left(2a(t)c(t) - a'(t) - \frac{3}{2}a(t)^2\right) + \left(2b(t)c(t) - b'(t) - \frac{3}{2}a(t)b(t)\right) + \frac{h\nu}{4l_0^2}(-a(t) + 2c(t)) = 0, \tag{B.89}$$

$$-4c(t)^2 + 2c'(t) + 3a(t)c(t) = 0. \tag{B.90}$$

We can split equation (B.89) by h and by x as these variables are now explicit in the equation and their coefficients must thus separately vanish. We see from this that $a(t) = 2c(t)$. Thus,

$$\xi^1 = 1, \quad \xi^2 = 2c(t)x + b(t), \quad \eta = c(t)h, \tag{B.91}$$

where

$$b'(t) + b(t)c(t) = 0, \tag{B.92}$$

$$c'(t) + c(t)^2 = 0. \tag{B.93}$$

The set of equations (B.92-B.93) can be solved exactly for $b(t)$ and $c(t)$. Cases where either $b(t) = 0$ or $c(t) = 0$ can also be examined.

BIBLIOGRAPHY

[1] M. Anthonyrajah, *Turbulent flow in channels and fractures: conservation laws and Lie group analysis*, MSc Dissertation, University of the Witwatersrand, 2011.

[2] M. Anthonyrajah, D. P. Mason and A. G. Fareo, *Propagation of a pre-existing turbulent fluid fracture*, International Journal of Non-Linear Mechanics, **54**, 105-114, 2013.

[3] R. K. Bansal, *A Textbook of Fluid Mechanics and Hydraulic Machines*, 2010. New Delhi, India: Laxmi Publications.

[4] R. E. Bellman, H. H. Kagiwada, and R. E. Kalaba, *Numerical studies of a two-point nonlinear boundary value problem using dynamic programming, invariant imbedding and quasilinearization*, 1964. California, USA: The Rand Corporation.

[5] R. E. Bellman and R. E. Kalaba, *Quasilinearization and Nonlinear Boundary-Value Problems*, 1965. USA: New York, American Elsevier Publishing Company Inc.

[6] J. Boussinesq, *Théorie de l'ecoulement tourbillant*, Mém. Prés. Acad. Sci., **46**, 1877.

[7] G. W. Bluman and S. C. Anco, *Symmetry and Integration Methods for Differential Equations*, 2002. New York, USA: Springer-Verlag.

[8] G. W. Bluman, A. F. Cheviakov and S. C. Anco, *Construction of conservation laws: how the direct method generalizes Noether's theorem*, Group Analysis of Differential Equations and Integrable Systems Conference Proceedings, 13-35, 2009.

[9] G. W. Bluman and J. D. Cole, *The General Similarity Solution of the Heat Equation*, Journal of Mathematics and Mechanics, **18**, 1025-1042, 1969.

[10] R. L. Burden and J. D. Faires, *Numerical Analysis*, 2010. Boston, USA: Cengage Learning.

[11] T. Chaolu and G. W. Bluman, *An algorithmic method for showing existence of nontrivial non-classical symmetries of partial differential equations without solving determining equations*, Journal of Mathematical Analysis and Applications, **411**, 281-296, 2014.

[12] P. A. Davidson, *Turbulence: An Introduction for Scientists and Engineers*, 2004. Oxford: Oxford University Press.

[13] M. R. Doshi and W. N. Gill, *A Note on the Mixing Length Theory of Turbulent Flow*, AIChE Journal, **16**, (5), 885-888, 1970.

[14] S. E. Emerman, D. L. Turcotte and D. A. Spence, *Transport of magma and hydrothermal solutions by laminar and turbulent fluid fracture*, Physics of the Earth and Planetary Interiors, **41**, 249-259, 1986.

[15] A. G. Fareo and D. P. Mason, *A group invariant solution for a pre-existing fluid-driven fracture in permeable rock*, Nonlinear Analysis: Real World Applications, **12**, 767-779, 2011.

[16] I. Farago, *Numerical Methods for Ordinary Differential Equations*, 2013. Hungary, Tankönyvtar. Retrieved from http://www.cs.elte.hu/ faragois/ODE_angol.pdf.

[17] A. D. Fitt, D. P. Mason, and E.A. Moss, *Group invariant solution for a pre-existing fluid-driven fracture in impermeable rock*, Zeitschrift für angewandte Mathematik und Physik, (ZAMP), **58**, 1049-1067, 2007.

[18] E. Fjær, R. M. Holt, P. Horsrud, A. M. Raaen and R.Risnes, *Petroleum Related Rock Mechanics*, 2008. Oxford, UK: Elsevier.

[19] R. F. Gillespie, *Integration*, 1959. Edinburgh: Oliver and Boyd.

[20] S. N. Ha, *A Nonlinear Shooting Method for Two-Point Boundary Value Problems*, Computers & Mathematics with Applications, **42**, 1411-1420, 2001.

[21] G. C. Howard and C. R. Fast, *Hydraulic Fracturing*, 1970. Texas, USA: Millet the Printer.

[22] S. Howison, *Practical Applied Mathematics: Modelling, Analysis, Approximation*, 2005. Cambridge University Press.

[23] M. K. Hubbert and D. G. Willis, *Mechanics of Hydraulic Fracturing*, Transactions of Society of Petroleum Engineers of AIME, **210**, 153-168, 1957.

[24] N. H. Ibragimov, *Elementary Lie Group Analysis and Ordinary Differential Equations*, 1999. West Sussex, England: John Wiley and Sons Ltd.

[25] V. B. Mandelzweig and F. Tabakin, *Quasilinearization Approach to Nonlinear Problems in Physics with Application to Nonlinear ODEs*, Computer Physics Communications, **141**, 268-281, 2001.

[26] J. Mathieu and J. Scott, *An Introduction to Turbulent Flow*, 2000. Cambridge: Cambridge University Press.

[27] D. A. Mendelsohn, *A review of hydraulic fracture modelling - Part I: General concepts, 2D models and motivation for 3D modelling*, ASME J. Energy Resources Technology, **106**, 369-376, 1984.

[28] N. Mindu and D. P. Mason, *Derivation of Conservation Laws for the Magma Equation using the Multiplier Method: Power Law and Exponential Law for Permeability and Viscosity*, Abstract and Applied Analysis, **Vol. 2014**, 13 pages, 2014.

[29] T. Y. Na, *Computational Methods in Engineering Boundary Value Problems*, 1979. New York, USA: Academic Press Inc.

[30] R. Naz, *Conservation Laws for Some Systems of Nonlinear Partial Differential Equations via Multiplier Approach*, Journal of Applied Mathematics, **Vol. 2012**, 13 pages, 2012.

[31] R. Naz, F. M. Mahomed, and D.P. Mason, *Comparison of different approaches to conservation laws for some partial differential equations in fluid mechanics*, Applied Mathematics and Computation, **205**, 212-230, 2008.

[32] R. Nordgren, *Propagation of vertical hydraulic fractures*, Journal of Petroleum Technology, **253**, 306-314, 1972.

[33] P. J. Olver and E. M. Vorob'ev, *Nonclassical and conditional symmetries*. In N. H. Ibragimov, CRC Handbook of Lie Group Analysis of Differential Equations, Volume 3, 1995. CRC Press.

[34] R. L. Panton, *Incompressible Flow*, 1996. USA: John Wiley & Sons, Inc.

[35] T. Perkins and L. Kern, *Widths of hydraulic fractures*, Journal of Petroleum Technology, **222**, 937-949, 1961.

[36] H. Oertel, *Prandtl - Essentials of Fluid Mechanics*, 2010. New York, USA: Springer.

[37] M. M. Rahman and M. K. Rahman, *A Review of Hydraulic Fracture Models and Development of an Improved Pseudo-3D Model for Stimulating Tight Oil/Gas Sand*, Energy Sources, **32**, 1416-1436, 2010.

[38] S. San and E. Yasar, *On the Conservation Laws and Exact Solutions of a Modified Hunter-Saxton Equation*, Advances in Mathematical Physics, **Vol. 2014**, 6 pages, 2014.

[39] H. Schlichting, *Boundary-Layer Theory*, 1970. USA: McGraw-Hill, Inc.

[40] H. Tennekes and J. L. Lumley, *A First Course in Turbulence*, 1972. Massachusetts, USA: The MIT Press.

[41] D. F. Young, B. R. Munson, T. H. Okiishi and W. W. Huebsch, *A Brief Introduction to Fluid Mechanics*, 2011. USA: John Wiley and Sons, Inc.